Funktionelle Analyse von krankheitassozierten *CASK missense Mutationen*

Dissertation

zur Erlangung der Würde des
Doktors der Naturwissenschaften (Dr. rer. nat.)
an der Fakultät für Mathematik, Informatik und Naturwissenschaften
Fachbereich Biologie
der Universität Hamburg

vorgelegt von

Yingzhou Edward Pan
aus Kanada

Hamburg, 2020

Datum der Disputation: 24.04.2020

Gutachter der Dissertation:

1. Prof. Dr. Hans-Jürgen Kreienkamp
2. Prof. Dr. Christian Lohr

Functional analysis of disease-associated *CASK* missense mutations

Dissertation

submitted for the Doctorate of Natural Sciences (Dr. rer. nat.)
in the Faculty of Mathematics, Computer Science and Natural Science
Department of Biology
University of Hamburg

By

Yingzhou Edward Pan
from Canada

Hamburg, 2020

The experimental part of the present work was carried out in the Institute for Human Genetics at the University Medical Center Hamburg-Eppendorf (UKE) under supervision of Prof. Dr. Hans-Jürgen Kreienkamp from February 2016 to March 2020

Date of Disputation: 24.04.2020

Reviewer of the dissertation:

1. Prof. Dr. Hans-Jürgen Kreienkamp (Supervisor)
2. Prof. Dr. Christian Lohr (Advisor).

Acknowledgements

I wish to express my sincere and heartfelt gratitude to my supervisor, Prof. Hans-Jürgen Kreienkamp. I thank you deeply for your unwavering support during the last 4 years, both professional and personal. It has been a wonderful experience to do my PhD and I could not have made the leap from Canada had it not been for your welcome and warmth.

I wish to thank Hans-Hinrich Hönck for your incredible technical and for being such a stabilizing presence in the lab.

I also want to thank all of my friends in the lab for having made our lab a place I looked forward to coming to every day. I will always cherish the moments we have spent together, both at the lab and all around Hamburg.

我非常感谢我的爸爸妈妈。你们给我创造了最好的机会也一直支持我。

我能达到今天的成就，是因为我站在你们的肩膀上。

To my brothers, Edgar, Edwin, and Edmond, you guys have been so patient with me during these last 4 years. Thank you for waiting for me as I wrote this chapter of my life.

Table of Content

Summary

The calcium/calmodulin-dependent protein serine kinase CASK is a member of the MAGUK (membrane-associated guanylate kinase) family of proteins. CASK fulfills several functions in neurons by interacting with several interaction partners. When binding to Liprin and Neurexin, CASK acts as a presynaptic scaffolding protein. When binding to Sap97, CASK can regulate the trafficking of postsynaptic glutamatergic receptors. When binding to Tbr1 and CINAP, CASK can regulate the transcription of genes with T-element promoters, such as *GRIN2B*, which encodes the NR2B subunit of the NMDA receptor.

The *CASK* gene is located on the X-chromosome, meaning that males can only be hemizygous for *CASK* mutations. Heterozygous female and hemizygous male patients with *CASK* loss-of-function mutations exhibit a recognizable set of phenotypes called microcephaly with pontine and cerebellar hypoplasia with intellectual deficiencies (MICPCH + ID). These symptoms are too severe to correlate to any specific molecular function of CASK. However, *CASK* missense mutations have also been reported in male patients who often exhibit either a subset or a milder form of the symptoms observed in patients with *CASK* loss-of-function mutations.

One possible explanation for the less severe symptoms observed in patients with *CASK* missense mutations is that *CASK* missense mutations may not disrupt all of CASK's molecular functions, but a subset of them. The single amino acid replacements may disrupt the ability of CASK to bind to specific interaction partners, and in turn, disrupt the function associated with each lost interaction partner. In principle, it should be possible to correlate the symptoms of patients with *CASK* missense mutations with the molecular phenotypes of each missense mutation.

In this project, I studied 12 *CASK* missense mutations identified in male hemizygous patients. My goals were to determine, first, whether each mutations was pathogenic; second, the pathogenic mechanism underlying each missense mutation; third, whether certain pathogenic mechanisms are shared across multiple missense mutations; and fourth, if certain pathogenic mechanisms correlated with patient symptoms.

In the first part of the project, I performed coimmunoprecipitation experiments to determine which partners were affected by which mutation. With the exception of Liprin-α2, which bound to all 12 CASK mutants, all other partners were affected by at least one mutation. CASK:Sap97 binding was disrupted by the L354P mutation, suggesting that this mutation affects CASK's ability to regulate postsynaptic glutamatergic receptor trafficking. The CASK:Tbr1 and CASK:CINAP interactions were disrupted by the Y723C and W914R mutations, suggesting these mutations disrupt CASK's ability to regulate gene transcription. However, the CASK:Neurexin interaction stood out as particularly sensitive, being mildly affected by the R489W and M507I mutations, and completely disrupted by the G521V, Y723C, and W914R mutations. This suggests that the loss of CASK:Neurexin interaction could be a major pathogenic mechanism underlying *CASK* missense mutations.

I then performed functional assays to determine whether the CASK functions associated with each partner were disrupted by the various mutations. The L354P mutation slightly decreased the trafficking of NMDA receptors compared to AMPA receptors, in accordance with previous literature, but not significantly. I did not observe any effect of CASK on the transcriptional activity of Tbr1, which made it impossible to study the effect of the Y723C and W914R mutations on this aspect of CASK function.

Studies of other MAGUKs suggest that CASK should be able to oligomerize when bound to Neurexin, a presynaptic adhesion protein. Oligomerization upon binding to Neurexin would both greatly aid in CASK's presynaptic scaffolding function and localize it to the correct subcellular compartment. Using split-YFP experiments, I confirmed that CASK oligomerizes in the presence of Neurexin. Furthermore, the G521V, Y723C and W914R mutations, which completely disrupted CASK:Neurexin interaction, also disrupted CASK's ability to oligomerize even in the presence of Neurexin, further supporting the hypothesis that CASK oligomerizes in the presynapse to scaffold the assembly of protein complexes.

Until now, the main proposed pathogenic mechanism underlying *CASK* loss-of-function mutations has been the disruption of its ability to upregulate the transcription of genes because some of the genes it regulates, such as *Reelin*, are necessary for brain laminar development. My results instead suggest that it is the loss of

CASK:Neurexin interaction, which mediates CASK's presynaptic scaffolding role, that may be the main pathogenic mechanism underlying CASK missense mutations. This notion is further supported by a recent study that also suggests that loss of the CASK:Neurexin interaction could also cause microcephaly in patients.

It remains difficult to specifically correlate specific molecular phenotypes to patient symptoms. However, the discovery that CASK:Neurexin interaction is disrupted by multiple *CASK* missense mutations and that it could underlie microcephaly provides an intriguing venue of therapy development. Multiple *CASK* missense mutations could potentially be responsive to a putative therapy that could compensate for the loss of CASK:Neurexin interaction.

Zusammenfassung

Die Calcium/Calmodulin-abhängige Protein Serine Kinase CASK gehört zu der Familie der Membran-assoziierten Guanylat-Kinasen (MAGUK). Durch die Interaktion mit mehreren Interaktionspartnern erfüllt CASK verschiedene Funktionen in Neuronen. Wenn CASK an Liprin und Neurexin bindet, wirkt es als präsynaptisches Gerüstprotein. Wenn CASK an Sap97 bindet, reguliert es den Transport von postsynaptischen Rezeptoren zur Zelloberfläche. Wenn CASK an Tbr1 und CINAP bindet, reguliert es die Transkription von Genen mit T-Element Promotoren, zum Beispiel *GRIN2B*, das für die NR2B-Untereinheit des NMDA-Rezeptors kodiert.

Da das *CASK*-Gen auf dem X-Chromosom liegt, können männliche Patienten nur hemizygot für *CASK*-Mutationen sein. Heterozygote weibliche und hemizygote männliche Patienten mit *CASK loss-of-function* Mutationen sind von einer Mikrozephalie mit pontinischer und zerebellärer Hypoplasie mit intellektueller Defizienz betroffen. Die Schwere dieser Symptome kann nicht mit bestimmten molekularen Funktionen von CASK korreliert werden. Aber in männlichen Patienten wurden *CASK missense* Mutationen entdeckt, die zu einer milderen Form oder nur zu einem Teil dieser Symptome führen.

Es könnte sein, dass die *CASK missense* Mutationen nur einen Teil der Funktionen von CASK stören und dass die Patienten deshalb weniger schwere Symptome zeigen. Der Austausch einzelner Aminosäure könnte die Bindung zwischen CASK und spezifischen Interaktionspartnern stören, und daher nur die Funktion, die mit diesem Interaktionspartner assoziert ist, stören. Die Untersuchung der *missense* Mutationen könnte daher eine Korrelation der Symptome der Patienten mit dem molekularen Phänotyp der Mutationen ermöglichen.

In diesem Projekt untersuchte ich 12 *CASK* missense Mutationen, die in männlichen hemizygoten Patienten identifiziert wurden. Meine Fragestellungen waren: (1) sind die Mutationen pathogen? (2) was sind die pathogenen Mechanismen der Mutationen (3) Gibt es gemeinsame pathogene Mechanismen zwischen mehreren Mutationen; und (4) können pathogene Mechanismen mit den Symptomen der Patienten korreliert werden?

Zuerst habe ich Koimmunopräzipitationsexperimente durchgeführt um festzustellen, welche Bindungspartner von welchen *missense* Mutationen betroffen sind. Mit Ausnahme von Liprin-α2, das alle 12 CASK-Mutanten binden konnte, waren alle anderen Bindungspartner zumindest von einer Mutation betroffen. Die CASK:Sap97 Bindung wurde durch die L354P Mutation gestört. Vermutlich beeinflusst diese Mutation die Fähigkeit von CASK, den Transport von postsynaptischen Rezeptoren zu regulieren. Die CASK:Tbr1 und CASK:CINAP Interaktionen wurden durch die Y723C und W914R Mutationen beeinflusst. Das deutet darauf hin, dass diese Mutationen die Rolle von CASK bei der Transkription stören. Die CASK:Neurexin Bindung wurde durch die R489W und M507I Mutationen teilweise, und durch die G521V, Y723C, und W914R Mutationen komplett gestört. Dies deutet darauf hin, dass der Verlust der CASK:Neurexin Bindung ein wichtiger pathogener Mechanismus ist, der viele Patienten betrifft.

In funktionellen Experimenten untersuchte ich, ob die *CASK* Mutationen die verschiedenen Funktionen von CASK betreffen. Die L354P Mutation reduzierte das Verhältnis von postsynaptischen NMDA-Rezeptoren zu AMPA-Rezeptoren an der Zelloberfläche. Ich beobachtete keinen Effekt von CASK auf die transkriptionelle Aktivität von Tbr1. Deshalb war es unmöglich die Wirkung der Y723C und W914R Mutationen in diesem Zusammenhang zu untersuchen.

Studien an anderen MAGUKs deuten darauf hin, dass CASK nach Bindung an Neurexin in der Lage sein sollte zu oligomerisieren.Die Oligomerisierung in Gegenwart dieses präsynaptischen Zelladhäsionsmoleküls würde die Funktion von CASK als Gerüstprotein der Präsynapse unterstützen.. In einem Split-YFP Experiment stellte ich fest, dass CASK in Gegenwart von Neurexin oligomerisiert. Die G521V, Y723C, und W914R Mutationen, die die CASK:Neurexin Bindung stören, stören auch die Fähigkeit von CASK, im Beisein von Neurexin, zu oligomerisieren. Diese Ergebnisse unterstützen die Hypothese, dass CASK in der Präsynapse oligomerisiert um die Komplexbildung präsynaptischer Komponenten zu fördern.

Der bisher angenommene pathogene Mechanismus von *CASK* loss-of-function Mutationen ist der Verlust der Transkription von Genen wie *RELN*, da das kodierte *Reelin*-Protein für die laminare Entwicklung des Gehirns

notwendig ist. Meine Ergebnisse zeigen stattdessen, dass der Verlust der CASK:Neurexin Bindung der hauptsächliche pathogene Mechanismus von *CASK* missense Mutationen ist. Dieser Befund wird durch eine kürzliche Studie unterstützt, die ebenfalls nahelegt, dass der Verlust der CASK:Neurexin Bindung die Entwicklung des Gehirns stören könnte.

Es bleibt weiterhin schwierig, die Symptome der Patienten mit den molekularen Phänotypen der Mutationen zu korrelieren. Die Entdeckung, dass die CASK:Neurexin Bindung durch viele *CASK* missense Mutationen gestört, und dass die Verlüst von CASK:Neurexin Bindung die Entwicklung des Gehirns stören könnte, stellen allerdings eine vielversprechende Möglichkeit für die Entwicklung von Therapien für Patienten mit *CASK missense* Mutationen dar. Da viele Mutationen die CASK:Neurexin Bindung stören, könnten viele Patienten auf Therapien ansprechen, die den Verlust dieser Interaktion kompensieren.

Résumé

CASK (calcium/calmodulin-dependent protein serine kinase, Sérine kinase calcium/calmoduline-dépendente) est une protéine de la famille des MAGUK (Membrane-associated guanlyate kinase, Guanylate kinase associée aux membranes). CASK remplit plusieurs fonctions dans les neurones en interagissant avec plusieurs partenaires d'interaction. Liée à la Liprine et la Neurexine, CASK agit comme une protéine d'échafaudage présynaptique. Liée à Sap97, CASK peut réguler le transport de récepteurs glutamatergiques post-synaptique. Liée à Tbr1 et CINAP, CASK peut réguler la transcription des gènes avec des promoteur à élément T, comme *GRIN2B*, qui code la sous-unité NR2B du récepteur de NMDA.

Le gène *CASK* se trouve dans le chromosome X, ce qui signifie que les hommes ne peuvent être que hémizygotes pour les mutations de *CASK*. Les patients hétérozygotes de sexe féminin et les patients hémizygotes de sexe masculin présentant des mutations non-fonctionnelles de CASK présentent un ensemble reconnaissable de phénotype appelé microcéphalie avec hypoplasie pontine and cérébelleuse avec déficiences intellectuelles (MICPCH + ID). Ces symptômes sont trop graves pour être corrélés à une fonction moléculaire spécifique de CASK. Cependant, des mutations faux sens de *CASK* ont été signalées chez des patients de sexe masculin qui présentent souvent un sous-ensemble ou une forme moins grave des symptômes observés chez les patients avec des mutations non-fonctionnelles de *CASK*.

Une explication possibles pour les symptômes moins graves observés chez les patients avec des mutations faux sens de *CASK* serait que les mutations faux sens de *CASK* ne perturbent pas toutes les fonctions de CASK, mais certaines d'entre elles. Le remplacement d'un seul acide aminé pourrait perturber l'interaction entre CASK et un partenaire spécifique, ce qui entraînerait que la perte de la fonction associée avec ce partenaire. En principe, il devrait être possible de distinguer les symptômes observés chez les patients présentant des mutations non fonctionnelles de *CASK* si les symptômes des patients présentant des mutations faux sens de *CASK* pouvaient être corrélés avec les phénotypes moléculaires de ces mutations faux sens.

Dans le cadre de ce projet, j'ai étudié 12 mutations faux sens de *CASK* identifiées chez des patients hémizygotes de sexe masculin. Mes objectifs étaient de déterminer, premièrement, si chaque mutation était pathogène; deuxièmement, le mécanisme pathogène de chaque mutation faux sens; troisièmement, si certains mécanismes pathogènes sont partagés entre plusieurs mutations faux sens; et quatrièmement, si certains mécanismes peuvent être corrélés avec les symptômes des patients.

Dans la première partie du projet, j'ai effectué des expériences de coimmunoprécipitation pour déterminer quels partenaires étaient affectés par quelle mutation. À l'exception de Liprin-α2, qui a pu interagir avec les 12 mutants de CASK, tous les autres partenaires ont été affectés par au moins une mutation. L'interaction CASK:Sap97 fut perturbée par la mutation L354P, ce qui laisse supposer que cette mutation affecte la capacité de CASK à réguler le transport des récepteurs glutamatergiques post-synaptiques. Les interactions CASK:Tbr1 et CASK:CINAP furent perturbées par les mutations Y723C and W914R, ce qui laisser supposer que ces mutations affectent la capacité de CASK de réguler la transcription de gènes. Ce fut cependant l'interaction CASK:Neurexine qui s'est révélée être la plus sensible, étant partiellement affectée par les mutations R489W et M507I, et complètement perturbée par les mutations G521V, Y723C, et W914R. Cela laisse supposer que la perte de l'interaction CASK:Neurexine pourrait être un mécanisme pathogène majeur des mutations faux sens de *CASK*.

J'ai ensuite effectué des essais fonctionnels pour déterminer si les fonctions de CASK associées aux partenaires étaient perturbées par les mutations faux sens. La mutation L354P a légèrement diminué le transport de récepteurs de NMDA, mais pas de façon statistiquement significative. Les mutations Y723C et W914R ont été testées pour déterminer leur capacité à perturber la capacité de CASK d'augmenter la transcription génétique. Cependant, je n'ai pas pu observer que CASK augmentait l'activité transcriptionelle de Tbr1 dans des expériences de double luciférase, ce qui a rendu impossible l'étude de l'effet des mutations Y723C et W914R.

Des études sur d'autres MAGUKs suggèrent que CASK devrait pouvoir s'oligomériser lorsqu'il interagit avec la Neurexine, une protéine d'adhésion présynaptique. L'oligomérisation de CASK liée à la Neurexine aiderait la

fonction d'échafaudage présynaptique de CASK et la localiserait dans le bon compartiment cellulaire. À l'aide d'expériences de YFP-divisée, j'ai confirmé que CASK s'oligomérise en présence de Neurexine. De plus, les mutations G521V, Y723C, et W914R, qui ont complètement perturbé l'interaction CASK:Neurexine, ont aussi perturbé la capacité de CASK à s'oligomériser, même en présence de Neurexine. Cela appuie d'avantage l'hypothèse selon laquelle CASK s'oligomérise dans la présynapse pour structurer l'assemblage de complexes protéiques.

Jusqu'à présent, le principal mécanisme pathogène proposé pour les mutations non-fonctionnelles de *CASK* a été la perte de sa capacité d'augmenter la transcription génétique parce que certains des gènes que CASK régule, comme *Reelin,* sont nécessaires au développement laminaire du cerveau. Mes résultats suggèrent plutôt que c'est la perte de l'interaction CASK:Neurexine qui pourrait être le mécanisme pathogène principal des mutations faux sens de *CASK*. Cette hypothèse est étayée par une étude récente qui suggère aussi que la perte de l'interaction CASK:Neurexine pourrait causer une microcéphalie chez des patients.

Il demeure difficile d'établir une corrélation précise entre les phénotypes moléculaires des mutations faux sens de *CASK* et les symptômes des patients chez qui ces mutations ont été trouvée. Toutefois, la découverte que l'interaction CASK:Neurexine est perturbées par de multiples mutations faux sens de *CASK*, et que ces dernières pourrait être à l'origine de la microcéphalie chez les patients, laisser entrevoir une possibilité excitante pour le développement de thérapies. En effet, une thérapie qui vise à compenser la perte de l'interaction CASK:Neurexine pourrait être efficace contre plusieurs mutations faux sens de *CASK*.

摘要

CASK（钙/钙调素依赖性蛋白丝氨酸激酶）是MAGUK（膜相关鸟苷酸激酶）家族的一员。CASK通过与多个相互作用的伙伴的相互作用来实现神经元的多种功能。当与Neurexin和Liprin结合时，CASK起着突触前支架蛋白的作用。当与Sap97结合时，CASK可以调节突触后谷氨酸受体的传输过程。当与Tbr1和CINAP结合时，CASK可以通过T系列启动子（如GRIN2B，由它编码NMDA受体的NR2B亚单位）来调节基因的转录。

CASK基因位于X染色体上，这意味着男性只能是CASK突变的半合子。具有CASK功能缺失突变的杂合子女性及半合子男性患者表现出一组可识别的表型，称为脑桥小头和小脑发育不全伴智力缺陷（MICPCH+ID）。这些症状太严重时，CASK的任何特定分子功能之间都无法相互关联。然而，CASK错义突变在男性患者中也有报道，这些患者通常表现出CASK功能丧失突变患者中观察到的症状的子集或更轻微的形式。

对CASK错义突变患者观察到的较轻症状的一种可能解释是，CASK错义突变可能不会破坏CASK的所有分子功能，而是其中的一部分。单一氨基酸替代物可能破坏CASK与特定相互作用伙伴结合的能力，进而破坏与每个丢失的相互作用伙伴相关联的功能。原则上，如果CASK错义突变患者的症状可以与每一个错义突变的分子表型相关，那么就有可能对CASK功能丧失突变患者的症状进行分类。

在本项目中，我研究了在男性半合子患者中发现的12个CASK错义突变。我的目标是，首先，确定每个突变是否致病；其次，确定每个错义突变背后的致病机制；第三，是否在多个错义突变之间共享某些致病机制；第四，确定某些致病机制是否与患者症状相关。

在本项目的第一部分中，我实施了共免疫切除实验，以确定哪些伴侣受到了哪些突变的影响。除了与所有12个CASK突变体结合的Liprin-α2外，所有其他伙伴都受到至少一个突变体的影响。CASK:Sap97结合被L354P突变破坏，这表明该突变影响CASK调节突触后谷氨酸受体传输的能力。CASK:Tbr1和CASK:CINAP相互作用被Y723C和W914R突变破坏，这表明这些突变破坏了CASK调节基因转录的能力。然而，受R489W和M507I突变的轻微影响，并被G521V、Y723C和W914R突变完全破坏的CASK:Neurexin相互作用特别敏感。这表明CASK:Neurexin相互作用的丧失，可能是CASK错义突变的主要致病机制。

然后，我进行了功能分析，以确定与每个伙伴相关的CASK功能是否被各种突变所破坏。根据以前的文献，与AMPA受体相比，L354P突变略微减少了NMDA受体的传输，但不显著。我还对Y723C和W914R突变进行了检测，以确定它们是否有能力破坏CASK上调基因转录的能力。然而，在双荧光素酶实验中，我未能观察到CASK增加Tbr1的转录活性，这使得我们无法研究Y723C和W914R突变的影响。

其他MAGUKs的研究表明，当绑定Neurexin（一种突触前粘附蛋白）时，CASK应该能够齐聚化。与Neurexin绑定的齐聚作用将极大地帮助CASK的突触前支架功能，并将其定位到正确的亚细胞室。使用分裂YFP实验，我证实了CASK在Neurexin存在下齐聚过程。此外，G521V、Y723C及W914R的突变完全破坏了CASK:Neurexin相互作用，甚至破坏了CASK在Neurexin存在下的齐聚化能力，从而进一步支持了CASK在突触前向支架组装蛋白质复合物过程中齐聚化的假设。

到目前为止，CASK功能丧失突变的主要致病机制是其上调基因转录的能力被破坏，因为它调控的一些基因，如颤蛋白，是脑层流发育所必需的。相反，我的结果表明，调解CASK的突触前支架作用的CASK:Neurexin相互作用的丧失，可能是CASK错义突变的主要致病机制。最近的一项研究也支持这一概念。该研究表明，CASK:Neurexin相互作用的损失也可能导致患者小头畸形。

很难将特定的分子表型与患者症状具体关联起来。然而，CASK:Neurexin相互作用被多 重CASK错义突变破坏，并且它可能是小头畸形的成因这一发现，为治疗的开发提供了一个引人入胜的场景。补偿CASK:Neurexin相互作用的损失，很可能是一种对多重CASK错义突变的治疗方式。

1 Introduction

1.1 CASK: A Highly Versatile Neuronal Protein

The Calcium/Calmodulin-dependent Serine protein Kinase (CASK) is a protein primarily expressed in the brain (Hata, Butz, & Südhof, 1996). CASK is a member of the Membrane-Associated Guanylate Kinase (MAGUK) superfamily of proteins, which can fulfill multiple functions but are primarily associated with a cellular scaffolding role (Funke, Dakoji, & Bredt, 2005; Lorenza González-Mariscal, Betanzos, & Ávila-Flores, 2000; Zheng, Seabold, Horak, & Petralia, 2011). By binding to various interaction partners, CASK is associated with a very wide spectrum of neuronal functions, including synaptic scaffolding, receptor trafficking, and transcription regulation (Y.-P. Hsueh, 2006).

As a synaptic scaffolding protein, CASK primarily interacts with Neurexin (Hata et al., 1996), Syndecan (Y. P. Hsueh et al., 1998), and Synaptic Cell Adhesion Protein (SynCAM) (Biederer et al., 2002). The binding of CASK to Neurexin and SynCAM is interesting as both of these synaptic adhesion proteins are involved in the development of synapses (Biederer et al., 2002; Dean et al., 2003; Graf, Zhang, Jin, Linhoff, & Craig, 2004; Scheiffele, Fan, Choih, Fetter, & Serafini, 2000). A recent discovery in the field of synaptic structure is the nanocolumn, an alignment of clusters of postsynaptic receptors and scaffolding proteins with presynaptic vesicle release sites. Presynaptic Neurexins have been shown to also form nanoclusters, which makes them, and by extension, CASK, interesting candidates as structural proteins mediating this very fine alignment.

CASK is also known to be involved in sorting of synaptic receptors by interacting with Sap97. Sap97 preferentially binds and traffics AMPA receptors (AMPARs) to the postsynapse. However, when in a complex with CASK, Sap97 preferentially binds to NMDA receptors (NMDARs) and traffics them to the postsynapse (Jeyifous et al., 2009; Lin, Jeyifous, & Green, 2013). CASK could therefore play a critical role in regulating the receptor composition of excitatory synapses.

CASK can also regulate the gene expression, a relatively rare function among MAGUKs. In a complex with Tbr1 and CINAP, CASK can regulate the expression of genes with T-element promoters, such as *Reelin* or the *NR2b* subunit of the NMDAR (Y.-P. Hsueh, Wang, Yang, & Sheng, 2000; G.-S. Wang et al., 2004; T.-F. Wang et al., 2004). *Reelin* is a gene necessary for the laminar development of the brain in mice (D'Arcangelo & Curran, 1998), which therefore suggests that CASK could have an important role in brain development.

Patients with loss of function mutations in *CASK* exhibit a severe set of phenotypes. Because the *CASK* gene is located on the X-chromosome (Dimitratos, Stathakis, Nelson, Woods, & Bryant, 1998), females can be heterozygous for *CASK* mutations while males can only be hemizygous. Male and female patients with *CASK* loss of function mutations exhibit a recognizable form of microcephaly called “microcephaly with pontine and cerebellar hypoplasia” (MICPCH) and exhibit severe intellectual deficiencies (ID). Additionally, male patients have severe epileptic seizures (Moog et al., 2015; Najm et al., 2008).

CASK missense mutations have also been reported. Most patients with missense mutations are males, often inheriting the mutations from an asymptomatic carrier mother (Hackett et al., 2009; Moog et al., 2015; Takanashi et al., 2012). However, a more recent study has reported two female patients who had heterozygous *CASK* missense mutations, yet exhibited severe phenotypes (L. E. W. LaConte et al., 2018). The male patients with *CASK* missense mutations sometimes exhibited either a milder form or a subset of the symptoms exhibited by the male patients with *CASK* loss-of-function mutations. For example, some did not exhibit microcephaly while others exhibited mild instead of severe ID. This suggests that the CASK protein in these patients may partially retain some of the functions associated with CASK that are normally all lost with *CASK* loss of function mutations.

In this study, I investigated a set of 12 missense mutations identified in male patients. I first determined whether or not each missense mutation is capable of disrupting the binding of CASK to various interaction partners. I then tested how the function of CASK associated with each partner was affected by the various missense mutations. My first goal was to find indications as to whether or not the 12 missense mutations are pathogenic.

This is in most cases not at all clear, as for individual mutations, there may be only one or very few patients worldwide. The second and third goals are to find out what pathogenic mechanisms underlie each mutation and whether each mutation has a unique pathogenic mechanism or whether some mechanisms are shared across multiple mutations. Finally, I sought to determine whether a correlation could be drawn between the molecular phenotypes associated with each mutation and the patients' symptoms.

1.1.1 *CASK* genetics and CASK protein structure

The *CASK* gene is located on the X chromosome in humans (Dimitratos et al., 1998). The gene is composed of 23 different exons, combined into 4 known *CASK* transcript variants numbered *CASK-TV1* to *TV4* (GeneBank NM_003688, NM_001126054, NM_001126055, & NM_001367721). These 4 transcript variants differ in their inclusions of 4 alternatively spliced exons: exons 11, 19, 20, and a 5' extension of exon 23 (23L) (Fig 3.1B).

From the N-terminus to the C-terminus, CASK is composed of a CaMK domain, 2 L27 domains (L27.1 and L27.2), followed by a PDZ, SH3, and GK domain motif that defines all MAGUKs (Y.-P. Hsueh, 2006). At its CaMK domain, CASK binds to presynaptic interaction partners associated with presynaptic scaffolding and vesicle regulation, such as α-Liprins (Olsen et al., 2005), Mint1 (Butz, Okamoto, & Südhof, 1998), and Caskin1 (Borg et al., 1998). The L27.1 domain of CASK binds to Sap97 and regulates Sap97's trafficking of NMDARs and AMPARs (Jeyifous et al., 2009; Lin et al., 2013). The L27.2 domain of CASK associates CASK with Velis, also known as MALS1, completing a Mint1:CASK:Velis complex that in mammalian neurons is thought to link vesicle exocytosis to synaptic presynaptic adhesion (Butz et al., 1998).

The PDZ domain of CASK binds to the presynaptic cell adhesion protein Neurexin (Hata et al., 1996) as well to Syndecan-2 (Y. P. Hsueh et al., 1998) and SynCAM (Biederer et al., 2002), all 3 being synaptic receptors involved in synapse formation and adhesion. The SH3 domain of CASK binds to N-type voltage calcium channels (Maximov & Bezprozvanny, 2002; Maximov, Südhof, & Bezprozvanny, 1999). Finally, the GK domain of CASK binds to Tbr1 and CINAP and is associated with CASK's function as a gene expression regulator (Y.-P. Hsueh et al., 2000; G.-S. Wang et al., 2004; T.-F. Wang et al., 2004).

The distinguishing feature of the CASK protein amongst MAGUKs is the CaMK domain at its N-terminus after which CASK is named. Like the GK domain of MAGUKs, it was initially believed that CASK-CaMK exclusively acts as a protein-protein binding site and that it did not possess kinase activity of its own on the basis that certain conserved residues of active CaM-kinases were changed in CASK (Cohen et al., 1998). However, a study by Mukherjee et al. (2008) showed that CASK-CaMK does in fact retain kinase activity. CaM-kinases require Mg^{2+} to work and bind to it via an Asp-Phe-Gly (DFG) motif. Because CASK replaces this DFG motif with GFG, it was initially expected that CASK could therefore not be an active kinase. Mukherjee et al., demonstrated that the change in residue did not disrupt the kinase activity of the CASK-CaMK domain, but instead only removed its need for Mg^{2+}. In fact, rather than requiring Mg^{2+}, CASK-CaMK is inhibited by both Mg^{2+} and Ca^{2+}. Interestingly, the target of CASK-CaMK is Neurexin (Mukherjee et al., 2008) which suggests that the kinase activity of CASK may regulate its presynaptic scaffolding role which will be discussed in the next section.

1.2 CASK in the context of synaptic structure

1.2.1 General structure of synapses

Neurons are specialized cells whose main function is information processing. Structurally, neurons consist of a soma which receives inputs via its dendrites and can generate and transmit a signal called an action potential via its axon (Chklovskii, 2004). Synapses are specialized cell adhesion sites which neurons use to communicate with each other by releasing neurotransmitters. The function of the synapse is to convert an action potential, an electric signal that travels down the length of the axon of the presynaptic neuron, into the release of chemical neurotransmitters onto the postsynaptic neuron. In the central nervous system (CNS), the two primary types of synapses are excitatory synapses and inhibitory synapses (van Spronsen & Hoogenraad, 2010). Excitatory synapses release the neurotransmitter glutamate from the presynapse, which binds to AMPA receptors (AMPARs) (Malinow & Malenka, 2002), NMDA receptors (NMDARs) (Wenthold, Al-Hallaq, Swanwick, & Petralia, 2008) and metabotropic glutamate receptors (mGluRs). The major effect of activation of these

receptors is a depolarization of the postsynaptic neuron via the influx of Na^+ ions, which may be associated with increases in Ca^{2+} levels. In inhibitory synapses, GABA (or glycine) is released from the presynapse and binds to GABA receptors (or glycine receptors), which then inhibits the postsynaptic cells via the influx of Cl^- ions (Jacob, Moss, & Jurd, 2008).

Excitatory and inhibitory synapses also differ in their structure. The specialized patch of membrane housing the various postsynaptic receptors is called the postsynapse. In excitatory synapses, the postsynapse usually forms at the tip of protrusions extending from dendrites called dendritic spines while in inhibitory synapses, the postsynapse typically occur directly on the dendrites or the neuronal soma (J. N. Bourne & Harris, 2008; Sheng & Kim, 2011).

Another key difference between excitatory and inhibitory synapses is the presence of the postsynaptic density (PSD) in excitatory synapses. When Palay (1956) first imaged inhibitory synapses, he noted an even thickening of the pre- and postsynaptic membranes at the site of contact. In excitatory synapses, however, the postsynaptic thickening is significantly thicker relative to the presynapse, and was thus termed Postsynaptic Density (PSD)(Gray, 1959). For this reason, excitatory synapses are also called "asymmetric" synapses while inhibitory ones are also called "symmetric" synapses (Siegelbaum, Kandel, & Yuste, 2013).

The thickenings on both sides of the synapse represent protein rich structures with specialized functions. The thickening of the presynaptic terminal is what we call now the presynaptic active zone. The main function of the active zone is to dock synaptic vesicles filled with neurotransmitters to the presynaptic membrane and ensure their release upon the presence of action potentials (Landis, Hall, Weinstein, & Reese, 1988; Sudhof, 2012). In the excitatory postsynapse, the PSD is a highly regulated structure consisting of postsynaptic neurotransmitter receptors anchored by a large network of scaffolding proteins (Sheng & Kim, 2011).

The exact physiological function of CASK in the presynapse is not yet well established. But based on its interaction partners, CASK may be involved in 3 general roles. CASK interacts with Neurexin (Hata et al., 1996), which has been involved in presynaptic and postsynaptic differentiation (Dean et al., 2003; Graf et al., 2004; Scheiffele et al., 2000), meaning CASK may be part of the signaling pathways involved in synaptogenesis. CASK also links Neurexin to the core components of the active zone via Liprin-α (Olsen et al., 2005; Sudhof, 2012) and to a CASK:Velis:Mint1 complex (Butz et al., 1998). Both complexes are involved in vesicle docking and fusion. CASK is thus well situated to link synaptic adhesion to vesicle release. Finally, via the Neurexin:CASK:Liprin-α set of interactions (Hata et al., 1996; Olsen et al., 2005), CASK is an interesting candidate as a component of nanocolumns, the most recently discovered element of synaptic structure (Tang et al., 2016) which will be discussed in more detail in section 1.2.4.

The binding between Neurexin and Neuroligin is a highly specific phenomenon, regulated through a mechanism called the "splice code" of transynaptic adhesion (Boucard, Chubykin, Comoletti, Taylor, & Südhof, 2005; Chih, Gollan, & Scheiffele, 2006; Graf, Kang, Hauner, & Craig, 2006). The coding mRNAs for both Neurexins and Neuroligins are extensively spliced in the mammalian brain (Ichtchenko et al., 1995; Ichtchenko, Nguyen, & Südhof, 1996; Missler, Fernandez-Chacon, & Südhof, 1998). Neurexin in particular has been estimated to be present in between 1000 and 2000 different isoforms, making it one of the most polymorphic proteins in mammals (Missler et al., 1998; Missler & Südhof, 1998; Ullrich, Ushkaryov, & Südhof, 1995). The splice code, a concept coined by Boucard et al. (2005), refers to the fact that specific isoforms of Neurexin are highly selective with respect to the isoform of Neuroligin they bind and vice versa (Chih et al., 2006; Graf et al., 2006).

The specificity of the Neurexin:Neuroligin interaction is particularly interesting in the light of the discovery that it is sufficient to induce the differentiation of both the presynapse and postsynapse. The first study to demonstrate this was performed by Scheiffele et al. (2000) who showed that primary neurons would form presynapses if their axons made contact with HEK293T cells overexpressing Neuroligin. Graf et al. (2004) performed the reverse experiment and showed that the dendrites of primary neurons would form postsynapses if their dendrites made contact with Cos-7 cells overexpressing Neurexin. Further work by Dean et al. (2003) then showed that Neuroligin triggers presynaptic differentiation by clustering Neurexin. Neuroligins likely possess an inherent ability to multimerize via their extracellular domains, as this domain is homologous to the extracellular

domain of acetylcholinesterases (AChEs), which are known to multimerize (Y. Bourne, Taylor, Bougis, & Marchot, 1999; Morel, Leroy, Ayon, Massoulié, & Bon, 2001). Neuroligin mutants deficient for multimerization are unable to induce presynaptic differentiation via Neurexin. Dean et al. were also able to trigger presynaptic differentiation by clustering Neurexin through attachment of primary and secondary antibodies, further showing that the signal for presynaptic differentiation begins with the clustering of presynaptic Neurexin.

Taken together, the results from Dean et al. (2003) and Graf et al. (2004) would also imply that Neurexin must have some ability to cluster Neuroligin, or that at least, Neuroligin multimerization is only possible after Neuroligin has bound to Neurexin. Indeed, if Neuroligin clustering were spontaneous, postsynaptic sites would also spontaneously form. Neurexin and Neuroligin may thus cluster each other to induce both pre and postsynaptic differentiation. However, Neurexin has no known inherent ability to cluster as none of its domains are associated with such a function (Missler et al., 1998). However, one of its interaction partners, CASK, likely has the ability to oligomerize, based on its similarity to other MAGUKs (Li et al., 2014). This gives rise to the possibility that CASK multimerization may be responsible for the downstream signaling that leads to synaptic differentiation via multimerization of Neuroligin and Neurexin.

How CASK is expected to oligomerize is worth discussing in more detail.

1.2.2 CASK likely oligomerizes via its PSG supramodule

MAGUKs constitute a large family of proteins primarily associated with scaffolding roles at cell junctions (Lorenza González-Mariscal et al., 2000). All MAGUK proteins are defined by a PDZ, SH3, and GK domain motif at their C-Terminus (Zheng et al., 2011; Zhu et al., 2016). It has become increasingly clear that within some MAGUKs, these 3 domains do not act as independent domains, but bind to each other in order to form a cohesive unit called the PSG supramodule. In MAGUKs with multiple PDZ domains, it is always the most C-terminal PDZ domain directly N-terminal up the SH3 domain that participates in the PSG supramodule. The three dimensional conformation of the PSG supramodule within a MAGUK is dependent upon a set of intramolecular PDZ:SH3 and SH3:GK interactions.

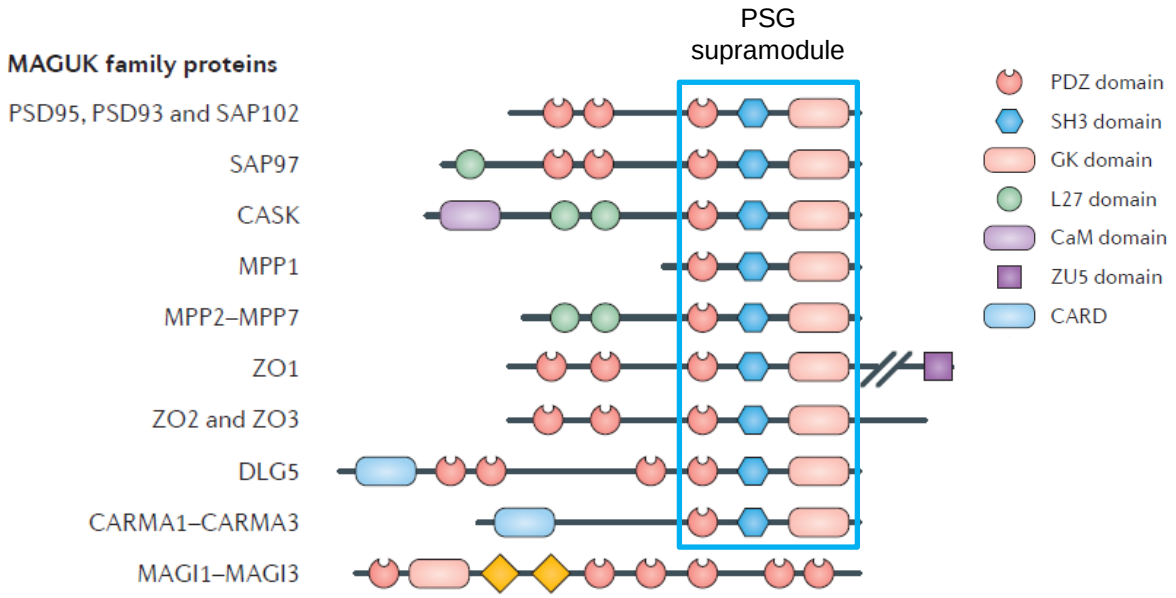

Figure 1.1: All MAGUKs are defined by a PDZ-SH3-GK motif at the C-Terminus, with the exception of MAGI (MAGuk protein Inverted). Studies have shown that a set of PDZ:SH3 and SH3:GK interactions allow for the formation of an integrated PSG supramodule. Figure taken from Zhu, Shang, and Zhang (2016)

The PDZ:SH3 interaction was first reported in ZO-1, a MAGUK primarily expressed in epithelial cells (L. González-Mariscal et al., 1999). A structural study by Pan, Chen, Yu, Yu, and Zhang (2011) suggested that the hydrophobic interface between the 3rd PDZ and SH3 domains in ZO-1 should mediate an intramolecular interaction. Another study by Nomme et al. (2011) showed that the binding of ZO-1 to its PDZ-ligand JAM requires both the PDZ and SH3 domains of ZO-1. They showed that both the PDZ and SH3 domains of ZO-1 contribute residues to form a hybrid binding pocket at the interface between the two domains (Fig 1.2A).

The SH3:GK interaction was studied in the MAGUKs PSD-95. Structural studies of PSD-95 by McGee et al. (2001) showed two main differences between canonical SH3 domains and the SH3 domain in MAGUKs. The first is the replacement of a β-strand normally found in canonical SH3 domains. Canonical SH3 domains are composed of 5 β-strands (named βA to βE) arranged in a criss-crossing pattern. In MAGUK-SH3 domains, the 5th β-strand (βE) is replaced by two β-strands named βE and βF that are not part of the SH3 domain itself but are instead part of the flanking regions of the GK domain and integrate themselves into the structure of the MAGUK-SH3 domains. This suggests that MAGUK-SH3 domains may not fold properly without associating in close proximity to the GK domains of MAGUKs. Further studies performed in Sap97 identified that a Tyrosine (Y710) from βE and a Tryptophan (W904) from βF of the GK domain extend into the SH3 domain, potentially acting as "anchors" that mediate the SH3:GK interaction (Zhu et al., 2011; Zhu et al., 2016) (Fig 1.2B).

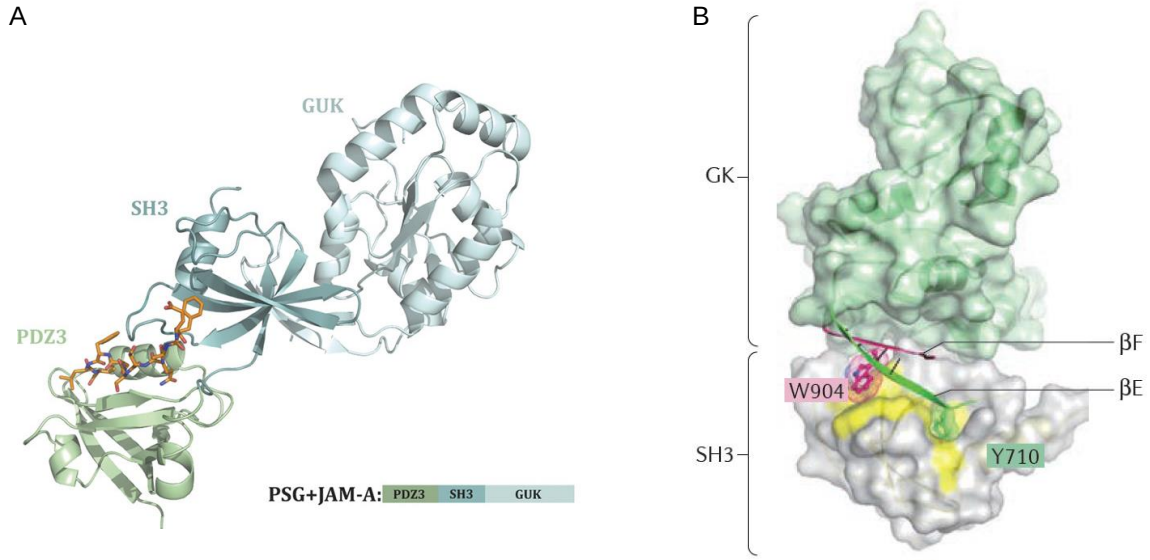

Figure 1.2 MAGUK possess a PSG supramodule **(A)** The most C-terminal PDZ domain of MAGUKs binds to the SH3 domain. In the MAGUK ZO-1, the PDZ:SH3 interaction creates a binding site for JAM, the PDZ-ligand of ZO-1. (Nomme et al., 2011) **(B)** The structure of the SH3 domain in MAGUKs is completed by two β-strands (βE and βF) provided by the GK domain of MAGUKs. In Sap97, two residues of the GK domain, Y710 and W904, mediate the SH3:GK interaction. (McGee et al., 2001; Zhu et al., 2016)

The second difference that distinguishes MAGUK SH3 domains from canonical SH3 domains is the presence of an extra stretch of amino acids called a "hinge" or "HOOK" domain between βD and βE in MAGUKs that is absent from canonical SH3 domains. This HOOK domain is also the reason why the βE and βF strands that integrated into the SH3 domain structure are considered part of the GK domain of MAGUKs rather than the SH3 domain.

McGee et al. propose that this extra "slack" between the SH3 and GK domain of MAGUKs is what confers PSD-95 and potentially MAGUKs in general the ability to multimerize. The HOOK domain gives the GK domain a certain degree of freedom and flexibility relative to the rest of the MAGUK protein. This makes it possible to form intermolecular SH3:GK interactions rather than intramolecular interactions. They propose that PSD-95 may dimerize if a first PSD-95 molecule "donates" its GK domain to stabilize the structure of a second PSD-95 molecule while the second PSD-95 reciprocates its GK domain to the first. Alternatively, this

mechanism could also allow PSD-95 to oligomerize if the first PSD-95 donates its GK domain to the SH3 of a second PSD-95, which in turn donates its GK domain to the SH3 domain of a third PSD-95 and so on.

A study by Li et al. (2014) integrated the previous concepts and showed that for the MAGUK PALS1, the formation of a PSG supramodule is necessary for the binding of its PDZ-ligand Crumbs, and that the binding of PALS1 to Crumbs is inherently linked to the dimerization of PALS1. They resolved the crystal structure of the PALS1:Crumbs complex and showed that Crumbs binds to a binding site formed at the interface between the PDZ and SH3 domains of PALS1 (Fig 1.3A). They also showed that in PALS1, the GK domain folds back onto the PDZ:SH3 domains to provide further binding sites for Crumbs. However, this conformation folds the GK domain far away from the SH3 domain and deprives the SH3 domain of the βE and βF sheets necessary for its formation, thus threatening the stability of the SH3 domain while exposing the previously intracellular SH3:GK interface to the cytoplasm. PALS1 solves this stability issue by forming a domain-swapped homodimer: rather than using its own GK domain to stabilize its SH3 domain, a folded-over PALS1 monomer will bind to a second PALS1 monomer in a similar folded conformation. The first PALS1 stabilizes its SH3 domain by binding to the exposed GK domain of the second monomer while simultaneously "donating" its GK domain to the exposed SH3 domain of the second PALS1 monomer (Fig 1.3B). Thus, PALS1 can only bind to Crumbs in a conformation that requires PALS1 to dimerize in order to be stable.

Li et al. demonstrated this functionally by showing that the binding affinity of the PDZ domain of PALS1 alone for Crumbs is 2 orders of magnitude weaker than the binding affinity of the PALS1-PSG (K_D values of 6.0μM vs 0.07μM). Interestingly, they also show a similar behaviour with the CASK-PDZ domain compared to the CASK-PSG supramodule when binding the C-terminus of Neurexin (undetectable binding vs K_D of 0.7μM). This therefore suggests that CASK also requires its entire PSG to bind to its PDZ-ligand. Given the sequence similarity between the PSG supramodule of CASK and PALS1, it strongly suggests that CASK likely also dimerizes or oligomerizes upon binding to its PDZ-ligand Neurexin.

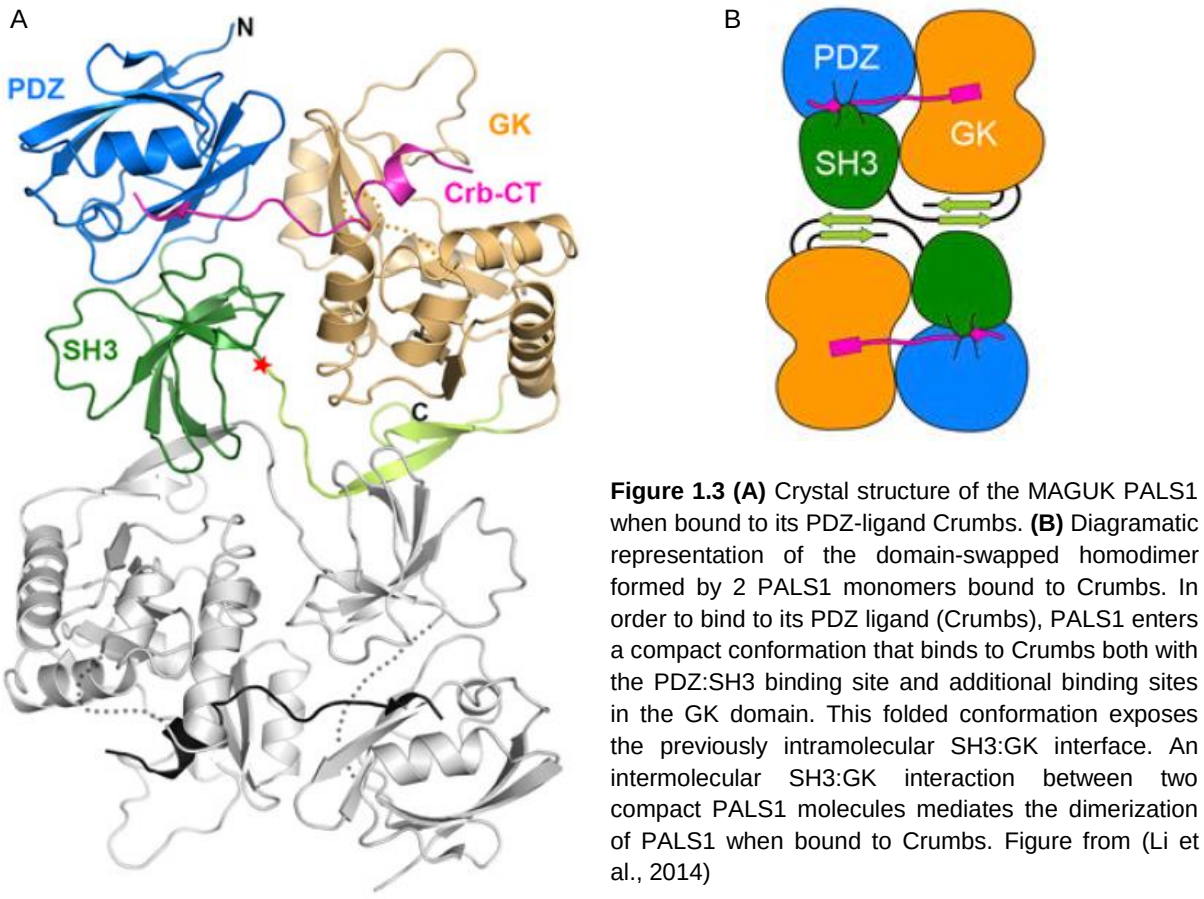

Figure 1.3 (A) Crystal structure of the MAGUK PALS1 when bound to its PDZ-ligand Crumbs. **(B)** Diagramatic representation of the domain-swapped homodimer formed by 2 PALS1 monomers bound to Crumbs. In order to bind to its PDZ ligand (Crumbs), PALS1 enters a compact conformation that binds to Crumbs both with the PDZ:SH3 binding site and additional binding sites in the GK domain. This folded conformation exposes the previously intramolecular SH3:GK interface. An intermolecular SH3:GK interaction between two compact PALS1 molecules mediates the dimerization of PALS1 when bound to Crumbs. Figure from (Li et al., 2014)

1.2.3 CASK couples synaptic adhesion to vesicle release

As an interaction partner of Neurexin (Hata et al., 1996), CASK is in an excellent position to anchor protein complexes to the presynaptic adhesion site. CASK is associated with two complexes involved in synaptic vesicle release: the evolutionarily conserved CASK:Mint1:Velis complex (Butz et al., 1998) and the core components of the presynaptic active zone (Sudhof, 2012).

CASK binds to Neurexin via its PDZ domain (Hata et al., 1996), to Velis via its L27.2 domain (Butz et al., 1998) and to Mint1 via its CaMK domain (Borg et al., 1998). The CASK:Velis:Mint1 likely mediates vesicle fusion through the interaction of Mint1 with Munc18 (Okamoto & Südhof, 1997). Munc18 is a protein that forms a complex with the SNARE proteins and both Munc18 and SNARE proteins are critical for the fusion of synaptic vesicles upon Ca^{2+} influx (Rizo & Südhof, 2002). The CASK:Velis:Mint1 complex likely also fulfills other presynaptic scaffolding roles, though these have not yet been formally demonstrated in mammals. But in *C. elegans*, the LIN2:LIN7:LIN10 homolog to this complex is necessary for the correction localization of the receptor LET-23 to the basolateral membrane of vulvar epithelial cells and therefore for vulvar development. The LET-23 receptor binds to the LIN7, the *C. elegans* homolog of Velis, as a PDZ-ligand (Kaech, Whitfield, & Kim, 1998; Simske, Kaech, Harp, & Kim, 1996). It is therefore likely that in the presynapse, the CASK:Velis:Mint1 complex also recruits and anchors presynaptic proteins to the active zone.

CASK may also play a role in anchoring the core components of the presynaptic active zone to the presynapse. Although multiple proteins are involved in docking of synaptic vesicles to the presynapse and in mediating their fusion to the presynaptic membrane upon Ca^{2+} influx, 5 have emerged as being of particular importance and constitute the "core components" of the active zone: RIM, RIM-BP, Munc13, ELKS, and α-Liprins (Sudhof, 2012). RIM is the central organizer among these 5 proteins, binding to all 4 others. CASK interacts with α-Liprins via its CaMK and L27.1 domains (Olsen et al., 2005; Wei et al., 2011) and therefore likely helps attach it to presynaptic adhesion sites. However, α-Liprins are able to bind to LAR-type receptor phosphotyrosine phosphatases (LAR-RPTPs), a class of synaptic adhesion proteins (C. Serra-Pagès et al., 1995; Carles Serra-Pagès, Medley, Tang, Hart, & Streuli, 1998), suggesting that α-Liprins may be sufficient for the anchoring of the active zone to presynaptic adhesion sites. Indeed, a study by Spangler et al. (2013) has shown that Liprin-α2 regulates the levels of both RIM and CASK and levels of both proteins and several of their interaction partners decreases when Liprin-α2 levels are knocked down.

It is therefore possible that anchoring the active zone core components to adhesion sites is a secondary function of CASK and that its main function is the recruitment of proteins involved in vesicle fusion whose function are complementary to the proteins recruited by the active zone core components. One example of this can be observed by how Munc13, recruited by RIM (Betz, Okamoto, Benseler, & Brose, 1997) and Munc18, recruited by the CASK:Velis:Mint1 complex (Okamoto & Südhof, 1997), coordinate to process Syntaxin, a SNARE protein necessary for vesicle fusion. SNARE proteins are a set of proteins present on both presynaptic vesicle and the presynaptic membrane which bind together to mediate vesicle fusion upon Ca^{2+} influx (Schiavo, Stenbeck, Rothman, & Söllner, 1997; Ungar & Hughson, 2003). After vesicle fusion, Syntaxin is present in closed conformation that cannot bind to other SNARE proteins and therefore cannot mediate vesicle fusion, but can bind to Munc18 (Dulubova et al., 1999). A study in *C. elegans* suggests that Unc13, the *C. elegans* homolog of Munc13, binds to Syntaxin and converts into an open conformation that cannot bind to Unc18, but can prime vesicle fusion (Richmond, Weimer, & Jorgensen, 2001). CASK and its complex may therefore have a role in retaining proteins necessary for vesicle fusion in the vicinity of the active zone core components until these can be re-integrated into the active zone.

The hypothesis that the active zone core components and the CASK:Velis:Mint1 complex may collaborate to recruit complementary proteins is further supported a study from L. E. LaConte et al. (2016). Both Mint1 (Butz et al., 1998) and α-Liprins (Olsen et al., 2005) bind to the CaMK domain of CASK. L. E. LaConte et al. (2016) show that Mint1 outcompetes Liprin-α3 for the CASK-CaMK, which fits well with previous results which showed that Mint1 also outcompetes Caskin, another presynaptic partner of CASK (Stafford, Ear, Knight, & Bowie, 2011; Tabuchi, Biederer, Butz, & Südhof, 2002). A priori, Mint1 out competing α-Liprins should preclude the possibility that the CASK can bind to the active zone core components via α-Liprins when it is also

bound to Mint1 and Velis. However, L. E. LaConte et al. (2016) show when CASK binds to Neurexin, the CASK:Neurexin interface forms a new binding site at the CASK-PDZ domain to which α-Liprins can bind, but Mint1 cannot. This mode of interaction is both distinctive and specific to CASK, suggesting that CASK plays a distinctive role in connecting the CASK:Velis:Mint1 complex to the active zone core components via α-Liprins.

1.2.4 CASK may mediate the formation of nanocolumns

Extensive mass spectrometry and electron microscopy studies have elucidated the identity, abundance, and spatial organization of the proteins of the postsynaptic density (PSD) of excitatory synapses. Electron microscopy studies have shown that the PSD exhibits a very fine laminar organization. Beneath the postsynaptic membrane and the receptors, the MAGUK protein PSD-95 forms the first scaffolding layer 10-20nm beneath the surface, oriented in vertical pillar with their PDZ-domains toward the postsynaptic membrane and their GK domains toward the cytoplasm (Chen et al., 2008). PSD-95 is one of the main scaffolding proteins of the PSD, binding to NMDARs (Kornau, Schenker, Kennedy, & Seeburg, 1995) and anchoring them to the postsynaptic adhesion protein Neuroligin (Irie et al., 1997). Deeper, the scaffolding proteins SAPAP and SHANK form a layer 24-26 nm beneath the postsynaptic membrane. Deeper still at 29-32nm beneath the membrane, proteins such as CRIPT and dynein light chain may act as a link between the PSD and the cytoskeleton (Valtschanoff & Weinberg, 2001).

The PSD also exhibits lateral organization. While NMDARs are generally localized towards the centre of the PSD, most AMPARs are localized on the periphery of the PSD (Kharazia & Weinberg, 1997; Racca, Stephenson, Streit, Roberts, & Somogyi, 2000). Certain scaffolding proteins, such as PSD-95 and PSD-93 seem well distributed throughout the PSD, while others like Sap97 are primarily located to the periphery of the PSD (DeGiorgis, Galbraith, Dosemeci, Chen, & Reese, 2006). The simultaneous localization of both AMPARs and Sap97 to the periphery of the PSD is interesting because Sap97 is the only known MAGUK to bind to AMPARs (Leonard, Davare, Horne, Garner, & Hell, 1998; Zheng et al., 2011). By contrast, PSD-95 requires adaptor proteins like Stargazin to bind to AMPARs (Schnell et al., 2002). Sap97 is also known to traffic AMPARs (and NMDARs) and their localization at the periphery of the PSD also fits well within the model whereby NMDARs are more durably inserted into the postsynaptic membrane while AMPARs are inserted and removed via exo- and endocytosis in response to long term potentiation (LTP) and long term depression (LTD) (Cognet, Groc, Lounis, & Choquet, 2006; Ehlers, 2000; Lu et al., 2001).

Nanodomains were discovered in more recent investigations of the lateral organization of the PSD that used newer superresolution nanoscopy techniques like STORM and PALM. These allow for optical imaging at resolution of down to 30-50nm, almost 10 times finer than was possible using conventional confocal microscopy (Maglione & Sigrist, 2013; Sigrist & Sabatini, 2012). A study by Nair et al. (2013) showed that within the PSD, AMPARs are not distributed homogenously, but instead form small clusters of about 20 AMPARs about 80nm across called nanodomains. They also showed that PSD-95 also forms such nanodomains, usually associated with AMPARs. Another study by MacGillavry, Song, Raghavachari, and Blanpied (2013) showed that the AMPAR nanodomains are not only associated with PSD-95, but also with deeper scaffolding proteins including Shank3 and Homer.

The concept of nano*columns* arose when a study by Tang et al. (2016) showed that the nanodomains of the PSD are aligned with vesicle release sites in the presynapse, forming functional “columns” that extend across the synaptic cleft. Their results showed that the presynaptic active zone protein RIM also forms nanodomains approximately 60nm wide and that these are aligned with nanodomains of AMPAR and PSD-95 in the postsynapse. However, the mechanism by which the presynaptic and postsynaptic nanodomains are aligned remains unknown. One study by Trotter et al. (2019) showed that Neurexin in the presynapse also forms nanodomains within excitatory synapses.

One hypothesis would thus be that nanocolumns are aligned by transsynaptic pairs of cell adhesion molecules, such as Neurexin and Neuroligin. Indeed, the postsynaptic PSD-95 containing nanodomains (MacGillavry et al., 2013; Nair et al., 2013) could be linked to presynaptic Neurexin via Neuroligin (Ichtchenko et al., 1995; Irie et al., 1997). However, Trotter et al. (2019) themselves point to several differences between the nanoclusters of Neurexin and the nanocolumns observed in previous studies to suggest that Neurexin may not necessarily be the

transynaptic mechanisms that underlies nanocolumns. They point to the fact that previous studies have shown approximately 2-3 nanocolumns per synapse while their studies show one nanocluster of Neurexin per synapse. Furthermore, they argue that nanodomains tend to form near the centre of synapses while their Neurexin nanoclusters usually form in the centre but eventually migrate towards the periphery over development.

A review by Biederer, Kaeser, and Blanpied (2017) also proposes that mechanisms other than transsynaptic adhesion proteins could mediate the alignment of nanocolumns. They also propose that postsynaptic adhesion proteins could bind directly to presynaptic calcium channels, thus aligning the sites of calcium influx to postsynaptic receptors. Another possibility is that diffusible signals could be secreted by the pre and postsynaptic sides to align pre and postsynaptic nanodomains.

Thus, it remains unclear which mechanism or combination of mechanisms underlies the alignment of nanocolumns. At the moment, however, the clustering Neurexin in the presynapse (Trotter et al., 2019) provides preliminary evidence for the transsynaptic adhesion model. That being said, it is also possible that Neurexin may not necessarily bind to postsynaptic Neuroligin. A study by Chamma et al. (2016) showed that the postsynaptic LRRTM2, which also binds to Neurexin, may be another candidate protein for the alignment of nanocolumns as it also can be found in clusters in the PSD and is more highly enriched within the PSD compared to Neuroligin. If Neurexin is the presynaptic adhesion protein mediating nanocolumn alignment, then CASK becomes a very likely component of the nanocolumns.

1.3 CASK regulates Gene Transcription with Tbr1 and CINAP

A distinctive ability of CASK among MAGUKs is its ability to act as a transcription regulator. In a complex with Tbr1 and CINAP, CASK can regulate the expression of genes with T-element promoters such as *GRIN2B* and *Reelin* (Y.-P. Hsueh et al., 2000; G.-S. Wang et al., 2004). Tbr1 (T-brain-1) is a transcription factor primarily expressed in the cerebral cortex. The structure of Tbr1 defines it as a T-box transcription factor (Bulfone et al., 1995). T-box transcription factors bind promoters which include a near-palindromic sequence called the T-box binding element (TBE). T-box transcription factors are involved in a wide variety of development processes, including cell fate specification and organ formation (Papaioannou, 2014). Befitting its cortical expression pattern, Tbr1 is involved in mammalian brain development. Mice deficient in Tbr1 exhibit a deficiency of brain laminar formation similar to *reeler* mice (Hevner et al., 2001). *reeler* mice are a line of mouse deficient in Reelin, a protein that promotes the axial migration of neurons during the development of cortical layers (D'Arcangelo & Curran, 1998).

Y.-P. Hsueh et al. (2000) showed that Tbr1 binds to the promoter of *Reelin* and that its transcription activity could be greatly amplified by the binding of CASK. They found that overexpressed Tbr1 on its own was capable of doubling transcriptional activity while CASK on its own had no effect. However, a combination of overexpressed Tbr1 and CASK increased transcriptional activity by a factor of 10 in cultured cells and a factor of 16 in primary neurons. CASK has no DNA binding domain of its own and these results confirm that CASK's function is to amplify the function of Tbr1. Hsueh et al. showed that the GK domain of CASK was required, but also sufficient for the ability of CASK to amplify Tbr1's transcription activity. However, the mechanism underlying this ability is uncertain.

A follow up study by G.-S. Wang et al. (2004) suggests that CASK may influence the transcription activity of Tbr1 by recruiting other co-factors. They identify one such co-factor: CINAP (CASK-Interacting Nucleosome Assembly Protein). Nucleosome assembly proteins are a family of proteins that regulates the assembly or disassembly of histones in nucleosomes, which in turns decreases or increases the accessibility to the DNA segments on those nucleosomes (Attia, Rachez, Avner, & Rogner, 2013; Walter, Owen-Hughes, Côté, & Workman, 1995). G.-S. Wang et al. (2004) showed that the CASK:Tbr1 complex could regulate the transcription of the *GRIN2B* gene, which encodes the NR2b subunit of the NMDAR. Their results show that CINAP could bind to the CASK:Tbr1 complex, and that in primary neurons, the CINAP:CASK:Tbr1 complex induces a higher *GRIN2B* transcription rate than the CASK:Tbr1 complex. However, they also show that in Neuro-A2 neuroblastoma cells, the CINAP:CASK:Tbr1 complex induces a lower *GRIN2B* transcription rate

than the CASK:Tbr1 complex, which suggests that other co-factors must be present to determine how CINAP regulates the CASK:Tbr1 complex.

G.-S. Wang et al. (2004) also show an intriguing negative feedback effect of the activity of NMDARs on the ability of the CINAP:CASK:Tbr1 complex to transcribe the *GRIN2B* gene. They report that activation of NMDARs induces the degradation of CINAP, which in turn decreases the transcription rate of the *GRIN2B* gene. During early postnatal development, NMDARs primarily incorporate the NR2b subunit and only later switch to NR2a (Liu, Murray, & Jones, 2004; Petralia, Sans, Wang, & Wenthold, 2005). This therefore suggests that NMDARs can downregulate their own expression during early development by decreasing the amount of CINAP present, which in turn downregulates the ability of the CASK:Tbr1 complex to transcribe the *GRIN2B* gene.

1.4 CASK sorts postsynaptic receptors with Sap97

In addition to regulating the expression of the NR2b subunit of the NMDAR as discussed above, CASK is also involved in the sorting and trafficking of NMDARs and AMPARs.

A study by Jo, Derin, Li, and Bredt (1999) showed that the previously discussed Velis protein is present in the postsynapse and binds to both NMDARs and PSD-95. Another study by Setou, Nakagawa, Seog, and Hirokawa (2000) shows that the motor protein KIF17 is able to bind to Mint1. They also show that NR2b, CASK, and Velis are part of the cargo transported by KIF17. They therefore propose that the CASK:Velis:Mint1 complex acts as an adaptor that tethers NR2b containing vesicles to KIF17 and mediates their transport.

CASK is also involved in the sorting of NMDARs away from AMPARs via an interaction with the MAGUK Sap97. Sap97 is known to bind to both NMDARs (Bassand, Bernard, Rafiki, Gayet, & Khrestchatisky, 1999) and AMPARs (Leonard et al., 1998; Sans et al., 2001). Although NMDAR and AMPARs travel to the postsynapse via distinct vesicles, (Malinow & Malenka, 2002; Rao, Kim, Sheng, & Craig, 1998), Sap97 has been shown to colocalize both with vesicles containing NMDARs (Jeyifous et al., 2009) and AMPARs (Sans et al., 2001).

A study by Jeyifous et al. (2009) shows that the sequestration of NMDARs from AMPARs occurs early in the secretory pathway. AMPARs traffic through the "classic" exocytosis pathway, trafficking from the endoplasmic reticulum (ER) to the somatic Golgi apparatus, before being sorted into transport vesicles that travel down the length of dendrites to the postsynapses (Greger & Esteban, 2007) in vesicles that, as said earlier, also contain Sap97 (Sans et al., 2001). Using Golgi and ER markers, Jeyifous et al. (2009) show that NMDARs bypass the somatic Golgi apparatus entirely and instead travel in ER-like vesicles for processing in Golgi outposts in the dendrites. These vesicles are enriched in NMDAR, Sap97, and CASK, suggesting that CASK is necessary for the sequestration of NMDARs away from AMPARs while the receptors are being processed in the endoplasmic reticulum. Furthermore, knock down of CASK in primary neurons decreased the amount of NMDARs in the postsynapse by 46%. These results strongly suggest that CASK is necessary for the trafficking of NMDARs to the postsynapse. However, CASK is not known to bind to NMDARs or AMPARs, and so they authors could not provide a mechanism by which CASK may mediate the sorting of the two receptor types away from each other.

A follow up study by Lin et al. (2013) shows that CASK can cause a conformational change in Sap97 that changes its binding preference for NMDARs or AMPARs. The notion that Sap97 may bind differentially to its interaction partners was first proposed by H. Wu et al. (2000), who showed that an intramolecular between the SH3 and GK domain can affect the binding of Sap97 to another interaction partner, GKAP. They generated models of Sap97 and proposed that this interaction may change the conformation of Sap97 from an extended conformation to a compact one where the N-terminus interacts with the C-terminus, and thus masks several binding sites. Later, Nakagawa et al. (2004) used electron microscopy to confirm that Sap97 exists both in an extended and a compact conformation.

Lin et al. (2013) used FRET assays to show that CASK can induce a change in the conformation of Sap97 and that the two conformations have difference preferences for NMDARs and AMPARs. Their results show that on its own, Sap97 is in a compact conformation that preferentially binds to AMPARs. However, when CASK binds

Sap97, it enters an extended conformation that preferentially binds to NMDARS. These results provide a mechanism that explains how the binding of CASK to Sap97 is necessary for Sap97's ability to bind to NMDARs and thus sort them away from AMPARs in the secretory pathway.

It is not yet clear whether or not the CASK:Velis:Mint1 mechanism and CASK:Sap97 mechanism of NMDAR trafficking are entirely separate or whether the two are in fact combined. From a protein interaction perspective, the two mechanisms are not inherently incompatible. Sap97 binds to the L27.1 domain of CASK (Feng, Long, Fan, Suetake, & Zhang, 2004; Lee, Fan, Makarova, Straight, & Margolis, 2002) while Velis binds to the L27.2 domain of CASK (Butz et al., 1998); thus the two proteins should not compete for binding to CASK unless steric hindrance becomes an issue. Both Velis (Jo et al., 1999) and Sap97 (Bassand et al., 1999) bind to NMDARs using their PDZ ligands and in both cases, with a preference for the NR2b subunit. However, given that NMDARs are a tetrameric complex, typically with 2 NR1 subunits and 2 NR2 subunits (Regan, Romero-Hernandez, & Furukawa, 2015), it remains possible that both Velis and Sap97 could bind to a NR2 subunit in a NMDAR. It would therefore be possible that CASK is linked via 2 partners to NMDARs while its interaction with Mint1 and KIF17 mediate the trafficking of the NMDAR-containing vesicles to the postsynapse.

1.5 *CASK* KO mouse models differ strongly from *CASK* KO patients

While CASK has many known molecular functions, its physiological functions remain unclear. A *Cask* knock-out mouse line was established by Atasoy et al. (2007) to study the physiological functions of CASK. However, these mice share very few phenotypes with patients with *CASK* loss-of-function mutations.

As mentioned earlier, the *CASK* gene is located on the X-chromosome (Dimitratos et al., 1998), meaning that female patients can be heterozygous for loss of function mutations while males can only be hemizygous. In both cases, these patients exhibit a severe but recognizable set of symptoms called Microcephaly with Pontine and Cerebellar Hypoplasia with Intellectual disability (MICPCH + ID). Male hemizygous patients additional exhibit severe epileptic seizures (Hackett et al., 2009; Moog et al., 2015; Najm et al., 2008; Takanashi et al., 2012).

By contrast, the *Cask* KO mice exhibit none of these phenotypes (Atasoy et al., 2007). Although these mice are non-viable, dying within hours of birth, they are also anatomically very normal, with the only notable anatomical phenotype being a cleft palate present in 80% of mice. These mice exhibit respiratory difficulties, which likely explain the post-natal lethality. However, these mice do not have brain morphology disruptions such as microcephaly as observed in human patients. This calls into question the relevance of these mice as a model for the physiological study of CASK, as it suggests CASK's functions may be compensated by other proteins in mice or that CASK may play different functions that have less impact on brain development.

That said, these mice may still be a useful source of primary neurons for study and can still be used for molecular and neuronal-level study of loss of CASK. A recent study by Mori et al. (2019) generated female heterozygous *Cask* mice. These *Cask* +/- mice were more viable than the male *Cask* Y/- mice with a 75% survival rate at 15 days post birth and weighed less than WT mice. Like the *Cask* Y/- mice, the *Cask* +/- mice were anatomically quite normal, with no observable microcephaly or anatomical disruption.

However, they found that the *Cask* +/- animals had an increased excitatory/inhibitory ratio of synapses in the brain as measured by electrophysiological recordings, followed by single cell genotyping. The authors could take advantage of mosaic status of cells, recording from CASK-expressing and CASK-deficient cells in the same animal, depending on X-chromosome inactivation. They show that postsynaptic neurons lacking CASK also express less NR2b and thus have fewer NMDARs in the postsynapse, which causes the presynaptic neurons to form more excitatory synapses on these neurons. While they do not provide a mechanism for this, they do show that the overexpression of NR2b can rescue the phenotype, supporting their hypothesis.

If a similar phenomenon occurs in human patients, it may explain why male patients exhibit epileptic seizures. Female heterozygous patients will also contain a functional mosaic of cells (Hao Wu et al., 2014) and thus may experience a smaller increase in the excitatory/inhibitory ratio of synapses compared to male patients, where all neurons lack CASK and thus all neurons would exhibit a higher excitatory/inhibitory synapse ratio.

1.6 *CASK* missense mutations identified in patients

The MICPCH + ID phenotype observed in male hemizygous and female heterozygous patients is most likely linked to the function of the CASK:Tbr1:CINAP complex in upregulating the expression of genes like *Reelin* (Y.-P. Hsueh et al., 2000; G.-S. Wang et al., 2004), which is known to be important in brain development (Chang et al., 2007; D'Arcangelo & Curran, 1998; Hong et al., 2000). However, given that these are loss of function mutations, all of CASK's molecular functions are necessarily lost in these patients and it therefore becomes impossible to determine how each of the molecular functions contributes to the symptoms observed in the patients.

However, some male patients have been diagnosed with *CASK* missense mutations, which cause single amino acid substitutions within the CASK protein. Some of these patients are just as strongly affected the patients with loss of function mutations. However, some exhibit only a subset or milder forms of the microcephaly, intellectual deficiency, and seizure symptoms observed in patients with *CASK* loss-of-function mutations.

Mutation	Intellectual Deficiency	Brain Malformations	Epilepsy
R140G	Developmental Delay	Microcephaly	ND
G161R	Severe	"No formal"	Severe
Y268H (1)	Severe	ND	Yes
Y268H (2)	Severe	ND	Yes
Y268H (3)	Severe	ND	No
L354P	Severe	MICPCH	Severe
P396S (1)	Severe	Yes, non-MICPCH	No
P396S (2)	Severe	Yes, non-MICPCH	No
P396S (3)	Severe	Yes, non-MICPCH	No
R489W	Severe	Yes, non-MICPCH	Yes
M507I	Developmental Delay	Microcephaly	Yes
G521V	Intellectual Deficiency	Microcephaly	<2 years old
Y723C (1)	Mild	MICPCH	ND
Y723C (2)	Mild ID	Microcephaly	ND
N798Y	Not Appropriate (Foetal diagnosis)	Non-microcephaly disruptions	N/A
V849A	Developmental Delay	Non-microcephaly disruptions	Yes
W914R (1)	Mild	Normal	ND
W914R (2)	Mild	Normal	ND
W914R (3)	Mid	Normal	ND

Table 1.1: Summary of symptoms of male patients with CASK missense mutations. **ID**: Intellectual deficiency **MICPCH**: Microcephaly with pontine and cerebellar hypoplasia, **N/A**: Not applicable, **ND**: not determined. Italic mutations are previously unpublished mutations reported by collaborators.

The fact that these missense mutations can cause a subset of the symptoms gives rise to the possibility that these mutations may also only affect a subset of CASK's molecular functions and are thus "milder" mutations. This notion is supported by the fact that the mothers of these patients can be asymptomatic (Hackett et al., 2009; Moog et al., 2015; Takanashi et al., 2012), though it should be noted that some of these mutations also affect females. Nevertheless, this gives rise to the possibility of using these missense mutations to study the various functions of CASK. One exciting possibility is to be able to correlate specific molecular functions of CASK to specific patient symptoms.

1.7 Project Rationale

The MAGUK CASK is involved in multiple molecular functions in neurons, acting as a presynaptic scaffolding protein, a gene transcription regulator, and a sorter and trafficker of postsynaptic receptors. Despite many years of work, however, the physiological functions of CASK remain unclear.

Part of the reason is the failure of "classical" approaches used in the study of patients. Patients with *CASK* loss of function mutations exhibit symptoms so severe that they cannot be reasonably tracked to any single CASK function. Furthermore, generated *Cask* KO mice are not viable and can therefore also not be used in the elucidation of CASK's physiological functions.

However, the diagnosis of patients with *CASK* missense mutations who exhibit milder forms of or a subset of the symptoms exhibited by the patients with *CASK* loss-of-function mutations provides a unique opportunity to dissect the various functions of CASK.

CASK fulfills its multiple functions by binding to various interaction partners. It is reasonable to expect that the replacement of single amino acids in the CASK protein may disrupt the ability of CASK to bind to specific interaction partners, which in turn may selectively affect the CASK function associated with that partner. The various mutations are distributed throughout the length of the *CASK* gene and cause amino acid substitution in almost every domain of CASK. This suggests that multiple binding partners are affected, which in turn suggests that multiple molecular functions may be disrupted by the mutations.

In this study, I study a set of 12 missense mutations. Five of these were previously published; seven have been reported to us by collaborators during the project. All were identified in male patients. I first tested how these mutations affect the ability of CASK to bind to a subset of its interaction partners. Once I found which interaction partner was affected by which mutation, I performed a functional assay to determine whether the CASK function associated with that specific partner was affected by a specific mutation.

My goals for this project were (1) to determine whether or not each mutation is pathogenic, (2) to determine the molecular pathogenic mechanism underlying each mutation, (3) to determine whether each missense mutation acts through a unique pathogenic mechanism or whether multiple mutations may share mechanisms, and (4) to determine whether certain pathogenic mechanisms could be correlated with the symptoms observed in patients.

2. Materials and Methods

2.1 Materials

2.1.1 Chemicals

Chemical were purchased from Merck, Sigma, or Carl Roth unless otherwise indicated.

2.1.2 Plasmids & Primers

2.1.2.1 Backbones plasmids

Plasmid	Description
pDONR223-CASK	Addgene #23470
pcDNA-DEST53	Invitrogen #12288015
pmRFP-C1	AG Stefan Kindler
FUW vector	Addgene #14882

2.1.2.2 CASK Plasmids

Plasmid name	Promoter	Transcript Variant	Backbone	Resistance	Backbone Source
CMV_GFP-CASK	CMV	TV3	pDEST53	Ampicillin	Invitrogen #12288015
CMV_RFP-CASK	CMV	TV1, TV2, TV3, TV5, TV6, TV7, TV8	pmRFP-C1	Kanamycin	AG Kindler
FUW_RFP-CASK	UbC	TV3	FUW	Ampicillin	AG Kreienkamp
hSynHH_RFP-CASK	hSyn	TV3, TV5	hSynHH	Ampicillin	AG Kreienkamp
CMV_CASK-YFP1	CMV	TV5	pcDNA3-cYFP1	Ampicillin	AG Braulke
CMV_CASK-YFP2	CMV	TV5	pcDNA3-cYFP2	Ampicillin	AG Braulke

2.1.2.3 CASK mutagenic and subcloning primers

Mutagenic Primer	Primer Sequence
R140G For	GATAATAACATAATTCACGGGGATGTGAAGCCCCACTGTG
R140G Rev	CACAGTGGGGCTTCACATCCCCGTGAATTATGTTATTATC
G161R For	CGGCACCTGTTAAACTTAGAGGCTTTGGGGTAGCTATTC
G161R Rev	GAATAGCTACCCCAAAGCCTCTAAGTTTAACAGGTGCCG
Y268H For	GCTGAAAGGATCACTGTTCATGAAGCACTGAATCACC
Y268H Rev	GGTGATTCAGTGCTTCATGAACAGTGATCCTTTCAGC
L354P For	GGTGCTGGACAGCCCGGAAGAGATTCATG
L354P Rev	CATGAATCTCTTCCGGGCTGTCCAGCACC
P396S For	CAAAATTAACACAAAGTCTTCATCACAAATCAGGAATCCTCCAAG
P396S Rev	CTTGGAGGATTCCTGATTTGTGATGAAGACTTTGTGTTAATTTTG
R489W For	TGGAGAATGTGACCAGAGTTTGGCTGGTACAGTTTCAAAAG
R489W Rev	CTTTTGAAACTGTACCAGCCAAACTCTGGTCACATTCTCCA
M507I For	GAACCAATGGGAATCACTTTAAAAATCAATGAACTAAATCATTGTATTGTTGC
M507I Rev	GCAACAATACAATGATTTAGTTCATTGATTTTTAAAGTGATTCCCATTGGTTC
G521V For	GTTGCAAGAATTATGCATGTGGGCATGATTCACAGGCAAGG
G521V Rev	CCTTGCCTGTGAATCATGCCCACATGCATAATTCTTGCAAC
Y723C For 23L+	TGATCAATTAGATCTTGTCACATGTGAAGAAGTAGTAAAACTGCCAG
Y723C Rev 23L+	CTGGCAGTTTTACTACTTCTTCACATGTGACAAGATCTAATTGATCA
Y723C For 23L-	CAATGCAGATCTTGTCACATGTGAAGAAGTAGTAAAACTGC
Y723C Rev 23L-	GCAGTTTTACTACTTCTTCACATGTGACAAGATCTGCATTG
N798Y For	GATGCAAGACATCTCTAATTACGAGTACTTGGAGTACGG
N798Y Rev	CCGTACTCCAAGTACTCGTAATTAGAGATGTCTTGCATC
V849A For	GAGTTTGCTCCTTTTGCTGTTTTCATTGCTGCACC
V849A Rev	GGTGCAGCAATGAAAACAGCAAAAGGAGCAAACTC
W914R For	CAGCCCCACAGCGGGTCCCTGTC
W914R Rev	GACAGGGACCCGCTGTGGGGCTG
hCASK_TV1_for	GTTTATGAAGCACTGAATCACCC
hCASK_TV1_rev	TTCTCCCAACACCATGTGCGCC

Primers were purchased from Sigma Aldrich as oligonucleotides.
Y723C primers overlap exon 23L. 2 versions were made for transcript variants with or without exon 23L

2.1.2.4 Partner plasmids

Partner	Resistance	Source
HA-Liprin-a2	Ampicillin	Hoogenraad Lab
Myc-Sap97	Kanamycin	AG Kreienkamp
HA-Neurexin-1b	Ampicillin	Addgene #58267
Myc-Tbr1	Ampicillin	Hsueh Lab
HA-CINAP	Ampicillin	Hsueh Lab

2.1.2.5 Other plasmids (lentivirus production & dual luciferase)

Plasmid	Source
psPAX.2	Addgene#: 12260
pMD2.G	Addgene#: 12259
NR2B-P. in pGL3-enhancer	AG Kutsche
Reelin-P. in pGL3-enhancer	AG Kutsche
pREN in pGL3-enhancer	AG Kutsche

2.1.3 Molecular Biology Materials

2.1.3.1 Reagents and Kits

Reagent	Manufacturer	Product #
Gateway® Technology	Invitrogen	12535-29 and 12535-027
Restriction enzymes (various)	Thermo Scientific	Various
10X FastDigest Green buffer	Thermo Scientific	B72
Midori Green Direct	NIPPON Genetics EUROPE	MG06
GeneRuler 1kb Plus DNA Ladder	Thermo Scientific	SM1333
T4 DNA Ligase enzyme	Thermo Scientific	EL0011
10X T4 Ligase Buffer	Thermo Scientific	B69
HiDi Formamide	Applied Biosystems	4311320

Kits	Manufacturer	Product #
GeneJet Gel Extraction Kit	Thermo Scientific	K0692
NucleoBond ® Xtra Midi kit	Macherey-Nagel	740410.100
BigDye Terminator v.1.1 Cycle Sequencing Kit (Sequencing Buffer & BigDye solution)	Applied Biosystems	4337452
QuikChange II XL Kit	Agilent	200522

2.1.3.2 Restriction Digest Enzymes & Buffers

Restriction digest enzymes were purchased from Thermo Fisher and were used in combination with 10X FastDigest Green buffer (Thermo Scientific: B72) to digest plasmids.

2.1.3.3 Agarose Gels

1% Agarose solutions

- 5g Agarose
- 500mL 1X TAE buffer (pH 8.0)

50X TAE buffer (pH 8.0) Stock

- 242g Tris-acetate
- 57.1mL glacial acetic acid
- 100mL 0.5M pH8.0 EDTA
- Top up to 1000mL with ddH_2O
- Or order from ROTH (Article # T845.2)

2.1.3.4 Bacterial transformation solutions

5X KCM buffer

- 500mM KCl
- 150mM $CaCl_2$
- 250mM $MgCl_2$
- Autoclave

LB Culture Medium (5L)

- 50g Bacto Tryptone
- 25g Yeast Extract
- 50g NaCl
- 4.5L veH2O
- Mix with large stirbar until dissolved
- Adjust pH of solution to 7.5
- Top up to 5L with veH2O
- Pour 500mL into bottles with 7.5g Agar (for LB-Agar) or empty bottles (for LB medium)
- Autoclave
- Add 500µL of stock antibiotic (if necessary) and let stir
    - Ampicillin: 100mg/mL stock (100µg/mL final)
    - Kanamycin: 35mg/mL stock (35µg/mL final)

2.1.4 Cell Biology Materials

2.1.4.1 HEK239T Culture and transfection Solutions

Solution	Manufacturer	Product #
DMEM Culture Solution	Gibco	41966.29
Fœtal Bovine Serum	Sigma Life Science	F7524 Lot: BCBV6321
Penicillin/Streptomycin Mix	Gibco	15140-122
10X Trypsin (2.5%)	Gibco	15090-046
Turbofect	Fisher Scientific	R0531

HEK293T culture medium (500mL)

- 450mL DMEM Culture Solution
    - 50mL of 500mL transferred into 50mL Falcon Tube for use as HEK293T Transfection Solution
- 50mL FBS
- 5mL Penicillin/Streptomycin Mix

HEK293T Transfection Solution

- DMEM Culture Solution without any additional solutions.

Versene Solution (5L)

- 1g EDTA
- 40g NaCl
- 1g KCl
- 4.66g anhydrous Na2HPO4, or 5.86g Na2HPO4●2H2O, or 8.8g Na2HPO4●7H2O
- 0.9g KH_2PO_4
- Top up to 5L ddH_2O
- Make 500mL bottles
- Autoclave

Trypsin-EDTA Solution

- 45mL Versene Solution
- 5mL 10X Trypsin

2.1.4.2 Lentiviral particle production

Product	Manufacturer	Product #
Lenti-X GoStix	Takara Bio Europe	631243
Lenti-X Concentrator Solution	Takara Bio Europe	631232

Phosphate Buffered Saline (PBS) Solution (5L)

- 1g KCl
- 1.2g KH_2PO_4
- 40g NaCl
- 8.85g Na2HPO4●2H2O or 13.4g Na2HPO4●7H2O
- 4.5L ddH_2O
- Adjust pH to 7.4
- Top up to 5L
- Split into 500mL bottles and autoclave

Lentivirus Production DMEM

- DMEM Culture Solution without any additional solutions (See 2.1.4.1 for Product Number)

2.1.4.3 Neuron Culture: Animals and Solutions

Animal	Source
Rattus norvegicus	Envigo

Solution	Manufacturer	Product #
HBSS	Gibco	24020-91
10X Trypsin (2.5%)	Gibco	15090-046
DMEM + Glutamax	Gibco	61965-026
Horse Serum	Sigma Scientific	H1138-500ML
Penicillin/Streptomycin Mix	Gibco	15140-122
Neurobasal	Gibco	21103-49
B27	Gibco	17504-044
Glutamax	Gibco	35050-038

HBSS Dissection Solution

- 500mL HBSS
- 5mL Penicillin/Streptomycin Mix (See 2.1.4.1)

DMEM Plating Solution

- 450mL DMEM + Glutamax
- 50mL Horse Serum
- 5mL Penicillin/Streptomycin Mix

Neurobasal Culture Solution

- 500mL Neurobasal
- 10mL B27
- 5mL Glutamax
- 5mL Penicillin/Streptomycin Mix

2.1.4.4 Neuron $Ca_3(PO_4)_2$ Transfection

Solution	Manufacturer	Product #
MEM + GlutaMAX	Gibco	42360-024
HBSS	Gibco	24020-91

2.5M $CaCl_2$
- 2.5M $CaCl_2$
- In ddH_2O
- Filter through 0.45µm filter

2X HBS
- 274mM NaCl
- 10mM KCl
- 1.4mM Na_2HPO_4
- 15mM D-Glucose
- 42mM Hepes
- In ddH_2O
- Adjust pH to 7.05 with NaOH
- Filter through 0.45µm filter

2.1.5 Experimental Materials

2.1.5.1 Cell Lysis

Phosphate Buffered Saline (PBS)
- See section 2.1.4.2 for recipe

RIPA Buffer (1L)
- 50mL 1M Tris, pH 8
- 30mL 5M NaCl
- 10mL NP40
- 50mL $10\%_{m/v}$ Sodium deoxycholate
- 10mL 0.5M EDTA
- 10mL $10\%_{m/v}$ sodium dodecyl sulphate (SDS)
- 1:500 Protease Inhibitors (PMSF, Leupeptin, and Pepstatin A)

RIPA Buffer + Protease Inhibitors

Solution	Single Plate Volume		(# Plate x 3.5) + 1		Volume
Lysis buffer	1000µL	X		=	
PMSF (0.125M)	2µL	X		=	
Leupeptin (5mg/mL)	2µL	X		=	
Pepstatin A (1mg/mL)	2µL	X		=	

2.1.5.2 RFP-Trap

RFP-Trap beads were purchased from Chromotek (Product# rta-20)

5X Lämmli Buffer (50mL)
- 15.65mL 1M Tris, pH 6.8
- 25mL Glycerin
- 3.75g SDS
- 3.855g DTT or 6.25mL β-mercaptoethanol
- 1 scoopula-tip of Bromophenol Blue

2.1.5.3 SDS-PAGE & western blotting solutions & equipment (antibodies above)

Product	Manufacturer	Product #
PageRuler Plus Prestained Protein Ladder	Thermo Scientific	26619
Whatman Chromatography Paper	GE	3030-392
Nitrocellulose Blotting Membrane	GE	10600002
WesternBright ECL	Biozym Scientific	541004 (WesternBright Kit)
WesternBright Peroxidase	Biozym Scientific	541004 (WesternBright Kit)

SDS-PAGE Running and Stacking Gels

	Separating Gel			Stacking Gel
Solution	Per 6% Gel	Per 10% Gel	Per 12% Gel	Per 5% Gel
ddH_2O	5.2mL	3.9mL	3.2mL	2.8mL
30% Acrylamide mix	2.0mL	3.3mL	4.0mL	700µL
1.5M Tris pH8.8 Buf.	2.6mL	2.6mL	2.6mL	
1.0M Tris pH 6.8 Buf.				500µL
10% SDS Solution	100µL	100µL	100µL	40µL
TEMED	7µL	7µL	7µL	3µL
Invert Tube to mix				
10% APS Solution	100µL	100µL	100µL	40µL
Invert Tube to mix				

WB Primary Antibodies

Target	Species	Dilution	Manufacturer	Product #
α-CASK (C-Term)	Rabbit	1:1000	Cell Signaling Technologies	9497S
α-HA	Mouse	1:1000	Sigma	9658
α-Myc	Mouse	1:1000	Sigma	M5546
α-GluR1 (AMPAR)	Rabbit	1:200	Alomone AGC-004	
α-NMDAR1	Mouse	1:1000	EMD Millipore	MAB363

Antibodies are diluted in 10mL 5% Milk Solution in TBS-T at appropriate antibodies

WB Secondary Antibodies

Target	Reporter	Dilution	Manufacturer	Product #
α-Rabbit	Horseradish Peroxidase (HRP)	1:2500	Jackson ImmunoResearch	GtxRb-003-EHRPX
α-mouse	Horseradish peroxidase (HRP)	1:2500	Jackson Immunoresearch	GtxMu-003-E2HRPX

Antibodies are diluted in 10mL TBS-T Solution

10X Running Buffer (5L)

- 500mL 10X Tris Glycine
- 50mL $10\%_{w/v}$ SDS
- Top up to 5L with ddH_2O

10X Transfer Buffer (5L)

- 1L Methanol
- 500mL 10X Tris Glycine
- 10mL 10% SDS
- Top up to 5L with ddH_2O

10X Tris Glycine

- 151.45g Tris
- 720.65g Glycine
- Check that pH is at 8.3 with pH sticks, do not adjust

10X TBS

- 60.57g Tris
- 438.3g NaCl
- 4.8L ddH_2O
- Adjust pH to 8.0
- Fill to 5L with ddH_2O
- Pour into 2L and 1L bottles
- Autoclave

1X TBS-T

- 5g Tween 20
- 500mL 10X TBS
- Top up to 5L with ddH_2O

Blocking Buffer (10mL per membrane)

- 0.5g Milk Powder
- 10mL TBS-T

2.1.5.4 Dual Luciferase kit (plasmid above)

The Dual Luciferase Report Assays kit was purchased from Promega (Product#: E1980)

2.1.5.5 Surface Biotinylation reagents

Solution	Manufacturer	Product#
cOmplete EDTA-free protease inhibitor	Roche	118 361 700 01
Sulpho-NHS-SS-Biotin	Thermo Scientific	21331
MEM	Gibco	31095-029
Streptavidin Beads	Sigma	E5529-1ML

Biotinylation RIPA Buffer for 12 samples

- 75mL RIPA Buffer (see Cell Lysis section for recipe)
- 3 tablets of cOmplete EDTA-free protease inhibitor

Biotinylation Solution (for 12 samples)

- 6.5mg Sulpho-NHS-SS-Biotin
- 6.5mL PBS+Ca+Mg

PBS+Ca+Mg Solution (1L)

- 100mL 10X PBS
- 1mL 1M $MgCl_2$ (1mM final)
- 100µM $CaCl_2$ (0.1mM final)
- Fill up to 1L with ddH_2O

PBS+Ca+Mg+Glycine

- 200mL PBS+Ca+Mg
- 1.501g Glycerol (100mM)

5X Lämmli Buffer

- See RFP-Trap section for recipe

2.1.5.6 FACS measured with Canto-II

Versene Solution

- See 2.1.4.1 for recipe

Trypsin-EDTA Solution

- See 2.1.4.1 for recipe

Phosphate Buffered Saline (PBS)

- See 2.1.4.2 for recipe

BD Canto II cell sorting machine was used for the experiment

2.1.5.7 Microscopy with SP8

Primary antibodies

Target	Species	Dilution	Manufacturer	Product #
α-vGlut1	Rabbit	1:2000	Synaptic Systems	135 303
α-Map2	Chicken	1:1000	Antibodies Online	ABIN 111 291
α-HA	Mouse	1:200	Sigma Aldrich	H9658
α-HA	Rabbit	1:200	Sigma Aldrich	H6908

Secondary antibodies

Target	Fluorophore	Dilution	Manufacturer	Product #
Alexa 405	α-chicken	1:1000	Abcam	Ab175674
Alexa 488	α-mouse	1:1000	Invitrogen	A11029
Alexa 488	α-rabbit	1:1000	Life Technologies	A11008
Alexa 633	α-mouse	1:1000	Invitrogen	A21050
Alexa 633	α-rabbit	1:1000	Life Technologies	A21072

Phosphate Buffered Saline (PBS)

- See 2.1.4.2 for recipe

4% PFA Stock (1L)

- In ventilated fume hood
- Heat 800mL of PBS to ~60°C while mixing with stir bar
- 40g Formaldehyde
- Add 1M NaOH drop by drop until powder dissolves
- Cool and filter (0.45µm) solution
- Top up to 1L with PBS
- Check pH, adjust to 7.4 with dilute HCl if necessary
- Aliquot into tubes of 50mL, store at -20°C

4% PFA + 4% Sucrose Solution

- 50mL aliquot of 4% PFA
- 2g Sucrose

10% Triton in PBS Stock Solution (in 50mL Tube)

- 5g Triton-X
- 1X PBS fill to 50mL

0.1% Triton in PBS Stock Solution (in 50mL Tube)

- 0.5mL 10% Triton in PBS
- 49.5mL PBS

10% Horse Serum in PBS (Blocking Buffer)

- 5mL Horse Serum
- 45mL PBS

ProLong™ Diamond Antifade Mounting Medium with DAPI was purchased from Invitrogen (Product#: P36962)

2.1.5.8 Quantification and Statistics Software

- Image Lab (Biorad)
- Office Excel (Microsoft)
- Prism 6 (GraphPad)
- ImageJ
- ZEN Blue 2.3 Lite (Zeiss)
- LAS X (Leica)
- BD FACSDiva (BD Biosciences)

2.2 Methods

2.2.1 Molecular Biology Methods

2.2.1.1 Gateway Cloning

In the beginning of this project, a GFP-CASK-TV3 plasmid was generated using Gateway® (Invitrogen) cloning to transfer the CASK gene contained in a PDONR223-CASK plasmid into a pcDNA-DEST53 plasmid according to the manufacturer's instructions. The *CASK* gene from this plasmid when then subcloned into other plasmids in order to generate *CASK* constructs with different tags or in other plasmids for different applications by restriction digest and ligation.

2.2.1.2 Restriction Digest of Plasmids

To subclone the *CASK* gene or regions of it, restriction enzymes were used to excise regions of interest out of plasmids and to open the plasmids into which the segments were to be inserted. A restriction digest premix was made by mixing 2µL of 10X FastDigest Green and 0.5µL of 1 or 2 restriction enzymes and then topping up to 10µL with ddH_2O per reaction. 10µL of plasmid or PCR product was added to 10µL of restriction digest premix. The mix was then incubated at 37°C for 1h.

2.2.1.3 Agarose Gel Electrophoresis for Analysis & Extraction

To analyze or purify the excised products and opened plasmids generated by restriction digest, digestion products were isolated by agarose gel electrophoresis.

To cast an agarose gel, 100mL of 1% Agarose solution and 6µL of Midori Green® were first mixed together. The mixture was then poured into a casting frame with an inserted comb. After the agarose gel solidified, the gel and the frame were submerged in a running chamber containing 1X TAE solution. The gel was then removed to open the samples wells. 10µL of GeneRuler 1 kb Plus DNA ladder was loaded into the first well followed by 18µL of the restriction digest products. The gel was run at 100V for 30 minutes to separate the DNA fragments.

For the purpose of restriction digest analysis, the DNA fragments were fluorescently imaged using an UV transilluminator and photographed in order to determine whether the fragments obtained were of the right size given the plasmid and restriction digest combination.

For the purpose of purifying DNA fragments, small sections of gel containing the desired DNA band were excised and the DNA was purified by GeneJet Purification.

2.2.1.4 GeneJet Purification of DNA out of Agarose Gel

DNA fragments isolated by agarose gel electrophoresis were further purified from the agarose matrix using the GeneJet Gel Purification kit from Fisher Scientific according to the manufacturer's instructions. The purified inserts and opened plasmids were then ligated by T4 ligation.

2.2.1.5 T4 Ligation of insert into plasmids

The purified DNA inserts were inserted into plasmids by T4 DNA Ligase ligation. The inserts and plasmid backbones were combined in ratios of 3:1 to 9:1 in a total volume of 18µL. 2µL of 10X Ligation Buffer containing 1mM of ATP and 1µL of T4 DNA Ligase enzyme was then added. The mixture was incubated overnight at 16°C.

The ligation products were then transformed into bacteria for amplification and analysis.

2.2.1.6 Transformation & Culture of Top10F' E. coli

Plasmids meant for transfection into HEK293T cells and neurons were produced using competent *E. coli* bacteria of the Top10F' strain. Bacteria were stored at -80°C in aliquots of 350µL for storage. Aliquots were thawed on ice for 15 minutes. Meanwhile, plasmids (1µL of Midiprep grade plasmids, 10µL of Miniprep grade plasmid or ligation products) were mixed with 20µL of 5X KCM buffer and topped up to 100µL with ddH_2O to make a plasmid mix. 100µL of thawed bacteria was then added to the plasmid mix and mixed by slowly pipetting up and down.

The bacteria were incubated on ice for 20min before being heat-shocked at 37°C for 5min. 1mL of room temperature LB culture medium without antibiotics was added to each tube and the bacteria were then incubated at 37°C for 1h. Meanwhile, LB-Agar plates with the appropriate selection antibiotic were warned in a 37°C incubator. After incubation, the bacteria were centrifuged at 17 000g for 1min and resuspended in 100µL of LB culture medium without antibiotics. 10µL and 90µL of the resuspension were spread on 2 LB-Agar plates with a selection antibiotic and incubated overnight at 37°C or over a weekend at room temperature.

The next day, the two plates were compared and colonies were picked from the plate with large but well isolated colonies. 100µL pipette tips were touched to the chosen colonies and then placed in a culture tube containing 3mL of LB culture medium with selection antibiotic. Typically, 3 colonies were picked per plate. The 3mL cultures were then placed in a shaker-incubator overnight (37°C, 200RPM). The next day, DNA was extracted by Miniprep.

Bacteria transformed with previously validated Miniprep or Midiprep grade plasmids were directly cultured in 100mL of LB culture medium with selection antibiotics rather than being plated on LB-Agar plates. The 100mL cultures were placed in a shaker-incubator overnight (37°C, 200RPM) before DNA was extraction by Midiprep.

2.2.1.7 DNA Extraction: Midiprep

DNA was extracted out of 100mL cultures of transformed bacteria using a NucleoBond® Xtra Midi kit from Macherey-Nagel according to the manufacturer's instructions. DNA pellets obtained from the process were resuspended in 200µL of TE buffer and left at room temperature for 3 hours or overnight at 4°C. DNA concentration was measured using an automatic plate reader and further diluted with more TE to a target concentration of 1µg/µL.

2.2.1.8 DNA Extraction: Miniprep

DNA was extracted out of 3mL cultures of transformed bacteria using the same reagents as the Midiprep protocol with a modified protocol. This protocol was used when multiple clones resulting from mutagenesis reactions needed to be analyzed before one was picked for retransformation and for higher purity isolation using Midiprep.

1.5mL of the 3mL culture was transferred into a small Eppendorf tube and centrifuged at 17 000g for 1min at room temperature. The supernatant was discarded and the bacteria pellet was resuspended in 100µL of 4°C RES buffer. 100µL of LYS buffer was then added to the resuspension which was mixed with 5 inversions and then incubated for 2min at room temperature. 100µL of NEU buffer was then added to the lysis mixture and mixed

with 5 inversions. The lysates were then centrifuged at 17 000g for 20min at room temperature. The supernatant was then transferred to a new Eppendorf tube and mixed with 210µL of 100% isopropanol to precipitate DNA. The solution was then vortexed and centrifuged at 17 000g for 5min at room temperature. The DNA pellet was then cleaned twice by discarding the supernatant, resuspending the pellet in 70%$_{v/v}$ ethanol and centrifuging at 17 000g for 5min at room temperature. After the supernatant was discarded, the DNA pellet was air dried at room temperature for 30min. The DNA pellet was then resuspended in ddH_2O for use in quality control analysis.

Miniprep grade plasmids are first controlled by restriction digest analysis. If the expected fragment sizes were obtained, the plasmids are then analyzed by Sanger sequencing.

2.2.1.9 Sanger Sequencing

Plasmids were typically subjected to Sanger sequencing follow mutagenesis to test for the presence of the desired missense mutation and the absence of undesired mutations. The Sequencing Buffer and BigDye solutions used were part of the BigDye Terminator v.1.1 Cycle Sequencing Kit from Applied Biosystems.

For each sequencing reaction, 5µL of ddH_2O, 2µL of 5X Sequencing Buffer, 1µL of BigDye, 1µL of the Miniprep or Midiprep grade plasmid, and 1µL of 10µM sequencing primer were mixed together. The mixture was then amplified in a PCR thermocycler running the following program:

Step #	Temp °C	Time	Go to	# Repeats
1	96	1min		
2	96	10s		
3	50	5s		
4	60	4min	2	30
5	4	Hold		

Lid Temp: 99°C

Following PCR amplification, 10µL ddH_2O, 2µL 3M sodium acetate, and 50µL of 100% ethanol were added to each tube. The mixture was vortexed and incubated at room temperature for 15min before being centrifuged at 3000g for 15min at room temperature. The supernatant was discarded and 100µL of 70%$_{v/v}$ ethanol was added. The tube was then centrifuged again at 3000g for 10 min at room temperature and the supernatant was discarded. The tube was further dried by being centrifuged upside at 500g for 1min at room temperature. The DNA pellet was then resuspended in 20µL of HiDi Formamide solution. The solution was then sent to the sequencing core facilities at the diagnostic department of the Institute of Human Genetics at the UKE. The sequence returned analyzed by BLAST alignment to the gene map.

2.2.1.10 Site directed mutagenesis by QuikChange II XL

Missense mutations were introduced into the CASK plasmids using the QuikChange II XL site-directed mutagenesis kit from Agilent according to the instructions from the manufacturer.

For each mutagenesis reaction, 5µL of 10X Reaction Buffer, 10ng of target plasmid, 1µL of 10mM forward and reverse mutagenic primers, 1µL of dNTP, and 3µL of QuikSolution were mixed and topped up to 50µL with ddH_2O. 1µL of Pfu Ultra was added last before the mix was amplified in a PCR cycler running the following program

Step #	Temp °C	Time	Go to	Repeat
1	95	1min		
2	95	50sec		
3	60	50sec		
4	68	**1min/kb plasmid:**	2	17
5	68	7min		
6	4°C	Hold		

Lid Temp: 99°C

After amplification by PCR, the original plasmid was digested by Dpn1 Restriction enzyme. The mutagenesis product was then transformed into bacteria, analyzed by miniprep and sequencing, retransformed into bacteria and isolated by Midiprep as described above.

2.2.2 Cell Biology Methods

2.2.2.1 HEK293T cell culture

HEK293T cells aliquots from long term storage at -80°C were thawed in a 37°C water bath for 10-15 minutes until thawed and transferred into a test tube with 5mL of prewarmed DMEM Culture Solution. The cells were then centrifuged at 3000g for 5min at room temperature. The supernatant was discarded and the cells were resuspended in 10mL of DMEM Culture Solution, transferred into a 10cm culture plate, and placed in a 37°C incubator with a 5% CO_2 atmosphere. The plate was allowed to grow until the cells were 95% confluent, typically after 4 days at which point the cells were split.

For splitting, plates confluent with HEK293T cells were first rinsed with 2mL of 37°C Versene Solution and then rinsed with 1mL of Trypsin-EDTA Solution. The cells were then resuspended in different volumes of DMEM Culture Solution and transferred into new 10cm plates with enough DMEM Culture Solution for the final volume to be 10mL.

2.2.2.2 HEK293T cell transfection

Plates of HEK293T cells meant for transfection were checked for a cell confluence of 20-50%. HEK293T cells were transiently transfected using Turbofect. For each transfection, a transfection premix consisting of the desired plasmids was mixed with 18µL of Turbofect and 950µL of DMEM Transfection Solution. The transfection premix was mixed and allowed to rest at 20min at room temperature. The transfection mixes were then transferred into the HEK293T plates which were then cultured in a 37°C incubator with a 5% CO_2 atmosphere

The total amount of DNA per premix was kept at 10 to 13µg, split between the different plasmids. For example, transfections for coimmunoprecipitation experiments had 5µg of *CASK* plasmid and 5µg of partner plasmid. Some plates for the Split-YFP experiments had 3µg of plasmids for *CASK-YFP1, CASK-YFP2, Neurexin-1β, Lirpin-α2*, and 1µg of *mRFP*.

2.2.2.3 Lentiviral particle production in HEK293T cells

Lentiviral particles encoding *CASK* meant for the infection of neurons were produced using HEK293T cells. Each plate was transfected as described above with a mixture of 4.5µg psPAX.2 (Addgene # 12260) packaging plasmid, 2µg of pMD2.G (Addgene 12259) envelope plasmid, 5µg of WT or mutant *RFP-CASK* cDNA in FUW-vector, and with 18µL Turbofect. The HEK293T cells were cultured for 6 hours in an incubator at 37°C with a 5% CO_2 atmosphere before the culture medium was replaced with 10mL of prewarmed Lentivirus Production DMEM and the cells were further cultured overnight.

On day 1 after transfection, if the HEK293T cells exhibited red fluorescence, the supernatant was checked for the presence of lentiviral particles using Lenti-X GoStix. 20µL of supernatant was placed into the well of the test stick and incubated for 10-20min. The appearance of a test band indicated the presence of lentiviral particles.

Harvesting and concentration of lentiviral particles was performed using a Lenti-X Concentrator solution. The 10mL of culture medium was harvested and replaced with 10mL of prewarmed Lentivirus Production DMEM. The collected culture medium was placed in a syringe and filtered through a 0.45µm filter into a 15mL Falcon tube. 3.7mL of Lenti-X Concentrator was mixed into the filtered supernatant to precipitate the lentiviral particles out of solution. The precipitated mix was stored at 4°C. On day 2 after transfection, the supernatant of the HEK293T cells was harvested, filtered and mixed with Lenti-X Concentrator like on day 1.

The 2 tubes of precipitated lentiviral particles were centrifuged at 1500g for 45min at 4°C to pellet the lentiviruses out of solution. The supernatant was discarded and the 2 lentiviral pellets were resuspended in 100µL of PBS solution and split into 50µL aliquots which were stored at -80°C.

2.2.2.4 Primary Hippocampal & Cortical Neuron Extraction and Culture

Primary hippocampal and cortical neurons were extracted from rats from Envigo. A pregnant rat at day E18 was euthanized by CO_2 followed by decapitation. The uterus was then surgically extracted and placed on an ice-chilled plate. In a laminar flow bench, the embryos were removed from the uterus and decapitated. The skin and skull on the dorsal side of the head were removed and the brains were extracted and placed in a 4cm dish with 8mL of HBSS Dissection Solution.

Using a dissection microscope, the 2 cortical hemispheres were separated from the midbrain and the meninges were removed from the hemispheres. The hippocampi were then extracted from the hemispheres and placed into a plate with fresh HBSS Dissection Solution. The hippocampi were aspirated into 4.5mL of HBSS Dissection Medium and transferred into a 15mL Falcon tube to which 500µL of 10X Trypsin was then added. The tube was placed in a 37°C water bath for 15min. Meanwhile, 4 Pasteur pipettes were made to have progressively narrower openings by rotating the pipette tip over a gas burner.

The hippocampi were then rinsed 5 times with 5mL of DMEM Plating Solution. After the last wash, DMEM Plating Solution was removed until 1.5mL remained in the tube. The neurons were then dissociated into individual cells by aspiration and ejection through the 4 Pasteur pipettes with the progressively narrower openings. The dissociated neurons were then diluted to 10mL of DMEM Plating Solution and the concentrations of cells in solution was counted using a haemocytometer. The neurons were then further diluted to a concentration of 150 000 neurons/mL. 1mL of neuron solution was seeded onto poly-L-lysine-coated coverslips in 12-well plates. The neurons were then placed into a 37°C incubator with a 5% CO_2 atmosphere and allowed to grow overnight. The next day, the DMEM Plating Solution in each well was replaced with 1mL of 37°C Neurobasal Culture Solution.

Cortical neurons were prepared and cultured in a similar manner with the same solutions. After the hippocampi were extracted, the hemispheres were transferred into a 4cm dish with 8mL of HBSS Dissection Solution. The hemispheres were cut into small pieces using sterile, surgical scissors before being aspirated into 4.5mL of HBSS Dissection Solution and transferred into a 15mL Falcon tube to which 500µL 10X Trypsin was added. The tube was then placed in a 37°C water bath for 20min. The cortices were then rinsed 5 times with 5mL of DMEM Plating Solution. After the last wash, the cortices were left in 1.5mL of DMEM Plating Solution and dissociated into individual cells by aspiration and ejection through 4 Pasteur pipettes with progressively narrower openings. After dissociation, the cortical neurons were sieved through a 70µm cell strainer and the elution was collected into a 50mL tube. The cortical neurons were then diluted in enough DMEM Plating Solution such that 2mL of plating medium contains the neurons from 1.5 embryos (~1.3mL / embryo). For a typical litter of 12 embryos, the cortical neurons were resuspended in 16mL of DMEM Plating Solution, which was then distributed into 6-well plates at 2mL per well. The 6-well plates were placed in a 37°C incubator with a 5% CO_2 atmosphere. The next day, the DMEM Plating Solution was replaced with 2mL of 37°C Neurobasal Culture Solution.

2.2.2.5 Neuron $Ca_3(PO_4)_2$ Transfection

7 days after neuronal extractions (7 DIV) hippocampal neurons were transfected using the $Ca_3(PO_4)_2$ method. 1 hour before transfection, the Neurobasal Culture Solution in each well was collected into a Falcon tube and replaced with 500µL per well of 37°C Neuron Transfection Solution (MEM + GlutaMax). The Falcon tube with Neuronal Culture Solution was topped to # of wells + 2mL with Neurobasal Culture Solution. The plate and the Falcon tube were then placed back in the 37°C incubator with 5% CO_2 atmosphere.

Meanwhile, the neuron transfection premix was prepared. In an Eppendorf tube, 10µg of DNA, 10µL of 2.5M $CaCl_2$ were mixed and then topped up to 100µL with ddH_2O. The tube was then vortexed continuously while 100µL of 2X HBS was added to the tube drop by drop. The transfection mix was then allowed to rest for 30min at room temperature.

100µL of transfection mix was then added to 2 wells with hippocampal neurons. The wells were then placed back in the 37°C incubator with 5% CO_2 atmosphere for 2 hours. Afterwards, the wells were rinsed 7 times with 1mL of 37°C HBSS Solution. After the final rinse, the previously collected Neurobasal Culture Solution was transferred back to the wells at 1mL per well. At 14 DIV, the neurons were then fixed, permeabilized and stained for immunocytochemistry as described later.

2.2.2.6 Neuron Infection

For biochemical experiments, a neuronal transfection rate higher than what can be achieved with $Ca_3(PO_4)_2$ transfection method was necessary. Therefore, cortical neurons were infected using lentiviral particles encoding WT and mutant *RFP-CASK-TV3*.

At 7 DIV, lentiviral particle aliquots stored at -80°C were thawed at room temperature. 20µL of lentiviral particles was used per well of cortical neuron. At 14 DIV, when nearly all the neurons were expressing RFP-CASK, the surface proteins of the neurons were biotinylated and analyzed by SDS-PAGE and western blot as described later.

2.2.3 Experimental Methods

2.2.3.1 Cell Lysis

HEK293T cells transfected for coimmunoprecipitation experiments were cultured for one day before being lysed using RIPA buffer. Protein complexes were then extracted by RFP-Trap and analyzed by SDS-PAGE and western blot as described later.

For lysis, each HEK293T plate was removed from the incubator and placed on ice. Each plate was then rinsed 3x with ~2mL 4°C PBS solution before 1mL RIPA Buffer + Protease Inhibitor (PI) was added into each plate. The plates were then placed on a teeter-totter for 15min while still on ice. The lysates were then collected into Eppendorf tubes and centrifuged at 20 000g for 15min at 4°C. The supernatant from the tubes was then collected for RFP-Trap coimmunoprecipitation and analysis by SDS-PAGE and western blot.

For lysates not requiring RFP-Trap, 50µL of lysate was removed and mixed with 12.5µL 5X Lämmli Buffer before being run on SDS-PAGE gels and analyzed by western blot.

2.2.3.2 RFP-Trap immunoprecipitation

RFP-tagged CASK was immunoprecipitated out of the lysate of HEK293T cells using RFP-Trap beads. RFP-trap beads were rinsed twice with 4°C RIPA Buffer + PI by adding 500µL 4°C RIPA Buffer + PI, centrifuging at 1000g for 1min at 4°C and discarding the supernatant. 50µL of the cell lysate was taken and mixed with 12.5µL 5X Lämmli Buffer for use as Input Sample. All remaining cell lysate was then used to resuspend the RFP-Trap beads and the mixture was placed in a rotator for 2h at 4°C. The beads were then rinsed 5 times: the beads were centrifuged at 1000g for 1min at 4°C, the supernatant was then discarded, and the beads were resuspended in 500µL 4°C RIPA Buffer + PI. After the fifth wash, the beads were centrifuged at 1000g for 1min at 4°C, the supernatant was discarded and the RFP-trap beads were resuspended in 60µL 1X Lämmli as “IP” (immunoprecipitated) Sample. The IP and Input samples were then denatured at 94°C for 5min before being run on an SDS-PAGE and analyzed by western blot.

2.2.3.3 SDS-PAGE & Western Blotting

Proteins in cell lysates were separated by molecular weight using electrophoresis in a SDS-PAGE gel using a Mini-PROTEAN II system from Biorad.

To make 10% separation gels, a premix consisting of 3.9mL ddH_2O, 3.3mL 30% Acrylamide, 2.6mL 1.5M Tris Buffer pH 8.8, 100µL 10%$_{w/v}$ SDS Solution, 7µL TEMED, and 100µL 10% APS solution per gel was mixed. 8mL of the separating gel mix was poured into a 1.5mm glass frame. 2mL of 100% Isopropanol was then added into each frame to remove air bubbles. The separation gel solution was allowed to polymerize.

Meanwhile, a stacking gel premix was made. 2.8mL ddH_2O, 700µL 30% acrylamide mix, 500µL 1.0M Tris pH 6.8, 40µL 10% SDS solution per gel were mixed together. The 3µL TEMED and 40µL 10% APS solution per

gel were added after the separation gel had polymerized and the isopropanol had been poured out and rinsed out with ddH_2O. 2mL of stacking gel was then added on top of the polymerized separation gel in each glass frame before a 1.5mm thick, 15-well comb was placed into each glass frame and the running gel was allowed to polymerize.

After the stacking gel had polymerized, the comb was removed from the gel + glass assembly and the gel + glass assembly was loaded into a running chamber with Running Buffer. 8µL of PageRuler Plus Prestained Protein Ladder and 15µL of protein samples were loaded into the wells of the gel. The running chambers were connected to a power supply unit and the proteins were electrophoresed at 100V for 15 minutes, then for 150V for 1h or 180V for 30-45 minutes.

After electrophoresis, the gels were removed from the glass running frame and were assembled into a transfer sandwich while submerged in Transfer Buffer. The sandwich was composed of, starting from the clear side of the cassette, a sponge layer, a sheet of Whatman paper, a nitrocellulose membrane, the SDS-PAGE gel, another sheet of Whatman paper, another sponge, and the black side of the cassette. The cassette was closed and was placed in the transfer chamber filled with Transfer Buffer, black side to black and red side to red. The transfer sandwiches were ran at 2 hours at 100V to transfer the proteins from the SDS-PAGE gels to the nitrocellulose membrane.

After transfer was completed, the nitrocellulose membranes were removed from the transfer sandwich and were blocked in 10mL of Blocking Buffer for 1h. They were then then incubated in primary antibody solutions overnight at 4°C. The next day, the membranes were removed from the antibody solutions and were rinsed 3x with 10mL of 1x TBS-T solution at 10min intervals. The membranes then incubated in secondary antibody solution for 1h, before being rinsed 3x again with 10mL of 1X TBS-T at 10min intervals. Each membrane was then incubated for 10-30s in a mixture of 4mL of WesternBright ECL and 4mL of WesternBright Peroxide before being imaged in a Biorad imager. The blots were quantified using the Image Lab program.

2.2.3.4 Dual Luciferase kit

For dual luciferase experiments, HEK293T cells were transfected using Turbofect as described in the sections above with 3µg of WT or mutant *CMV_RFP-CASK-TV3*, *Myc-Tbr1*, *HA-CINAP*, *Renilla Luciferase*, and *NR2b-P*. (Firefly luciferase under the control of a *Grin2b* promoter). The next day, the HEK293T cells were lysed and Firefly and Renilla luciferase luminescence was measured with a Dual Luciferase Reporter Assay kit from Promega according to the manufacturer's instructions.

2.2.3.5 Cortical Neuron Surface Protein Biotinylation

Cortical neurons were infected with lentiviral particles encoding WT and mutant *FUW_RFP-CASK-TV3* as described previously. To measure the quantity of NMDARs and AMPARs on the surface of cortical neurons, surface proteins were tagged with biotin and then purified for quantification by SDS-PAGE and western blot.

For 2 6-well plates of cortical neurons, 75mL of Biotinylation RIPA Buffer and 6.5mL of Biotinylation solution were prepared ahead of time and placed on ice. To biotinylated surface proteins, cortical neurons were rinsed with 1mL of 4°C MEM and then 3X with 1mL of 4°C PBS+Ca+Mg. 500µL of Biotinylation Solution was then added into each well and the plates were incubated on ice on a shaker for 30min.

Meanwhile, 1300µL of Streptavidin beads were centrifuged at 1000g for 1min at 4°C. The beads were then rinsed 3x by the addition of 500µL of Biotinylation RIPA Buffer, centrifugation at 1000g for 1min at 4°C, and removal of the supernatant. After the final wash, the Streptavidin beads were resuspended in half the initial volume of beads (650µL) of Biotinylation RIPA Buffer, and split into 6 tubes of 100µL and placed on ice.

After Biotinylation, the cortical neurons were rinsed 3X with 1mL of 4°C PBS+Ca+Mg+Glycin, leaving the 3rd rinse on for 20min in order to quench all unbound Biotin in solution. The neurons were then rinsed 2x with 1mL of 4°C PBS+Ca+Mg. The neurons were then incubated in 400µL of 4°C Biotinylation RIPA for 15min on ice on a teeter-totter. The cells were then homogenized in the Biotinylation RIPA buffer, transferred into Eppendorf tubes and centrifuged at 20 000g for 20min at 4°C.

50µL of the supernatant was transferred into an Eppendorf Tube and mixed with 12.5µL 5X Lämmli Buffer as "Input" sample. Remaining cell lysate was mixed with Streptavidin beads in an Eppendorf Tube, topped up to 1.4mL of Biotinylation RIPA buffer and placed on a rotator for 3 hours at 4°C. The beads were then centrifuged at 1000g for 1min at 4°C and the supernatant was discarded. A long wash was performed by resuspending the beads in 1mL Biotinylation RIPA buffer and placing them in a rotator for 5min at 4°C before centrifuging the beads at 1000g for 1min at 4°C and discarding the supernatant. The beads were then rinsed 3X times with the same steps but without rotation. After the supernatant was removed from the 3rd rinse, the beads were resuspended in 65µL 5X Lämmli to the beads. The samples were then incubated at 4°C overnight before being used for SDS-PAGE and western blot analysis as described previously.

2.2.3.6 Split-YFP & FACS

For split-YFP experiments to gauge CASK oligomerization, HEK293T cells were transfected with 3µg of WT or mutant *CMV_CASK-TV5-YFP1, CMV_CASK-TV5-YFP2, HA-Neurexin-1β, HA-Liprin-α2,* 1µg *mRFP,* and *pcDNA3* (to bring the DNA load per plate up to 13µg) in various combinations using Turbofect as described previously.

The cells were then given 2 days to express the proteins before being prepared for analysis by FACS. The culture medium in the plates was aspirated and the cells were rinsed twice with pre-warmed Versene Solution. 1mL of Trypsin-EDTA solution was added onto the plates and immediately removed. The cells were left for 1min before being resuspended in 2mL of DMEM and transferred to a 15mL Falcon tube. The cells were then centrifuged at 1200g for 3min at room temperature and the supernatant was discarded. The cells were then resuspended in 1mL of PBS and pipetted up and down a few times to make sure the cells were well separated.

The cells were then transferred into FACS-compatible test tubes and brought to the FACS core facilities for measurement on a Canto II system.

In FACS assays, analyzed "events" are any fragment, cells and cell clumps that flow through an analysis chamber where multiple lasers probe the samples. Before fluorescence in the channels of interest can be measured, the FACS machine must first be setup to distinguish dead cells and cell fragments from viable cells, and then to distinguish individual cells from cell clumps of 2-3 cells.

Separating dead cells from viable cells is done by a set of criteria called the "Cell Survivability Gate" (Fig 3.13A, P1). It is done by shining a light source meant to for that purpose onto the sample and measure the amount of light reflected back towards the light source (Front Scatter Intensity) and the amount of light scattered towards the side of the cells at a right angle from the light source (Side Scatter Intensity). Fluorescent events scoring too low on both metrics are interpreted as dead cells and rejected while cells falling within higher ranges of front and side scatter defined by the gate P1, set by the user, are considered alive and further analyzed.

Separating cell clumps from individual cells is done by a set of criteria called the "Single Cell Gate" (Fig 3.13B). With the same light source as the cell survivability gate, the total front scattered light as the cells pass through the measurement chamber (Front Scatter Intensity) are compared to the peak front scatter intensity (Front Scatter Height). Cells scoring too high on these two metrics are interpreted as being cell clumps and are rejected while cells falling within a range of Front Scatter Intensity and Front Scatter Height values defined by the gate P2, set by the user, are considered individual cells and passed on for fluorescence analysis.

Cells that fulfill the selection criteria of the Survivability Gate and the Single Cell Gate are then analyzed based on their fluorescence in the RFP and YFP channel. Our goal is to measure the YFP-fluroescence of transfected cells. Because we co-transfect all the cells of our experimental conditions with *mRFP*, RFP fluorescence can be used as a measure of transfection. We used negative control cells which were not transfected with any fluorescent protein to define the threshold separating RFP-fluorescent cells from non-fluorescence cells (Fig 3.13C, vertical line). Only cells above the RFP-fluorescence threshold were considered transfected and were analyzed for YFP-fluorescence.

2.2.3.7 Microscopy with SP8

Hippocampal neurons used for imaging were transfected 7 days *in-vitro* (DIV) as described above. At 14 DIV, the neurons were rinsed 2X with ~1mL of 4°C PBS before being fixed in 500µL of 4°C 4% PFA + Sucrose solution for 15min on a teeter-totter. The neurons were then rinsed 2X with ~1mL of 4°C PBS solution. The neurons were then permeabilized for 3min in 500mL of 0.1% Triton-X on a teeter-totter, after which the neurons were again rinsed 3X with ~1mL of 4°C PBS. The neurons were then blocked with 500µL of 10% Horse Serum solution for 1h. After blocking, the neurons were labelled with primary antibodies by placing the coverslips face down on 100µL droplets of 2% horse serum solution with primary antibodies. The coverslips were protected from light and placed at 4°C overnight for labelling.

The next day, the coverslips were placed back into the 12-well plates and rinsed 3X with ~1mL of 4°C PBS at 10min intervals. The neurons were then labeled with secondary antibodies by placing the coverslips face down on 100µL droplets of PBS with secondary antibodies. The coverslips were shielded from light and allowed to incubate at room temperature for 1h. The coverslips were then placed back in the 12-well plates and rinsed 3X with ~1mL of 4°C PBS at 10min intervals.

The coverslips were then dipped in ddH_2O, blotted on paper, and placed face down on a drop of ProLong™ Diamond Antifade Mounting Medium with DAPI on glass slides. The slides were then left to polymerize at room temperature while shielded from light.

Coverslips were imaged using a Leica SP8 microscope with a 63x oil-immersion objective.

2.2.3.8 Data Processing and Statistics

SuperMean Correction was a data processing step used to compensate for uneven western blot exposures. The imagers used to quantify the western blot membranes exposed the membranes until the signals began to saturate the sensor of the imager. However, due to occasional uneven protein distribution, a localized cluster of proteins in one band on a membrane could trigger the saturation point earlier than on a membrane with well distributed proteins. The result is that certain membranes had a much shorter exposure time, and thus much weaker signals for the bands than others. However, the relative signal intensity between the bands within a single membrane is preserved, even with shorter exposure times.

The SuperMean Correction proportionally increases or decreases all the bands on a particular membrane such that membranes of the same condition (for example, CASK IP membranes of 3 repeats) across multiple repeats have the same average signal intensity. This removes the statistical variance that would be introduced from uneven exposure, a non-biological source of variance, while preserving the relative values between the bands on a single membrane, which corresponds to the amount of protein present, a biologically relevant source of variance.

An important aspect of the SuperMean Correction is that it can only be used if all the membranes grouped together share the same conditions. For example, 3 CASK IP membranes must have the same mutants present in order to be processed by SuperMean correction.

After SuperMean Correction, significance between WT and mutant conditions was calculated as usual using 1 or 2-way ANOVAs as appropriate, followed by Tukey's or Dunnett's multiple comparisons tests.

3. Results

3.1 *CASK* Transcript Variants

3.1.1 *CASK* Transcript Variants differ in their inclusion of 3 exons and 1 exon fragment

Before considering the missense mutations identified in male patients, I first wanted to address another aspect of *CASK*: the various transcript variants of *CASK* and the various CASK isoforms that result from these.

The *CASK* gene is subject to alternative splicing and there are currently 4 confirmed variants named *CASK-TV1* to *CASK-TV4* in the human reference transcript database (GeneBank NM_003688, NM_001126054, NM_001126055, & NM_001367721). These transcript variants differ in their inclusion of 3 exons and a small exon fragment: exon 11, 19, 20, and a 5' extension of exon 23 (23L). *CASK-TV4* is the longest variant of *CASK*, including all 4 alternatively spliced axons (Fig 1B). Interestingly, the 4 alternatively spliced axons (Fig 1B, yellow blocks) encode segments of amino acids only located within the linker region between protein domains of the CASK protein.

Exon	Start in TV4	End in TV4	Length	Position
Exon 11	1016	1033	18bp, 6aa	CamK-L27.1 linker
Exon 19	1738	1806	69bp, 13aa	PDZ-SH3 linker
Exon 20	1807	1842	36bp, 12aa	PDZ-SH3 linker
Exon 23L	2156	2170	15bp, 5aa	SH3-GK linker

Table 3.1: Alternatively spliced exons of *CASK*

These various *CASK* transcript variants need to be considered for two reasons.

The first reason is a pragmatic one. Different research groups have been using different *CASK* transcript variants to define the position of their mutations. For example, Takanashi et al. (2012) report a L348P mutation in patients, which fits within *CASK-TV3*. When Moog et al. (2015) discussed this mutation this mutation in their review, they renamed it L354P, which fits within *CASK-TV1*. However, they state that Takanashi et al., had "wrongly" described it as L348P, suggesting that Moog et al., were simply unaware of the existence of different *CASK* transcript variants. This is thus a potential source of confusion when discussing *CASK* mutations.

The second reason is that no study has yet investigated whether or not the different isoforms encoded by the various *CASK* transcript variants are functionally distinctive. The missense mutations identified in patients suggest that the replacement of even a single amino acid can have a strong effect on the function of CASK. It can therefore reasonably be expected that the inclusion or removal of 5 to 13 amino acids long segments could also have an effect on the function of CASK, even if these region are located in linker regions between domains.

To test this, I generated plasmids encoding the various *CASK* transcript variants. For this, the central, variable region of *CASK* was amplified out of human brain cDNA by PCR and cloned it into the *CMV_RFP-CASK* plasmid by Dr. Frederike Harms. 29 clones were generated this way which were sequenced by Sanger sequencing. These experiments were performed in cooperation with Debora Tibbe, whom I supervised during an internship for her master's course.

We identified 7 transcript variants (Fig 3.1B) and calculated their relative abundance (Fig 3.1C). *CASK-TV1* incorporates exon 11, 19, and 20, and accounted for 6 of the 29 clones (20.7%). *CASK-TV2* incorporates exons 11 and 20, and accounted for 4 of the 29 clones (13.8%). *CASK-TV3* incorporates exon 20 and 23L and accounted for 3 of the 29 clones (10.3%). *CASK-TV4* which incorporates all 4 alternatively spliced exons, however, was not found among the analyzed 29 clones.

Surprisingly, we were also able to find new *CASK* transcript variants that are not listed among the confirmed *CASK* transcript variants in the reference human transcript database. We tentatively named them *CASK-TV5* through *CASK-TV8* (Fig 3.1B,C). *CASK-TV5* incorporates exons 11 and 19, and accounted for 12 of the 29 clones (41.4%), making it the single most abundant *CASK* transcript variant in our population. *CASK-TV6* incorporates exons 19 and 20, and accounted for 1 of the 29 clones (3.4%). *CASK-TV7* incorporates exons 19,

21, and 23L, and accounts for 2 of the 29 clones (6.9%). *CASK-TV8* incorporates exon 19, and accounts for 1 of the 29 clones (3.4%).

Fig 3.1

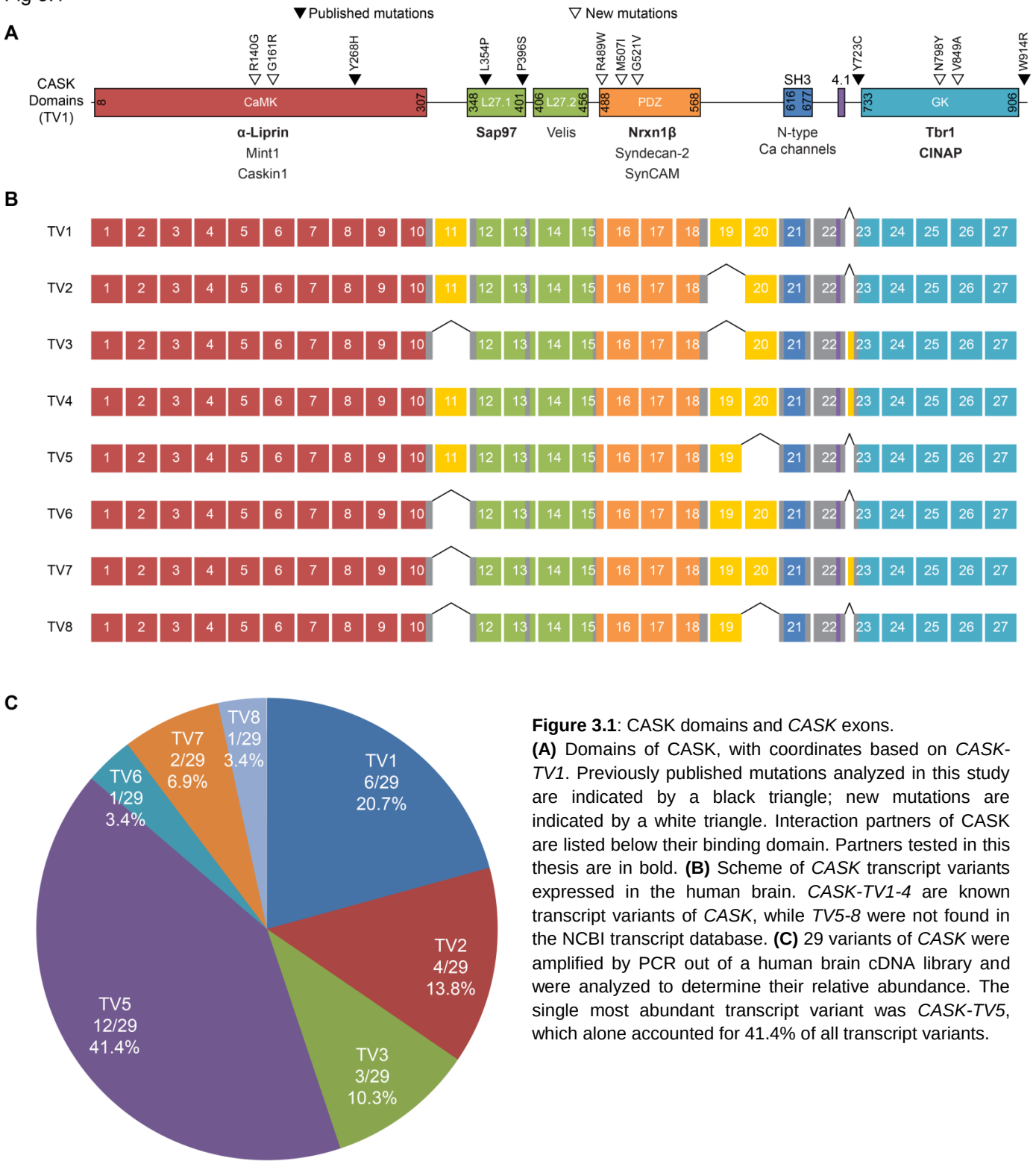

Figure 3.1: CASK domains and *CASK* exons.
(A) Domains of CASK, with coordinates based on *CASK-TV1*. Previously published mutations analyzed in this study are indicated by a black triangle; new mutations are indicated by a white triangle. Interaction partners of CASK are listed below their binding domain. Partners tested in this thesis are in bold. **(B)** Scheme of *CASK* transcript variants expressed in the human brain. *CASK-TV1-4* are known transcript variants of *CASK*, while *TV5-8* were not found in the NCBI transcript database. **(C)** 29 variants of *CASK* were amplified by PCR out of a human brain cDNA library and were analyzed to determine their relative abundance. The single most abundant transcript variant was *CASK-TV5*, which alone accounted for 41.4% of all transcript variants.

One pattern that was observed among the analyzed clones is the obligate inclusion of either exon 19 or 20; *CASK* transcript variants included one or both, but never lacked both. These are the two longest alternatively spliced exons of *CASK*, which in the protein product would contribute 26 and 12 amino acids to the 47aa long linker region between the PDZ and SH3 domains of CASK. The C-terminus of MAGUKs is known to act as a PSG supramodule (Li et al., 2014; Zeng, Ye, Xu, & Zhang, 2018), which depends on an intramolecular interaction between the PDZ and SH3 domains of MAGUKs. It can therefore be speculated that the correct orientation of the PDZ and SH3 domains requires that the PDZ-SH3 linker region be of a minimum length.

With 4 alternatively spliced exons, a theoretical 16 different transcript variants exist. It is not possible to say at this point whether all of these transcript variants exist in the human brain but in amounts too low for our sample of 29 clones to detect, or whether some are not physiologically produced.

CASK transcript variant 5 stands out in 2 ways. *CASK-TV5* is by far the single most abundant transcript variant, being almost as abundant as the 3 confirmed *CASK* transcript variants combined (12 vs 13 of 29). When I searched for a match of the 4 new *CASK* transcript variants in the NCBI nucleotide database, *CASK-TV5* was a very close match to the rat *Cask* cDNA (GenBank: U47110.1). *CASK-TV5* and rat *Cask* share 95% sequence identity and align without continuous mismatch segments. The rat CASK protein (GenBank: AAB19127) and the translation product of *CASK-TV5* also align very closely, with 99% identity, differing in 4 amino acids, 2 of which are conservative substitutions.

Since many articles used a rat *Cask* plasmid and *CASK-TV5* is the single most abundant *CASK* transcript variant, I decided to replace *CASK-TV3*, which I used in the beginning of my project, with *CASK-TV5* in order to bring my experiments in line with previously published work. As a result, some of the functional experiments in this thesis were performed with CASK-TV3 while some were performed with CASK-TV5. Which CASK isoform was used will be clearly stated in text and in figure legends.

3.1.2 CASK-TV2 binds more strongly to Tbr1 than other CASK-TVs

I suspected that the different transcript variants of *CASK* may have developed certain biases for certain functions among *CASK*'s repertoire of functions. To test this, I asked whether the transcript variants of CASK bind with more or less affinity to CASK binding partners. I chose 3 interaction partners, Tbr1, Sap97, and Neurexin-1β as these binding partners represent the 3 main functions of CASK: transcription regulation, receptor sorting, and presynaptic scaffolding.

To analyze the binding affinity of various interaction partners to CASK, I performed coimmunoprecipitation (CoIP) experiments using RFP-Trap in HEK293T cells. The HEK293T cells were transfected plasmids coding for *Myc-Tbr1*, *Myc-Sap97*, or *HA-Neurexin-1β* in combination with WT *RFP-CASK-TV1*, *TV2*, *TV3*, *TV5*, *TV6*, and *TV7*. *CASK-TV8* was not included in the functional assays. 1 day after transfection, the cells were lysed using RIPA buffer with protease inhibitors. Proteins were isolated using RFP-Trap beads and both the immunoprecipitated (IP) and input samples were quantified by SDS-PAGE and Western Blot. Each binding partner was tested against the CASK transcript variant 3 times. Within each experiment, the signals from the immunoprecipitated partner (IP) membrane were normalized against their corresponding signals on the CASK IP membrane in order to analyze the amount of partner coimunoprecipitated out of solution by each CASK isoform.

In the experiments that compared the CASK transcript variants' ability to bind to Tbr1, the Tbr1(IP)/CASK(IP) ratio was higher with CASK-TV2 than with the other transcript variants. Tbr1 showed significant preference for CASK-TV2 over TV3, TV5, and TV6 ($P<0.05$), and near significant preference over CASK-TV1 ($P=0.0506$) and TV7 (0.073) (Fig 3.2A,B). Why CASK-TV2 binds more strongly to Tbr1 is not possible to tell at this point. Tbr1 binds to the GK domain of CASK (Y.-P. Hsueh et al., 2000). Of the 4 segments encoded by alternatively spliced exons, the segment encoded by 23L is the closest to the GK domain and is missing in CASK-TV2. However, CASK-TV1, TV5, and TV6 also lack the segment encoded by exon 23L, yet they bind weakly to Tbr1 compared to CASK-TV2. Therefore, the stronger CASK:Tbr1 binding cannot be attributed to the absence of the exon 23L-encoded segment. A protein folding model of this region could provide valuable insight. It

would also be interesting to test whether CASK-TV2 also binds more strongly to other GK domain partners, such as CINAP.

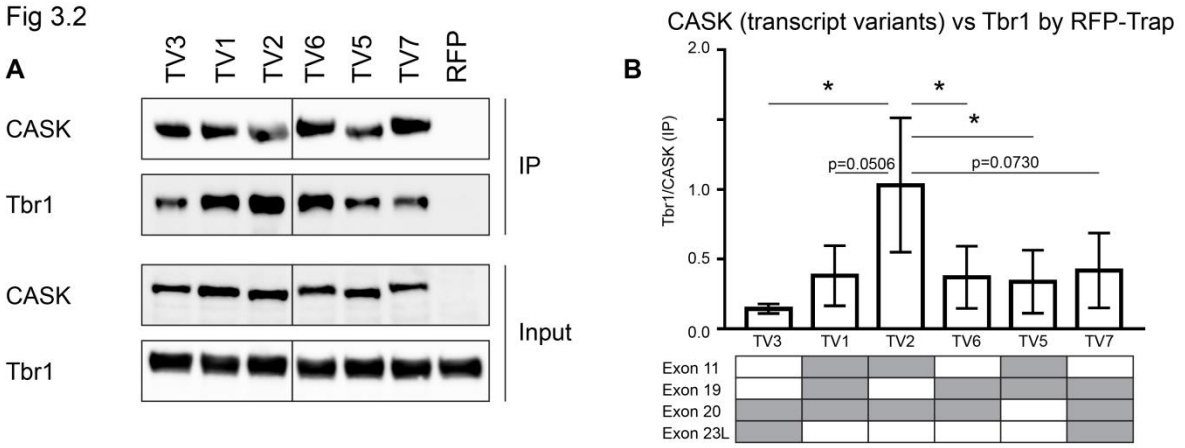

Figure 3.2: Tbr1 preferentially binds to CASK-TV2
(A) HEK293T cells were transfected with plasmids coding for multiple transcript variants of *RFP-CASK* with *Myc-Tbr1*. CASK was immunoprecipitated after cell lysis by RFP-Trap and input and IP samples were analysed by SDS-PAGE and Western Blot. **(B)** After SM correction, each Tbr1(IP) signal was normalized against the appropriate CASK(IP) signal to determine the binding efficiency of the different CASK transcript variants to Tbr1. CASK-TV2 bound significantly more to Tbr1 compared to the other transcript variants of CASK. N=3, *P<0.05, 1-way ANOVA with Tukey's multiple comparisons test.

3.1.3 The sequence encoded by exon 11 decreases CASK:Sap97 interaction

To measure the ability of the various CASK transcript variants' ability to bind to Sap97, HEK293T cells were transfected with plasmids coding for multiple transcript variants of WT *RFP-CASK* and *Myc-Sap97*. The signals of immunoprecipitated Sap97 and CASK were then quantified and analyzed as described above.

In these experiments, isoforms could be roughly divided into strong and weak binders. More Sap97 was coimmunoprecipitated by CASK-TV3, TV6, and TV7 than by CASK-TV1, TV2, and TV5 (Fig 3.3A). Statistically, however, the effect was less clear. CASK-TV3 coimmunoprecipitated significantly more Sap97 than CASK-TV2 (P=0.036) or CASK-TV5 (P=0.001), but not significantly more than CASK-TV1 (P=0.168). CASK-TV6 coimmunoprecipitated significantly more Sap97 than CASK-TV2 (P=0.019) and CASK-TV5 (P=0.001), but not significantly more than CASK-TV1 (P=0.0103). CASK-TV7 coimmunoprecipitated significantly more Sap97 than CASK-TV5 (P=0.028), but not significantly more than CASK-TV1 (P=0.633) or CASK-TV2 (P=0.263). It is possible that 3 repeats were too few to have the statistical power required to show the difference between certain isoforms. However, if the data points for the strong binders (TV3, 6, and 7) and the weak binders (TV1, 2, and 5) are pooled into 2 groups, a two-tailed Student's t-test between the 2 groups returns a significant difference (P=0.0005), suggesting that the groups are indeed distinct.

One mechanism that could explain the difference in CASK:Sap97 binding strength between the 2 groups of CASK isoforms is the exclusion or inclusion of the exon 11-encoded region. CASK-TV3, TV6, and TV7 all lack the segment encoded by exon 11 while CASK-TV1, TV2, and TV5 all incorporate it (Fig 3.3B). Of the 4 alternatively spliced exons, exon 11 encodes the segment closest to the L27.1 domain of CASK where Sap97 binds (Fig 3.1A) (Jeyifous et al., 2009). This suggests that the inclusion or exclusion of the 6 amino acids in the CaMK-L27.1 linker region can change the conformation of the L27.1 domain to respectively decrease or increase the binding affinity of CASK to Sap97.

Fig 3.3

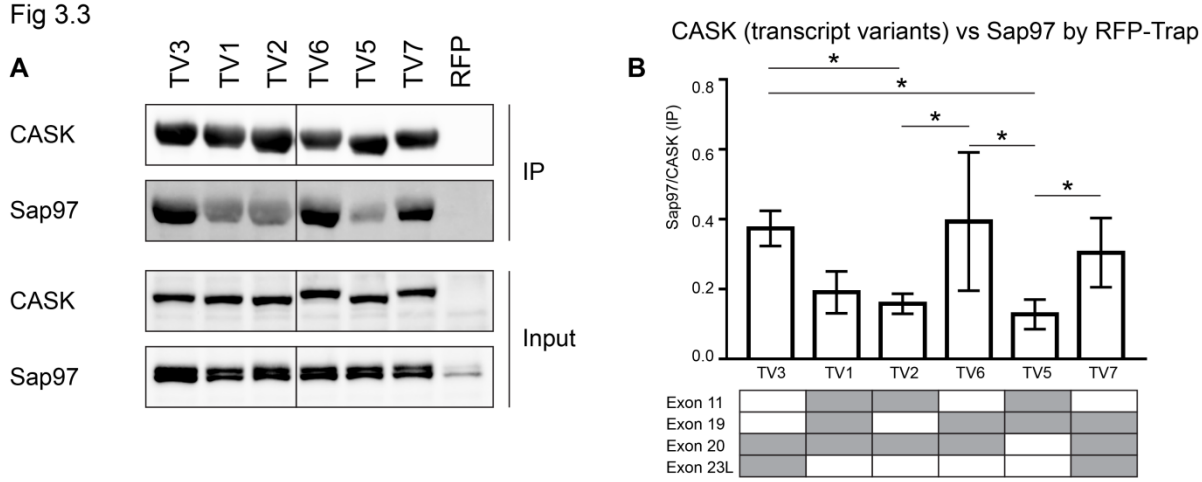

Figure 3.3: Sap97 binds more strongly to CASK isoforms without exon 11
(A) HEK293T cells were transfected plasmids coding for with multiple transcript variants of *RFP-CASK* with *Myc-Sap97*. CASK was immunoprecipitated after cell lysis by RFP-Trap and input and IP samples were analysed by SDS-PAGE and Western Blot. **(B)** After SM correction, each Sap97(IP) signal was normalized against the appropriate CASK(IP) signal to determine the binding efficiency of the different CASK transcript variants to Sap97. CASK isoforms lacking the exon 11 encoded segment (TV3, TV6, & TV7) bound significantly more strongly to Sap97 than CASK isoforms including it. N=3, *P<0.05, 1-way ANOVA with Tukey's multiple comparisons test.

3.1.4 Neurexin-1β does not show preferential binding to any of the CASK-TVs

To measure the ability of the various CASK transcript variants' ability to bind to Neurexin-1β, HEK293T cells were transfected with plasmids coding for multiple transcript variants of WT *RFP-CASK* and *HA-Neurexin-1β*. The signals of immunoprecipitated Neurexin-1β and CASK were then quantified and analyzed as described above.

In these experiments, no transcript variants bound to Neurexin-1β significantly more or less strongly than any other. The biggest difference between two conditions was between CASK-TV1 and TV2, but even they were not significantly different from each other (P=0.096) (Fig 3.4A,B). The work of Li et al. (2014) and Zeng et al. (2018) have shown that MAGUKs bind to their PDZ ligands via the assembly of their PDZ, SH3, and GK domains into an integrated PSG supramodule. By contrast, the interaction partners I discussed so far bind to a single domain of CASK. This collaboration between multiple domains to bind to Neurexin-1β may explain why the inclusion or exclusion of the segments encoded by the alternatively spliced exons had no effect on the binding of CASK to Neurexin-1β.

As mentioned earlier in section 3.1.2, all of the *CASK* transcript variants I test here include either exon 19 or 20, or both, but cannot lack both. Exon 19 and 20 encode the sequence of amino acids between the PDZ and SH3 domains of CASK. The formation of the PSG supramodule in MAGUKs requires the hydrophobic interaction of the PDZ and SH3 domains (Pan et al., 2011). The fact that all CASK isoforms bound equally well to Neurexin suggests that the inclusion of either or both of the segments encoded by exon 19 and 20 do not affect the ability of the PSG supramodule to form. However, it would be highly interesting to test whether the simultaneous absence of the segments encoded by exon 19 and 20 could disrupt the formation of the PSG supramodule and by extension, the binding of CASK to Neurexin.

These CoIP assays provide the first indication that the transcript variants of CASK may exhibit functional specificity. For example, CASK is known to play both a role in transcription regulation via Tbr1 (Y.-P. Hsueh et al., 2000; G.-S. Wang et al., 2004) and regulate NMDAR & AMPAR receptor sorting by binding to Sap97 (Jeyifous et al., 2009; Lin et al., 2013). CASK-TV2 binds strongly to Tbr1 but weakly to Sap97. One may therefore speculate that *CASK* may be spliced into its *TV2* variant when neurons need to upregulate CASK's

transcriptional regulation role without upregulating its protein trafficking role. CASK is also expressed in multiple tissues (Hata et al., 1996) and it would be interesting to see if different tissues express different *CASK* transcript variant profiles.

Fig 3.4

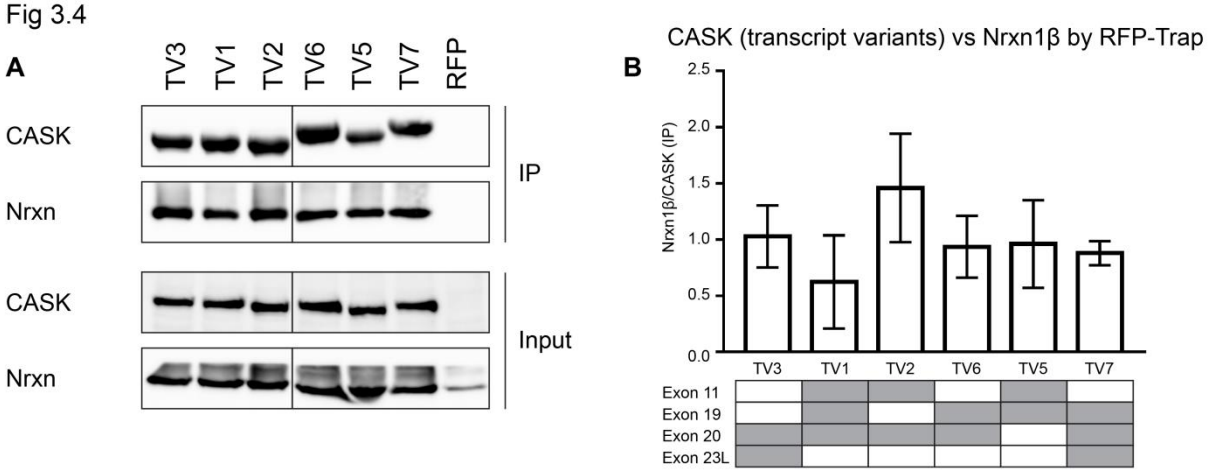

Figure 3.4: Neurexin-1β binds equally well to all CASK isoforms
(A) HEK293T cells were transfected with plasmids coding for multiple transcript variants of *RFP-CASK* with *HA-Nrxn1β*. CASK was immunoprecipitated after cell lysis by RFP-Trap and input and IP samples were analysed by SDS-PAGE and Western Blot. **(B)** After SM correction, each Nrxn1β(IP) signal was normalized against the appropriate CASK(IP) signal to determine the binding efficiency of the different CASK transcript variants to Nrxn1β. All CASK isoforms bound equally well to Nrxn1β. N=3, *P<0.05, 1-way ANOVA with Tukey's multiple comparisons test.

3.2 Missense mutations alter the binding of CASK-TV3 to its partners

Next, I pursued the primary goal of my thesis: to investigate how missense mutations identified in hemizygous male patients affect the functions of CASK. As in the previous sections, the simplest way to screen for important mutations was to investigate how these mutations affect the binding of CASK to its interaction partners using CoIP by RFP-Trap. The most interesting CASK mutant and partner combinations were then further investigated using various functional assays appropriate for the CASK function associated with each partner.

I investigated 12 missense mutations of *CASK* identified in hemizygous male patients: 5 were previously published mutations and 7 were new mutations reported by collaborators (Fig 3.1A). Because the new mutations were reported to our lab over the course of 3.5 years, the 12 mutations could not be simultaneously tested in a single screening experiment. Mutations were therefore split into 2 groups whose statistics were computed separately. The first group of 9 mutations consists of 5 published mutations (Y268H, L354P, P396S, Y723C, and W914R) and 4 new mutations (R489W, M507I, G521V, and N798Y) that were reported early enough to be tested with the first 5 mutations in both the coimmunoprecipitation experiments and the functional assays. 2 new mutations (G161R and V849A) were reported after the functional assays had been concluded. Therefore, new binding assays were performed with WT *CASK* and only these two mutants. Because these 2 mutations did not significantly change CASK:Partner binding, they were not tested in functional assays. The CASK:Liprin-α2 binding affinity tests were performed late enough for all 11 mutations to be combined into a single group. The 12th and last mutation, R140G, came too late to be included in the coimmunoprecipitation experiments but was included in one of the functional assays.

3.2.1 CASK:Tbr1 and CASK:CINAP binding are affected by the Y723C and W914R mutations

To test the effects of the missense mutations on CASK:Tbr1 binding, I performed a CoIP experiment using RFP-Trap on HEK293T cells transfected with WT and mutant *RFP-CASK-TV3* and *Myc-Tbr1*. However, this experimental setup gave very unstable results. The amount of Tbr1 coimmunoprecipitated by any one CASK

mutant could be higher than WT in one experiment and lower in the next in an unpredictable manner. This experimental setup therefore showed no significant difference in the binding affinity of WT or mutant CASK to Tbr1 (data not shown).

Knowing that CASK and Tbr1 also form a complex with CINAP (G.-S. Wang et al., 2004), I wondered if adding CINAP may somehow stabilize the binding behaviour of Tbr1. Therefore, I repeated the experiment, but triple transfected the HEK293T cells with WT and mutant *RFP-CASK-TV3*, *Myc-Tbr1*, and *HA-CINAP*. The addition of CINAP stabilized the behaviour of Tbr1 and made it possible to analyze the effects of CASK missense mutations on CASK:Tbr1 binding. In this +CINAP condition, 2 of the 4 mutations in the GK domain of CASK significantly decreased the ability of CASK to bind to Tbr1. CASK:Tbr1 binding was decreased to 47% of WT by Y723C (P=0.02) and decreased to 14% of WT by W914R (P<0.0001) (Fig 3.5A,B). This was not due to a lack of Tbr1 expression: the Tbr1 (Input) blots for these 2 mutations were similar in intensity to the WT condition, meaning that a similar amount of Tbr1 was expressed in these two conditions as in the WT condition. The other 2 mutations of the GK domain, N798Y and V849A did not significantly alter CASK:Tbr1 binding relative to WT (Fig 5C,D).

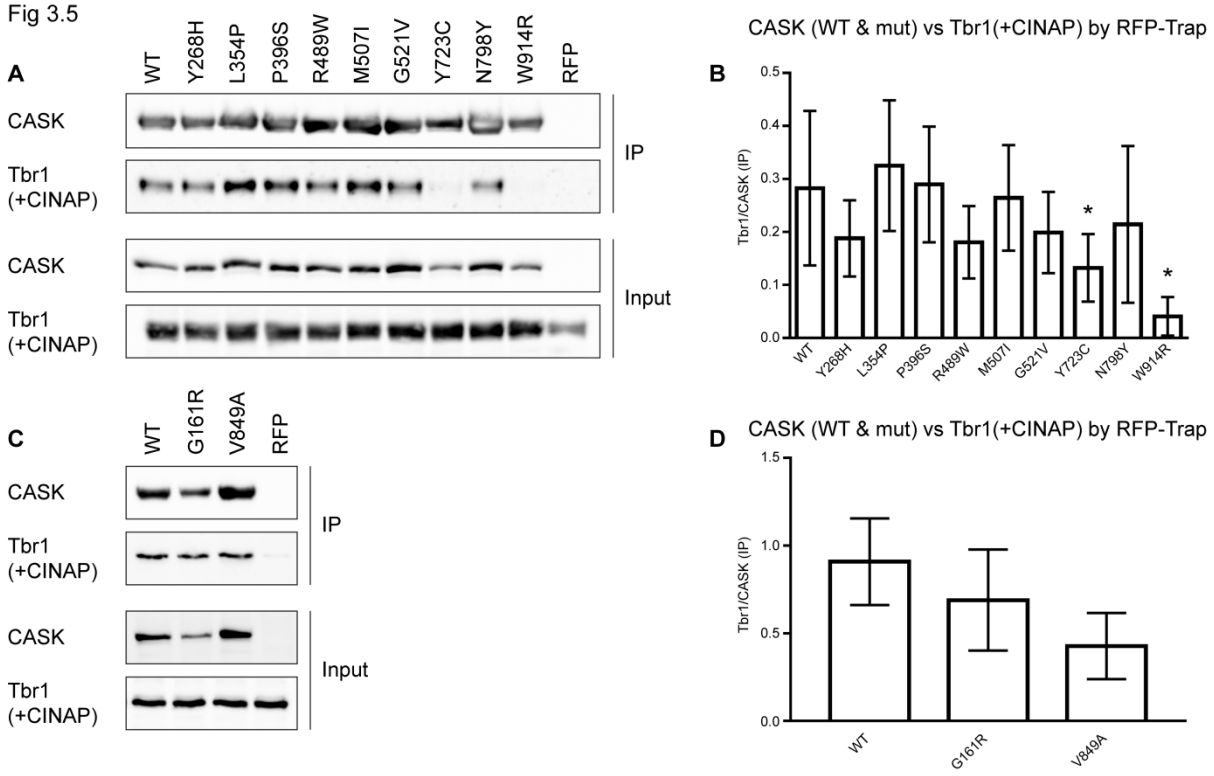

Figure 3.5: CASK:Tbr1 binding is decreased by the Y723C and W914R mutations in a CASK, Tbr1, CINAP triple overexpression context. **(A+C)** HEK293T cells were transfected with plasmids coding for WT and mutant *RFP-CASK-TV3* with *Myc-Tbr1* and *HA-CINAP.* CASK was immunoprecipitated after cell lysis by RFP-Trap and input and IP samples were analysed by SDS-PAGE and Western Blot. **(B+D)** After SM correction, each Tbr1(IP) signal was normalized against the appropriate CASK(IP) signal to determine the binding efficiency of the different CASK mutants to Tbr1. CASK:Tbr1 binding was decreased by the Y723C and W914R mutations compared to WT. N=7 for A & B, N=3 for C & D, *P<0.05, 1-way ANOVA with Dunnett's multiple comparisons test against WT.

The Y723C and W914R mutation are particularly interesting because they correspond to the Y710 and W904 residues of Sap97. These residues were identified as being of key importance to the SH3:GK interaction that mediates the formation of the PSG supramodule in Sap97 and other MAGUKs (Zhu et al., 2011; Zhu et al., 2016) as discussed in section 1.2.3. It is therefore possible that the SH3:GK interaction is also required for the binding of CASK to Tbr1. This may also explain why the N798Y and V849A did not disrupt CASK:Tbr1

binding as they are not known to be important for SH3:GK interaction. How the SH3:GK interaction may impact CASK:Tbr1 binding, however, is not yet clear.

The PSG of MAGUKs has so far been shown to form two conformation, one straight, one folded. Studies of PSD-95 (McGee et al., 2001) and Sap97 (Zhu et al., 2011; Zhu et al., 2016) suggest that both as monomers and multimers, the conformation of the PSG supramodule can be linear. A study of PALS1 (Li et al., 2014) suggests that MAGUKs could also take on a folded conformation, though this one is strictly possible upon dimerization. The current results suggest that CASK:Tbr1 interaction requires the formation of a functional PSG supramodule, though it is not possible to determine whether CASK is in a linear or folded conformation when bound to Tbr1.

Having seen that CINAP could stabilize CASK:Tbr1 binding, I then investigated how CASK:CINAP interaction was affected by the various missense mutations in the presence and absence of Tbr1.

To test the CASK:CINAP binding affinity in the triple-overexpression context, I analyzed the same RFP-Trap lysates from section 3.2.1 but stained membranes for CINAP in western blot and normalized the CINAP (IP) signal against the same CASK blots from 3.2.1 (Fig 3.5A vs 3.6A, CASK blots).

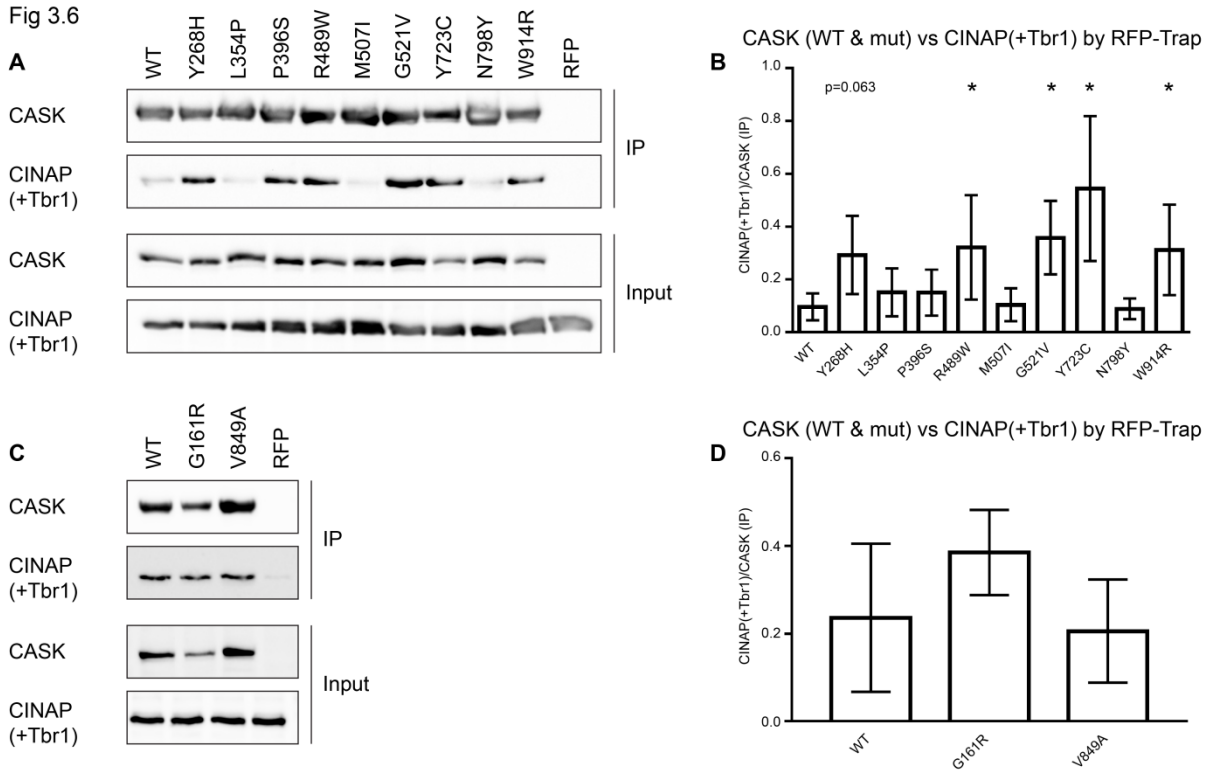

Figure 3.6: CASK:CINAP binding is increased by the R489W, G521V, Y723C, and W914R mutations in a CASK, Tbr1, and CINAP triple overexpression context. **(A+C)** HEK293T cells were transfected with plasmids coding for WT and mutant *RFP-CASK-TV3* with *Myc-Tbr1* and *HA-CINAP.* CASK was immunoprecipitated after cell lysis by RFP-Trap and input and IP samples were analysed by SDS-PAGE and Western Blot. **(B+D)** After SM correction, each CINAP(IP) signal was normalized against the appropriate CASK(IP) signal to determine the binding efficiency of the different CASK mutants to CINAP. CASK:CINAP binding was increased by the R489W, G521V, Y723C, and W914R mutations compared to WT. N=7 for A & B, N=3 for C & D, *P<0.05, 1-way ANOVA with Dunnett's multiple comparisons test against WT.

In the CASK + Tbr1 + CINAP context, CASK:CINAP interaction was made significantly stronger by the Y723C and W914R mutations (Fig 3.6B), the same two mutations which decreased CASK:Tbr1 interaction (Fig 3.5B). The Y23C mutation increased CASK:CINAP binding to 480% of WT (P=0.0001) and the W914R increased CASK:CINAP binding to 290% of WT (P=0.0138). The other two mutations of the GK domain, N798Y (Fig 3.6B) and V849A (Fig 3.6D) did not significantly affect CASK:CINAP affinity.

Interestingly, 3 mutations outside the GK domain also increased CASK:CINAP affinity. In the PDZ domain, the R489W mutation increased CASK:CINAP binding to 286% of WT (P=0.0228) and the G521V mutation increased CASK:CINAP binding to 330% of WT (P=0.0054). In the CaMK domain, the Y268H mutation was also able to increase CASK:CINAP binding (Fig 3.6A), though not quite significantly (P=0.063).

I also investigated the CASK:CINAP interaction in the context of cells only overexpressing CASK and CINAP (Fig 3.7). In this CASK + CINAP overexpression context, the effect of the GK domain mutations was proportionally even more dramatic than in the triple overexpression context. The Y723C mutation increased CASK:CINAP binding to 650% of WT (P=0.0001) and the W914R mutation increased CASK:CINAP binding to 450% of WT (P=0.0001). The higher percentage difference observed may likely be due to the low amount of CINAP bound by CASK-WT relative to CASK-Y723C and W914R (Fig 3.7A, CINAP IP) despite the presence of CINAP in all conditions (CINAP Input). In contrast to the GK domain mutations, the mutations outside the GK domain no longer increase CASK:CINAP binding (Fig 3.7A,B) compared to the triple overexpression context (Fig 3.6A,B).

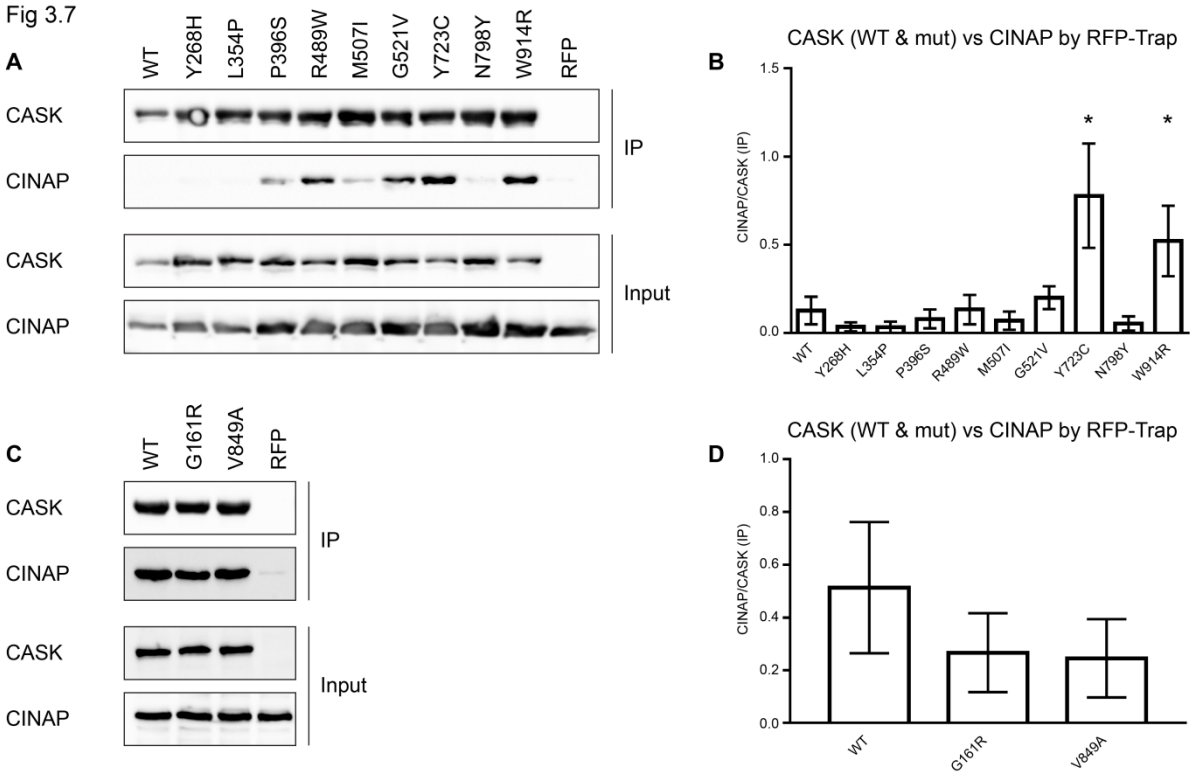

Figure 3.7: CASK:CINAP binding is increased by the Y723C and W914R mutations in a CASK and CINAP double overexpression context. **(A+C)** HEK293T cells were transfected with plasmids coding for WT and mutant *RFP-CASK-TV3* with *Myc-Tbr1* and *HA-CINAP.* CASK was immunoprecipitated after cell lysis by RFP-Trap and input and IP samples were analysed by SDS-PAGE and Western Blot. **(B+D)** After SM correction, each CINAP(IP) signal was normalized against the appropriate CASK(IP) signal to determine the binding efficiency of the different CASK mutants to CINAP. CASK:CINAP binding was increased by the Y723C and W914R mutations compared to WT. N=7 for A & B, N=3 for C & D, *P<0.05, 1-way ANOVA with Dunnett's multiple comparisons test against WT.

The ability of the Y723C and W914R to increase CASK:CINAP binding strength while decreasing CASK:Tbr1 binding strength was somewhat surprising as I expected binding to both partners to be decreased by the two mutations. The mechanism underlying this difference in effect is unclear. One possible explanation is that Tbr1 and CINAP may compete for a shared binding site and that the Y723C and W914R mutations favour the binding of CINAP over Tbr1. However, the study from G.-S. Wang et al. (2004) suggests that the two partners simultaneously bind to CASK and do not compete.

3.2.2 CASK:Sap97 interaction is completely inhibited by the L354P mutation

Next, I wanted to investigate whether any of the missense mutations I studied could disrupt CASK:Sap97 binding. If so, it would suggest that the disruption of NMDAR trafficking could be a pathogenic mechanism underlying CASK missense mutations. To investigate whether any of the *CASK* missense mutations could affect CASK:Sap97 interaction, I performed a coimmunoprecipitation experiment using RFP-Trap in HEK293T cells transfected with plasmids coding for WT or mutant *RFP-CASK-TV3* and *Myc-Sap97*.

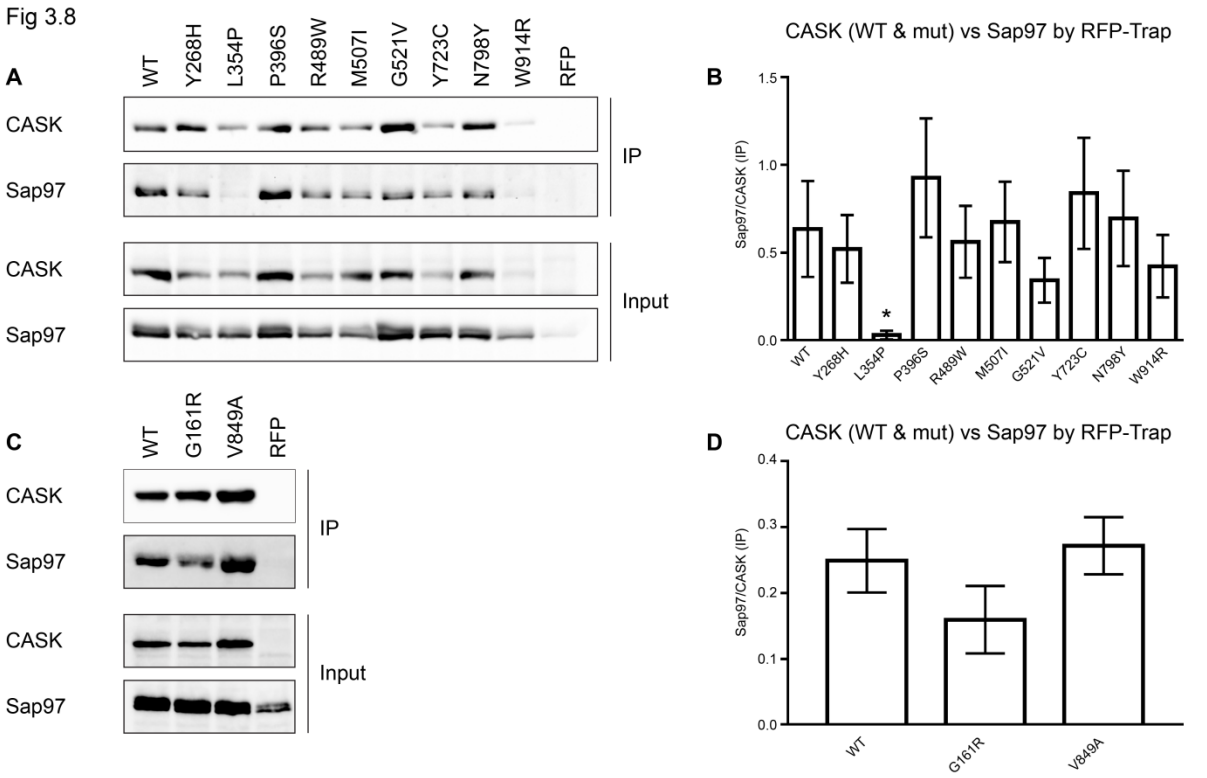

Figure 3.8: CASK:Sap97 interaction is disrupted by the L354P mutation **(A+C)** HEK293T cells were transfected with plasmids coding for WT and mutant *RFP-CASK-TV3* with *Myc-Sap97.* CASK was immunoprecipitated after cell lysis by RFP-Trap and input and IP samples were analysed by SDS-PAGE and Western Blot. **(B+D)** After SM correction, each Sap97(IP) signal was normalized against the appropriate CASK(IP) signal to determine the binding efficiency of the different CASK mutants to Sap97. CASK:Sap97 binding was decreased to ~5% of WT by the L354P mutation (P=0.0001). N=7 for A & B, N=3 for C & D, *P<0.05, 1-way ANOVA with Dunnett's multiple comparisons test against WT.

Here, I observed that CASK:Sap97 binding was strongly inhibited by a mutation of the L27.1 domain. The L354P mutation dramatically decreased CASK:Sap97 binding to ~5% of WT (P=0.0001) (Fig 3.8A,B). However, the P396S mutation of the same domain did not have any effect on CASK:Sap97 binding and was in fact the strongest binder, though not significantly stronger than WT. None of the other CASK missense mutations had a significant effect on the CASK:Sap97 interaction. The complete lack of CASK:Sap97 interaction resulting from the L354P mutation suggests that the ability of Sap97 to traffic NMDARs could be disrupted in the neurons with the CASK-L354P mutation.

3.2.3 CASK:Liprin-α2 binding was not affected by any missense mutations

In the presynapse, CASK primarily plays a scaffolding role and anchors multiple protein complexes to presynaptic adhesion sites via its interaction to Neurexin (Hata et al., 1996). For example, CASK may couple synaptic adhesion to vesicle release by forming the CASK:Velis:Mint1 complex (Butz et al., 1998). CASK may also anchor the core components of the presynaptic active zone to presynaptic adhesion sites via its interaction to Liprin-α2 (Olsen et al., 2005).

A study by Spangler et al. (2013) revealed that CASK levels in the presynapse are regulated by Liprin-α2. Thus, in addition to the CASK:Neurexin interaction, which I will explore in the next section, the CASK:Liprin-α2 interaction also needs to be investigated. Loss of this interaction could be expected to both disrupt the ability of CASK to link not only the presynaptic active zone, but also other presynaptic complexes to adhesion sites, and thus could be a potent pathogenic mechanism. To test whether the *CASK* missense mutations could impact CASK:Liprin-α2 binding, I performed coimmunoprecipitation experiments using RFP-Trap in HEK293T cells transfected with plasmids coding for WT or mutant *RFP-CASK-TV3* and *HA-Liprin-α2*.

CASK:Liprin-α2 binding proved to be very robust. None of the missense mutations located in the CaMK domain or L27.1 domain, where Liprin-α2 binds to CASK (Olsen et al., 2005; Wei et al., 2011), or any of the other missense mutations affected the amount of Liprin-α2 coimmunoprecipitated by CASK (Fig 3.9). The consistency of the Liprin-α2/CASK signal across WT and mutant CASK was impressive: the L354P mutant which deviated furthest from WT only increased to 117% of WT.

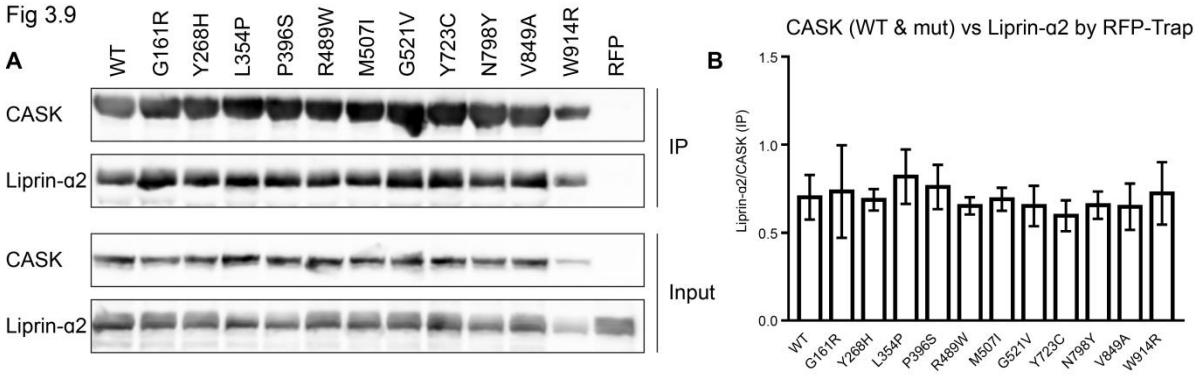

Figure 3.9: CASK:Liprin-α2 interaction is not disrupted by any mutation **(A+C)** HEK293T cells were transfected with plasmids coding for WT and mutant *RFP-CASK-TV3* with *HA-Liprin-α2.* CASK was immunoprecipitated after cell lysis by RFP-Trap and input and IP samples were analysed by SDS-PAGE and Western Blot. **(B+D)** After SM correction, each Liprin-α2(IP) signal was normalized against the appropriate CASK(IP) signal to determine the binding efficiency of the different CASK mutants to Liprin-α2. CASK:Liprin-α2 binding was not changed by any of the missense mutations. N=3 *P<0.05, 1-way ANOVA with Dunnett's multiple comparisons test against WT.

3.2.4 CASK:Neurexin-1β binding was affected by mutations in the PDZ and GK domains

The other presynaptic binding partner of CASK that I tested was Neurexin-1β. Neurexins are presynaptic adhesion proteins that are of critical importance for the formation and maintenance of synapses (Craig & Kang, 2007; Dean et al., 2003). Neurexin-1β binds to the PDZ domain of CASK (Hata et al., 1996) and underlies CASK's ability to anchor multiple other protein complexes to presynaptic adhesion sites. Loss of CASK:Neurexin-1β binding could be an important pathogenic mechanism for CASK missense mutations. To test whether the *CASK* missense mutations could affect CASK:Neurexin-1β binding, I performed coimmunoprecipitation experiments using RFP-Trap in HEK293T cells transfected with plasmids coding for WT or mutant *RFP-CASK-TV3 and HA-Neurexin-1β.*

The interaction between CASK and Neurexin-1β was the most interesting. The 3 mutations of the CASK-PDZ domain affected CASK:Neurexin-1β as expected. CASK:Neurexin-1β binding was decreased to 53% of WT by the R489W mutation (P=0.0014) and to 50% of WT by the M507I mutation (P=0.0006). The 3rd PDZ domain mutation was far more disruptive: G521V decreased CASK:Neurexin-1β to 1% of WT (P=0.0001) (Fig 3.5B).

Surprisingly, 2 mutations of the GK domain, Y723C and W914R, also severely decreased CASK:Neurexin-1β binding. The Y723C mutation decreased CASK:Neurexin-1β interaction to 1% of WT (P=0.0001) and the W914R mutation decreased it to 2% of WT (P=0.0001). These two mutations thus have an even stronger effect than the R489W and M507I mutations of the PDZ domain. These were the same 2 mutations that decreased CASK:Tbr1 binding (Fig 3.5B) and increased CASK:CINAP binding (Fig 3.6B, 3.7B).

Re-analysis of the data using Tukey's multiple comparisons test to compare every mutation against every other showed that the R489W and M507I mutations are statistically distinguishable from the G521V, Y723C, and W914R mutations. This suggests that the mutations can be grouped into a mild and strong category.

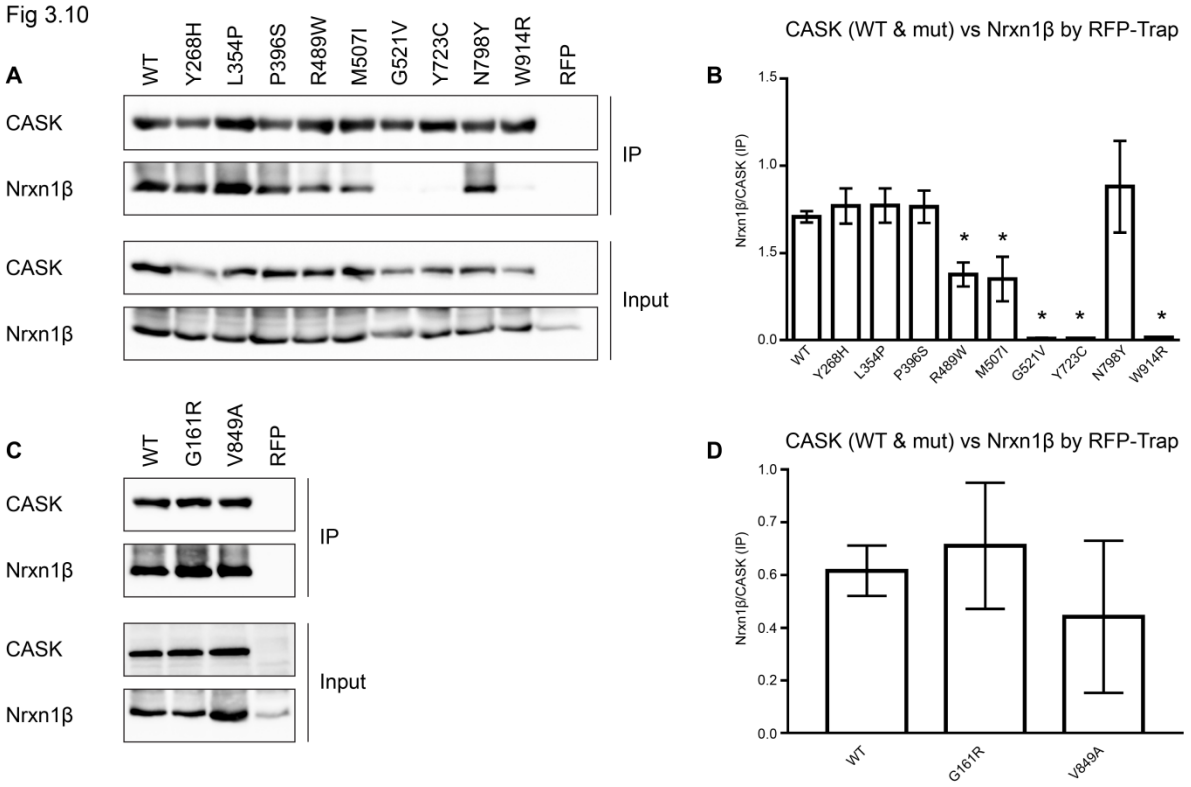

Figure 3.10: CASK:Neurexin-1β (Nrxn1β) interaction is partially disrupted by the R489W and M507I mutations, and completely disrupted by the G521V, Y723C, and W914R mutations **(A+C)** HEK293T cells were transfected with plasmids coding for WT and mutant *RFP-CASK-TV3* with *HA-Nrxn1β*. CASK was immunoprecipitated after cell lysis by RFP-Trap and input and IP samples were analysed by SDS-PAGE and Western Blot. **(B+D)** After SM correction, each Nrxn1β(IP) signal was normalized against the appropriate CASK(IP) signal to determine the binding efficiency of the different CASK mutants to Nrxn1β. CASK:Nrxn1β binding was decreased to 50% of WT by the R489W and M507I mutations and to ~1% of WT by the G521V, Y723C and W914R mutations. N=3 *P<0.05, 1-way ANOVA with Dunnett's multiple comparisons test against WT, and with Tukey's multiple comparisons test.

3.3 Functional Consequences of CASK:Partner Interaction Loss

Because CASK relies on its interaction partners to fulfill its molecular functions, it is highly likely that the mutations which disrupt CASK:Partner binding will in turn disrupt the function associated with each specific partner. I therefore tested the 3 functions of CASK with 3 separate assays.

3.3.1 The transcriptional activity of the CASK:Tbr1 complex could not be measured

Tbr1 and CINAP are the CASK interaction partners associated with CASK's transcription regulation function. Coimmunoprecipitation experiments showed that the Y723C and W914R mutations decrease CASK:Tbr1 binding and increase CASK:CINAP binding (Section 3.2.1 & 3.2.2). In order to determine whether or not this affects the ability of CASK to regulate gene transcription, I performed dual luciferase experiments.

A dual luciferase assay works by transfecting cultured cells with a mix of 2 plasmids encoding 2 different chemoluminescent Luciferase proteins. The first Luciferase, *Firefly*, is put under the control of a promoter of interest. The more the promoter is active, the more Firefly Luciferase is expressed.

In order to compensate for changing transfection efficiencies from plate to plate, a second Luciferase, *Renilla* is put under the control of a constitutively active promoter. The use of a premix of plasmids ensures that the ratio

of *Firefly* to *Renilla Luciferase* plasmids stays constant across the conditions of one experiment, so that when the chemoluminescence from Firefly is normalized against the chemoluminescence from Renilla, it is only indicative of the transcriptional activity of the promoter of interest controlling *Firefly* expression and not transfection efficiency. The cells are then further transfected with additional plasmids to test their effect on the activity of the promoter of interest. At the time of measurement, the chemoluminescent signal from Firefly and Renilla Luciferase are measured sequentially and the Firefly signal is normalized to the Renilla signal.

Fig 3.11

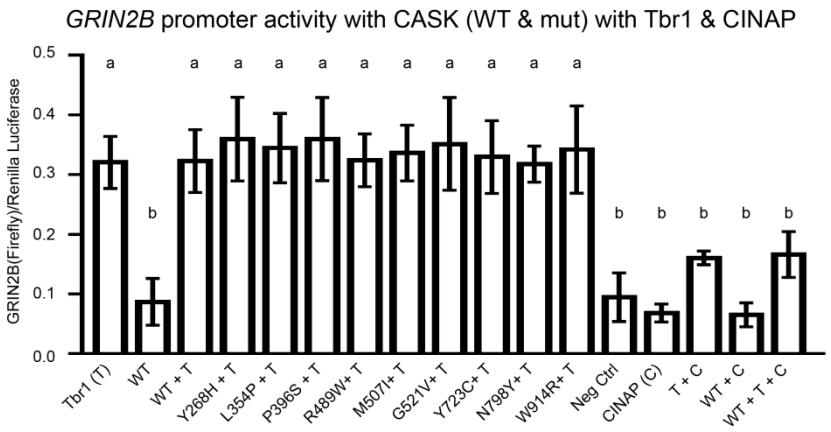

Figure 3.11: CASK:Tbr1 transcriptional activity could not be measured
HEK293T cells were transfected with plasmids coding for *GRIN2B promoter-controlled Firefly Luciferase*, constitutively expressed *Renilla Luciferase*, WT or mutant *RFP-CASK-TV3*, and *Myc-Tbr1* and/or *HA-CINAP*. The chemoluminescence of Firefly luciferase was normalized against the chemoluminescence of Renilla luciferase to determine the transcriptional activity of the *GRIN2B* promoter. Tbr1 was capable of increasing transcriptional activity relative to negative control, but the further addition of CASK-WT did not further increase transcriptional activity. Therefore, whether the Y723C and W914R mutation inhibit CASK:Tbr1-mediated transcriptional activity could not be determined. The addition of CINAP decreased the transcriptional activity of Tbr1 or CASK + Tbr1 conditions back to negative control levels. N=3, 1-way ANOVA followed by Tukey's multiple comparisons test. Columns not sharing a letter are significantly different at P<0.05.

CASK is known to regulate the expression of *GRIN2B*, which encodes the NR2b subunit of the NMDAR, and the expression of the *Reelin* gene (Y.-P. Hsueh et al., 2000; G.-S. Wang et al., 2004). I therefore performed dual luciferase experiments using Firefly luciferase under the control of the *GRIN2B* promoter and *Reelin* promoter. HEK293T were transfected with *Firelfy* and *Renilla Luciferase* plasmids as well as plasmids encoding WT or mutant *RFP-CASK-TV3*, *Myc-Tbr1*, and *HA-CINAP* in various combinations.

Despite using an experimental design similar to Y.-P. Hsueh et al. (2000), I was not able to replicate all of their results. I also saw that Tbr1 increased transcriptional activity of the *GRIN2B* promoter relative to negative control (P=0.001) and that CASK-WT on its own did not (P=0.9999) (Fig 3.11A). However, when Tbr1 and CASK-WT were transfected together, I was not able to see a further increase in the transcriptional activity of the *GRIN2B* promoter compared to Tbr1 alone (P=0.9999). The Tbr1+CASK-Y723C and Tbr1+CASK-W914R conditions did not have lower transcriptional activity of the *GRIN2B* promoter relative to Tbr1+CASK-WT. However, this is more likely due to the Tbr1+CASK-WT condition not having been able to further increase the transcriptional acitivity of the *GRIN2B* promoter relative to the Tbr1 only condition rather than a lack of effect from the mutation.

G.-S. Wang et al. (2004) showed that CINAP downregulates Tbr1+CASK transcription activity at the *GRIN2B* promoter in Cos cells but upregulates it in primary cultured neurons. I similarly showed that the addition of CINAP to Tbr1 and Tbr1+CASK-WT supressed the transcriptional activity at the *GRIN2B* promoter back down to levels indistinguishable from negative control.

One explanation for the inability of overexpressed CASK to further increase the transcriptional activity of Tbr1 at the *GRIN2B* promoter is the presence of endogenous CASK. HEK293T are based on human embryonic

kidney cells (Graham, Smiley, Russell, & Nairn, 1977) which express CASK (Hata et al., 1996). It is therefore possible that the Tbr1-only condition actually reflects the transcriptional activity of Tbr1+CASK. This would also explain the lack of effects from the Y723C and W914R CASK mutants. Since these two mutants cannot bind to Tbr1, they would not be able to out-compete endogenous CASK for Tbr1 despite being overexpressed.

I repeated this experiment with *Firefly luciferase* under the control of the *Reelin* promoter (data not shown). However, in this experiment, the Tbr1-only and Tbr1+CASK-WT/mutant conditions all failed to increase the transcriptional activity at the *Reelin* promoter relative to negative control. Furthermore, the CASK-only condition and all the conditions with CINAP exhibited transcriptional activity at the *Reelin* promoter even lower than the negative control condition. These results are difficult to explain, but may suggest that the endogenous proteins expressed in HEK293T have the ability to increase transcription at the *Reelin* promoter. How CASK or CINAP could then inhibit the activity, however, is not possible to explain with the current data.

3.3.2 The surface NMDAR/AMPAR ratio in cortical neurons is not affected by the L354P mutation

Sap97 is involved in the trafficking of both NMDARs and AMPARs in neurons but shifts its binding preference from AMPARs to NMDARs when it forms a complex with CASK. Having seen in the coimmunoprecipitation experiments that the L354P mutation disrupts CASK:Sap97 binding, I wanted to investigate how this loss of binding may affect the trafficking of NMDARs and AMPARs. To test this, I infected primary culture cortical neurons with lentiviral particles encoding WT or mutant *RFP-CASK-TV3* at 7 days in-vitro (7 DIV). At 14 DIV, surface proteins were then purified by surface biotinylation and analyzed by SDS-PAGE and western blot. The ratio of NMDARs and AMPARs within this biotinylated fraction was calculated for neurons infected with WT and mutant *CASK*.

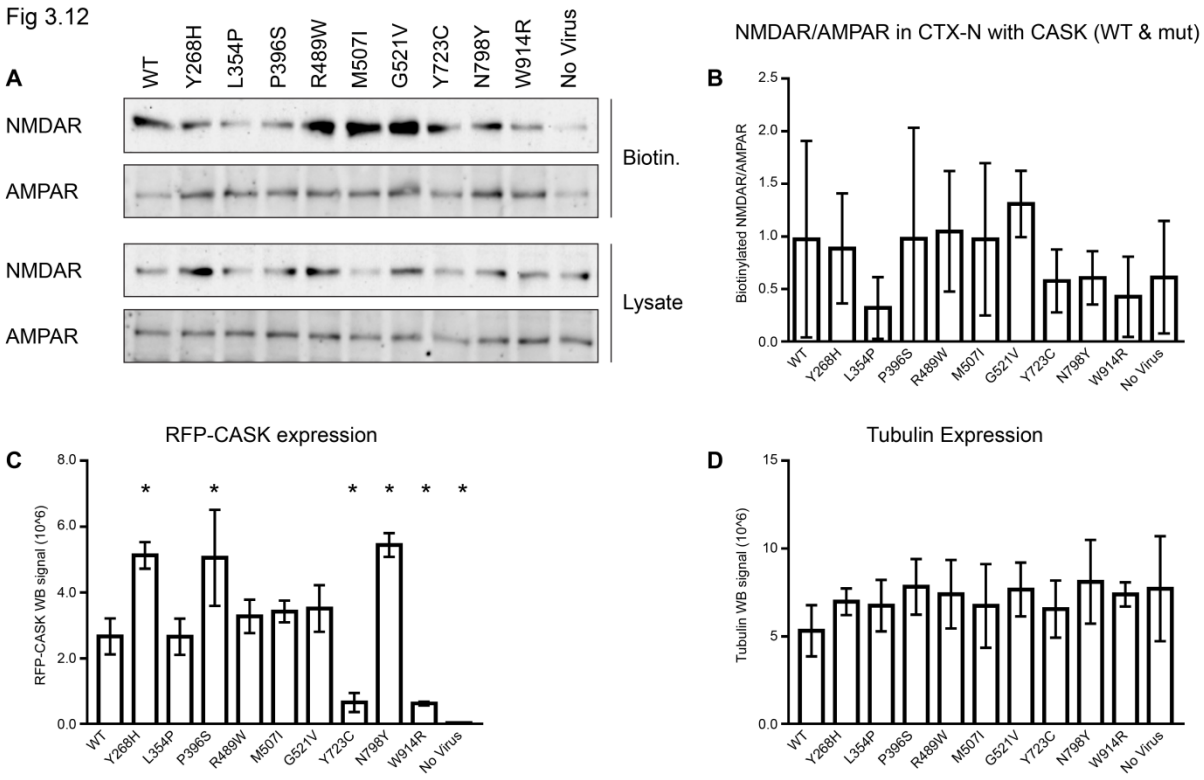

Figure 3.12: The ratio of surface NMDAR/AMPAR on cortical neurons was not affected by the L354P mutation. **(A)** Primary embryonic rat cortical neurons were infected at 7 days *in-vitro* (7DIV) with lentiviral particles encoding WT or mutant *RFP-CASK-TV3*. Surface proteins were purified by biotinylation and the amount of NMDARs and AMPARs in the biotinylated fraction were analyzed by SDS-PAGE and western blot. **(B)** The ratio of NMDARs/AMPARs on the surface of neurons overexpressing CASK-L354P was 33% that of neurons overexpressing CASK-WT. However, the difference was not significant (P=0.9712) due to high variance across conditions. **(C)** The level of CASK-L354P expressed was comparable to CASK-WT levels. **(D)** Similar Tubulin signal across conditions means that a similar amount of cortical neurons was processed across conditions. N=3, P<0.05, 1-way ANOVA followed by Dunnett's multiple comparisons test against WT

I decided to use lentiviral infection of cortical neurons because it would allow for a near 100% infection rate of all cultured neurons. Such high transfection rate is required in order to avoid the effect from transfected cells being masked by non-transfected cells. Viral particles were produced using a 2nd generation lentiviral system by transfecting HEK293T with an envelope plasmid, a packaging plasmid, and a lentiviral transfer plasmid encoding WT or mutant *RFP-CASK-TV3* as described in the methods section.

The L354P mutation decreased the NMDAR/AMPAR ratio to 33% of WT (Fig 3.12B). However, the standard deviation in each condition was very high and therefore, the difference between the WT and L354P conditions was not significant (P=0.9712). To ensure this was not due to lack of RFP-CASK expression, the full lysates were analyzed for expression of RFP-CASK and Tubulin. Western Blot analysis using anti-CASK showed that RFP-CASK-L354P was expressed at similar levels to RFP-CASK-WT (P=0.9999) (Fig 3.12C). Some CASK mutants, such as Y268H, P396S, Y723C, N798Y and W914R, were expressed significantly more or less than WT, though they do not explain the lack of effect from the L354P mutant. Tubulin staining was even across condition indicating that the amount of cells in each condition was similar (Fig 3.12D).

3.3.3 CASK oligomerization induced by Neurexin-1β and Liprin-α2 is inhibited by the G521V, Y723C, and W914R mutations

A previous study of the MAGUK PALS1 has provided evidence that PALS1 dimerizes when it binds to its PDZ-ligand Crumbs in a mechanism that involves its PSG supramodule (Li et al., 2014). The authors also suggest that CASK may behave in a similar way when it binds to its PDZ-ligand, Neurexin. In section 3.2.4, I have identified missense mutations of *CASK* that completely disrupt its ability to bind to Neurexin: G521V, Y723C, and W914R. I therefore wanted to test if these mutations also disrupt CASK oligomerization. If so, it would provide further evidence that CASK also oligomerizes upon binding to its PDZ ligand, a behaviour that has so far been shown in few MAGUKs, including PALS1 (Li et al., 2014) and PSD-95 (Rademacher et al., 2019; Zeng et al., 2018)

To test this, I performed split-YFP experiments measured by FACS with Debora Tibbe. HEK293T cells were transfected to express 2 versions of *CASK-TV5*, one fused to the N-terminal half of a YFP protein (CASK-YFP1) and one fused to the C-terminal half of YFP (*CASK-YFP2*). Interaction between a CASK-YFP1 and CASK-YFP2 protein should allow both halves of the YFP protein to reassemble and fluoresce. Yellow fluorescence was therefore used as a measure of CASK oligomerization and was measured in individual cells using Fluorescence Activated Cell Sorting (FACS). FACS allows for the measurement of the multiple fluorophores in a very large number of cells and therefore allows for measurement of an effect at the population level.

HEK293T cells used as controls were transected with plasmids coding for *eYFP* only, *mRFP* only, *CASK-YFP1 + mRFP*, *CASK-YFP2 + mRFP*, or left entirely untransfected in order for the appropriate fluorescence thresholds to be set for FACS analysis. HEK293T cells used in experimental conditions were transfected with plasmid coding for WT or mutant versions of *CASK-YFP1* and *CASK-YFP2* along with *HA-Neurexin-1β, HA-Liprin-α2*, or both, and *mRFP*. *Liprin-α2* was included even though it binds to the CaMK domain of CASK (Wei et al., 2011), not to its PDZ domain. However, it is also one of the presynaptic partners of CASK and in preliminary test experiments, it induced oligomerization as much as Neurexin-1β did. *mRFP* was included to act as a transfection indicator such that transfected cells could be distinguished from non-transfected cells, even in the absence of a YFP signal. Cells were given 2 days to grow after transfection to express the proteins before being resuspended in PBS and measured by FACS. We tested the R489W, M507I, and G521V mutations which strongly disrupted CASK:Neurexin-1β because we wanted to test the mutations with the greatest effect. We also tested the 3 mutations of the CaMK domain as negative control since they did not have any effect on CASK:Neurexin-1β interaction, but are within the domain where Liprin-α2 binds.

In the FACS assays, 10 000 analyzed "events" were recorded, which include dead cell fragments, clumps of multiple cells, or individual live cells that flowed through the fluorescent analysis chamber. In order to analyze only individual live cells, 2 selection criteria called "gates" were used. The first "cell viability gate" (Fig 3.13A) excludes dead cell fragments by selecting against events that cause too little frontal and side scattering of a light beam shined onto the analysis chamber. The second "single cell gate" (Fig 3.13B) selects for individual cells

and against multi-cell "clumps" by selecting only for events that have a certain value of front light scatter relative to peak front light scatter. The selection of the appropriate gates was done according to the recommendation of the staff of the FACS core facilities.

Fig 3.13

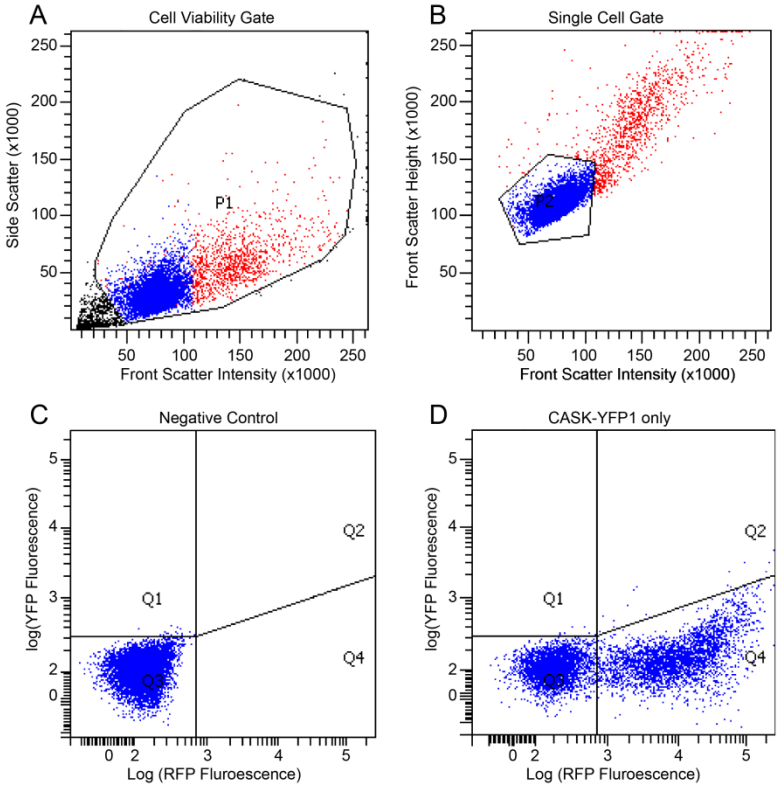

Figure 3.13 Controls and gate setting for FACS assay
(A) To exclude dead cells from analyzed cell population, cells with low Front Scatter and Side Scatter values were excluded. Viable cells have Front and Side scatter values within region defined by P1. **(B)** To exclude multi-cell clumps and to only analyze single cells, only fluorescent events within certain values of Front scatter and Side Scatter, defined by P2, were analyzed. **(C)** RFP fluorescence was used as the indicator of transfection. Threshold of RFP fluorescence (vertical line) was set using negative control cells that do not fluorescence in the RFP or YFP channels. **(D)** YFP fluorescence threshold (diagonal line) was set using cells transfected with *mRFP* only.

Cells that pass through both gates were then analyzed based on their RFP and YFP fluorescence. Non-transfected negative control cells which glowed in neither RFP or YFP were used to set the threshold for RFP fluorescence (Fig 3.13C). Cells whose RFP fluorescence was lower than this threshold were considered non-transfected and were not analyzed.

We used cells transfected with *mRFP*, which are RFP-fluorescent, but not YFP-fluorescent to define the threshold between non-YFP-fluorescent cells and YFP-fluorescent cells (Fig 3.13D, diagonal line on right between Quadrant 2 and Quadrant 4). The gate was then tested with cells transfected with *CASK-YFP1 + mRFP*, and *CASK-YFP2 + mRFP* as a negative control as these cells should also be non-YFP-flureoscent (Fig 3.13D, Q4). The need for a diagonal line between Q2 and Q4 is reflective of the imperfect separation of the RFP and YFP fluorescent channels. A certain degree of the RFP signal will always leak into the YFP channels detector and this contribution to the YFP channel signal must be rejected.

As cells were analyzed, they fell into one of the 4 quadrants based on their RFP and YFP fluorescence. Cells in quadrants 1 and 3 were not RFP fluorescence and therefore were not analyzed. Cells in quadrant 4 are transfected (based on their RFP-fluorescence) but are interpreted as having no CASK oligomerization (based on the absence of YFP-fluorescence). Cells in quadrant 2 are transfected cells (based on RFP fluorescence) that have CASK oligomerization (based on YFP fluorescence).

Observing the scatterplots produced, starting with the CASK-YFP1+2 without partner condition as baseline (Fig 3.14 Row 1), it can be seen that most transfected cells (Q2 & 4) fall below the threshold of YFP-fluroescence and are mostly in quadrant 4. However, slightly more cells are present in Q2 in this condition than in the negative CASK-YFP1 + RFP condition (Fig 3.14A vs 3.13D). This low degree of YFP fluorescence suggests that CASK may slightly oligomerize even in the absence of Neurexin or it may be indicative of a small degree of spontaneous YFP1 + YFP2 assembly simply due to the presence of the two proteins.

Fig 3.14

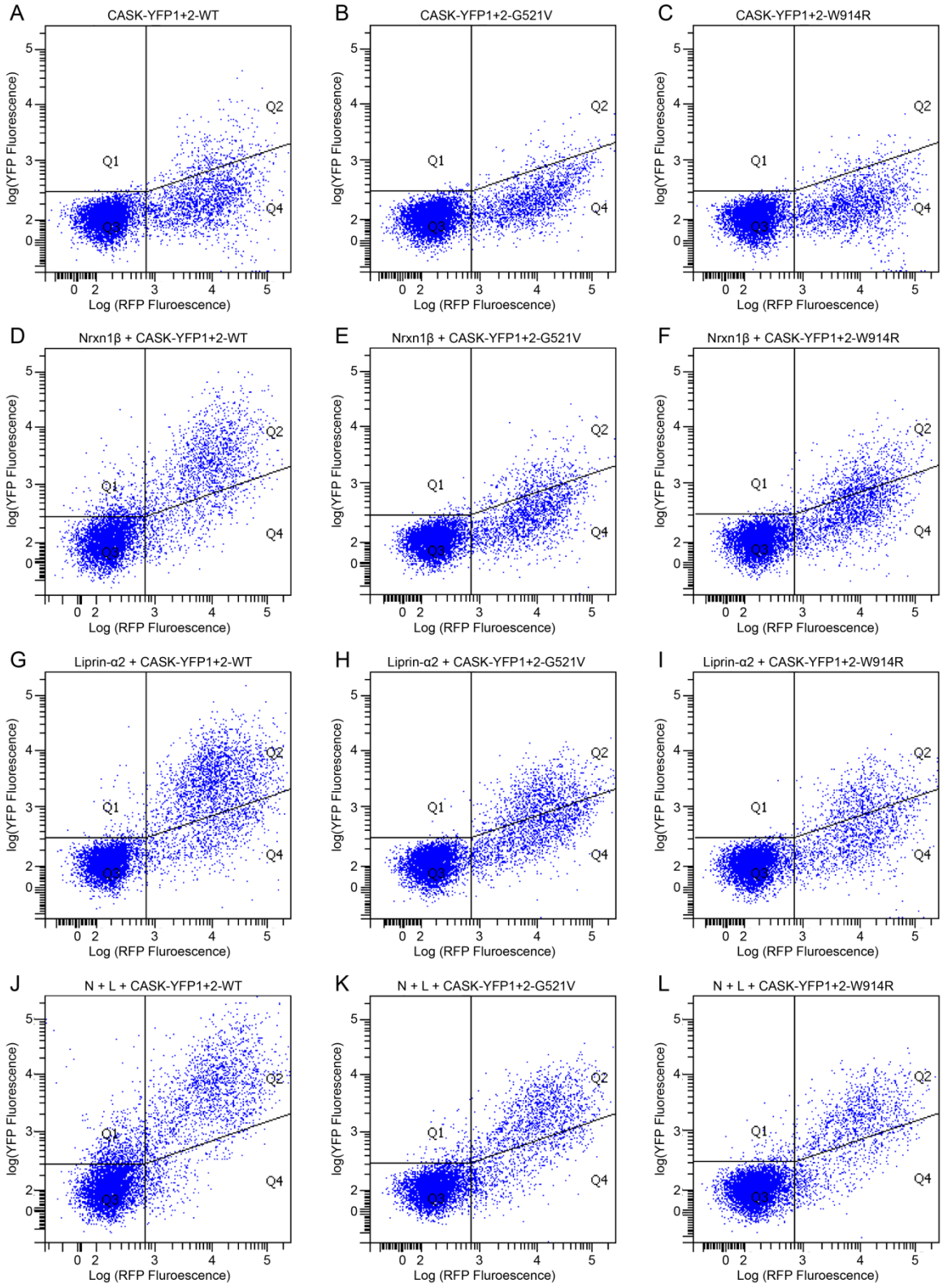

Figure 3.14: Oligomerization of WT and mutant CASK in the presence of presynaptic partners.
HEK293T cells were transfected with plasmids coding for WT or mutant *CASK-TV5-YFP1* and *CASK-TV5-YFP2* constructs with *HA-Nrxn1β*, *HA-Liprin-α2*, or both. RFP-fluorescence (Q2+4) is interpreted as transfection, and YFP-fluorescence (Q2) is interpreted as CASK oligomerization. Compared to CASK without partners **(Row 1)**, adding Nrxn1β **(Row 2)**, Liprin-α2 **(Row 3)**, or both **(Row 4)** increases the amount of CASK oligomerization. However, within each partner (Row), the G521V **(Col2)**, Y723C (not shown), and W914R **(Col3)** CASK mutants oligomerize less than CASK WT **(Col1)**.

When Neurexin-1β (Fig 3.14 Row 2), Liprin-α2 (Fig 3.14 Row3), or both (Fig 3.14 Row4) were added, YFP-fluorescence greatly increased (Fig 3.14, left columns) as indicated by the shift of the cells from Q4 towards Q2. However, in the conditions where CASK mutants had been expressed (Fig 3.14 G521V: middle column, W914R: right column), the increase in oligomerization is much lower. Furthermore, within each partner condition (Fig 3.14 Rows), the CASK mutants always oligomerize less than WT CASK.

To analyze the degree of CASK oligomerization, the mean YFP fluorescence of all transfected cells (Q2+4) was taken and compared across conditions (Fig 3.15). These values were recorded for 3 experiments and analyzed by 2-way ANOVA followed by Dunnett's multiple comparisons tests and Tukey's multiple comparisons test to determine the effect of adding binding partners vs no partner, the effect of the CASK mutations vs WT overall, and the effect of the CASK mutations vs WT within each partner condition.

Compared to the No Partner condition (Fig 3.15 left group), the addition of Neurexin-1β (Fig 3.15 centre left group), Liprin-α2 (Fig 3.15 centre right group), or both partners (Fig 3.15 right group) all significantly increases the oligomerization of CASK (P=0.0001). Interestingly, the mean YFP-fluorescence shows that the Neurexin-1β + Liprin-α2 condition (Fig 3.15 right group) increased oligomerization more than the two partners on their own (Fig 3.15 centre 2 groups) (P=0.0001).

Across partner conditions, the G521, Y723C, and W914R CASK mutants oligomerized significantly less than WT CASK (P=0.0001). Within the No Partner condition, none of the mutants were significantly different from WT (P>0.99). Within the Neurexin-1β, Liprin-α2, and both partner conditions, the G521V, Y723C, and W914R mutant CASK oligomerized significantly less than WT CASK (P<0.032).

Fig 3.15

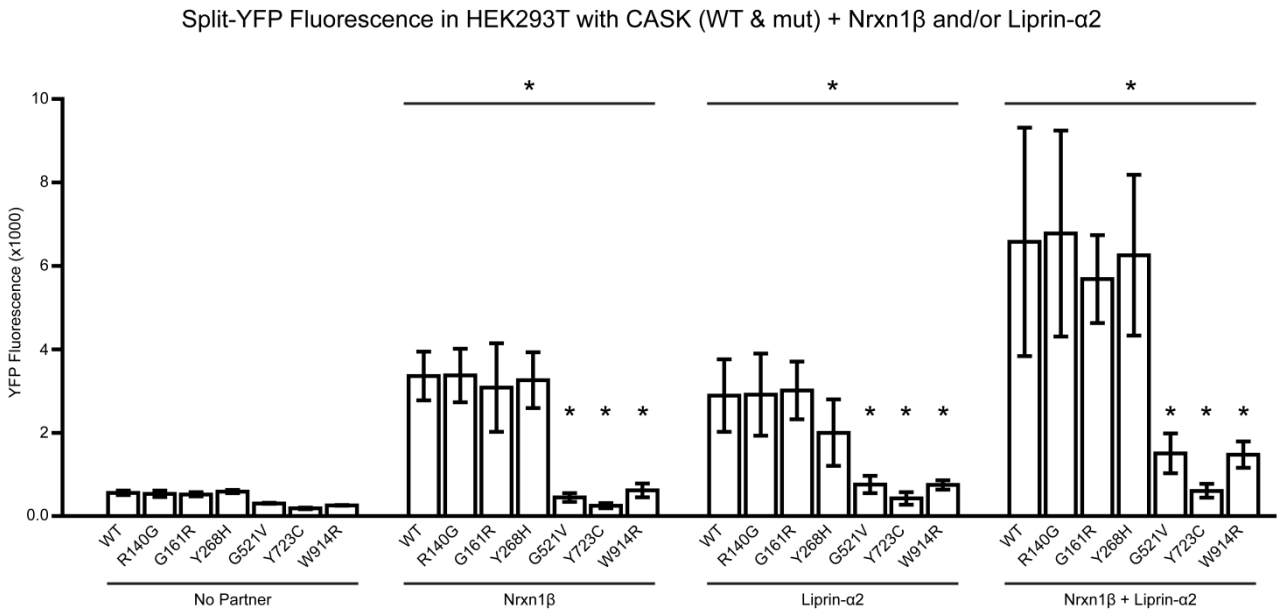

Figure 3.15: Quantification of CASK oligomerization by Split YFP and FACS.
(A) The first method to quantify CASK oligomerization was based on the mean YFP-fluorescence of the transfected cells. **(B)** The second was to quantify the percentage of transfected cells that had above threshold YFP fluorescence. In both conditions, the addition of Neurexin-1β, Liprin-α2, and both significantly increased CASK oligomerization compared to No Partner (P=0.0001). Within all the partner conditions, the G521V, Y723C, and W914R CASK mutants oligomerized significantly less than WT CASK (P<0.032). N=3, P<0.05, 2-way ANOVA followed by Dunnett's multiple comparisons test against WT and No Partner

Fig 3.16

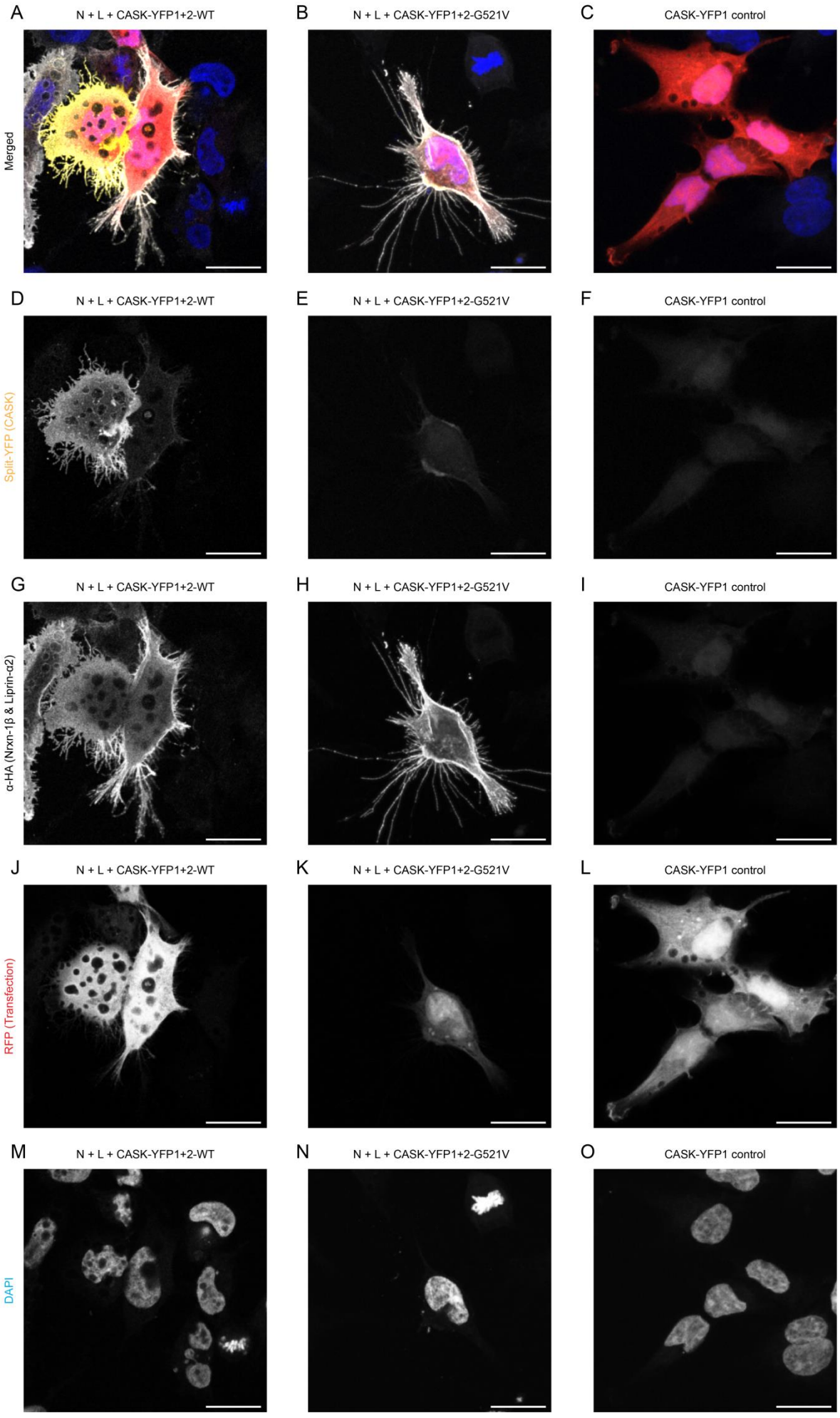
A
N + L + CASK-YFP1+2-WT
B
N + L + CASK-YFP1+2-G521V
C
CASK-YFP1 control
Merged
D
N + L + CASK-YFP1+2-WT
E
N + L + CASK-YFP1+2-G521V
F
CASK-YFP1 control
Split-YFP (CASK)
G
N + L + CASK-YFP1+2-WT
H
N + L + CASK-YFP1+2-G521V
I
CASK-YFP1 control
α-HA (Nrxn-1β & Liprin-α2)
J
N + L + CASK-YFP1+2-WT
K
N + L + CASK-YFP1+2-G521V
L
CASK-YFP1 control
RFP (Transfection)
M
N + L + CASK-YFP1+2-WT
N
N + L + CASK-YFP1+2-G521V
O
CASK-YFP1 control
DAPI

Figure 3.16 (Previous Page): Immunofluorescent imaging of HEK293T cells imaged by FACS.
(A) In HEK293T cells transfected with *CASK-YFP1+2-WT*, *HA-Nrxn1β*, and *HA-Liprin-α2,* CASK oligomerization, as revealed by YFP-fluorescence **(D)** colocalizes with **(G)** HA-Nrxn1β and HA-Liprin-α2. **(B)** Cells transfected with *CASK-G521V* have much weaker YFP-fluorescence compared to CASK-WT **(E vs D)**, though what little is present is localized to the plasma membrane, where HA-Nrxn1β and HA-Liprin-α2 are localized **(H)**. HEK293T cells transfected with *CASK-YFP1-WT* + *mRFP* were used as negative control and exhibit no YFP-fluorescence **(F)**. The presence of RFP fluorescence **(L)** shows that these cells are transfected and thus that the lack of YFP-fluorescence (F) is due to the inability of CASK-YFP1 to fluoresce on its own. The lack of signal in the shared HA-Nrxn1β and HA-Liprin-α2 channel shows that the anti-HA antibodies were specific. Scale bar = 20μm

During these experiments, some cells were taken out of the PBS resuspension meant for FACS analysis and imaged by fluorescence microscopy. They were fixed and stained with anti-HA antibodies to label overexpressed HA-Neurexin-1β and HA-Liprin-α2, and with DAPI to label cellular nuclei. Cells were imaged with a channel for YFP to gauge the amount and localization of oligomerization, a shared channel for Neurexin-1β and Liprin-α2 (both have an HA-tag and therefore could not be distinguished when staining), and for DAPI. The images were taken with consistent settings across images (except for the DAPI channel) in order to be able to compare the brightness between images. The effects described by the FACS assay could also be observed in the fluorescent images, with the added benefit of showing that the YFP-fluorescence signal in the HEK293T colocalizes with Neurexin-1β and Liprin-α2, further supporting the hypothesis that CASK oligomerizes in the presence of Neurexin-1β.

In HEK293T transfected with *CASK-WT-YFP1+2*, *HA-Neurexin-1β*, and *HA-Liprin-α2* (Fig 3.16 left column), CASK oligomerization, as revealed by YFP-fluorescence (Fig 3.16D, yellow in A), was colocalized with the shared staining for HA-Neurexin-1β and HA-Liprin-α2 (Fig 14G, white in A).

If CASK-G521V was used (Fig 3.16B & centre column), YFP-fluorescence was far dimmer (Fig 3.16E) despite the presence of HA-Neurexin-1β and HA-Liprin-α2 (Fig 3.16H). The presence of RFP in these cells (Fig 3.16K) suggests that these cells were successfully transfected and therefore, that the lack of YFP fluorescence is more likely due to failure of CASK to oligomerize than a lack of CASK expression.

Control cells transfected only with *CASK-YFP1* and *mRFP* (Fig 3.16C & right column) were imaged and show that the anti-HA antibodies were specific and did not stain any endogenous proteins in the HEK293T cells (Fig 3.16I). The cells imaged were transfected, as indicated by the RFP-fluorescence (Fig 3.16L). The lack of signal in the YFP channel shows that CASK-YFP1 cannot fluorescence on its own (Fig 3.16F).

One particularity of cells transfected with *HA-Neurexin-1β* is the formation of long tendrils (Fig 3.16G,H), which were absent from cells without *HA-Neurexin-1β* (Fig 3.16L). This effect was also present in cells with only *HA-Neurexin-1β* as interaction partner but absent in cells with only *HA-Liprin-α2* as interaction partner (data not shown), suggesting that Neurexin-1β is sufficient for inducing this morphology. It is unclear what the nature of these extensions is, but their similarity to neurites, especially in the cell from Fig 3.16H is striking. One could speculate that the presence of Neurexin-1β may be inducing a signaling pathway in the HEK293T cells that triggers an exploratory behaviour similar to that of neurites, even in non-neuronal cells.

The increase in YFP-fluorescence resulting from the addition of Neurexin-1β to the CASK-YFP1+2-WT conditions suggests that Neurexin-1β can induce the oligomerization of CASK, as was suggested by Li et al. (2014) and Zeng et al. (2018). As expected, the G521V, Y723C, and W914R mutations which strongly inhibit CASK:Nrxn1β binding were capable of inhibiting this oligomerization. As will be discussed in the discussion section 4.2.3, the G521V, Y723C, and W914R mutations likely simultaneously disrupt CASK:Neurexin-1β interaction and CASK oligomerization by disrupting the formation of the CASK PSG supramodule.

The most surprising results from these experiments, however, was that Liprin-α2 could also induce CASK oligomerization. Even more puzzling, the mutations that disrupted CASK:Neurexin-1β interaction-mediated CASK oligomerization also disrupted CASK:Liprin-α2 interaction-mediated oligomerization. Finally, analysis of the mean YFP-fluorescence of transfected HEK293T cells showed that Neurexin-1β and Liprin-α2 induced more YFP-fluorescence together than either could on their own (Fig 3.15A, right column vs centre 2 columns).

3.3.4 CASK trafficking is not disrupted by loss of Neurexin-1β binding

The results from the previous section demonstrated that loss of CASK:Nrxn1β binding can severely disrupt its ability to oligomerize and presumably, function as a scaffolding protein of the presynapse. Although CASK was first discovered as a presynaptic protein, the trafficking pathways that bring it there are not entirely understood. I therefore wanted to investigate if the loss of CASK:Neurexin-1β binding may be deleterious to the trafficking or retention of CASK to the presynapse.

To investigate this, I transfected primary cultured hippocampal neurons using calcium phosphate with plasmids coding for WT and mutants of *RFP-CASK-TV3* at 7 days in vitro (7 DIV). At 14 DIV, the neurons were fixed with 4% PFA and stained for the presynaptic marker vGlut1, for the dendritic marker Map2 and for the nucleus using DAPI. Images of these neurons were then collected using a Leica SP8 confocal microscope.

In general, RFP-CASK-WT localization is cytosolic in hippocampal neurons. This may be surprising for a MAGUK, but CASK has been previously shown to be diffusely cytoplasmic both in the soma (Y.-P. Hsueh et al., 2000) and in proximity to synapses (Samuels et al., 2007). I imaged cytoplasmic CASK both in the soma as well as in neurites (Fig 3.17A,B). The G521V mutation of CASK does not appear to change CASK localization, as it is also seen in the soma and neurites (Fig 3.17J,K). Although overexpressed RFP-CASK is primarily cytoplasmic, it was nevertheless possible to see concentrations of CASK in presynapses. Axons could be seen growing past the imaged neurons (Fig 3.17A, box enlarged in E). Axons were defined as neurites that were CASK-positive (Fig 3.17F,O) but Map2-negative (Fig 3.17H,Q). Presynapses were identified by the presence of vGlut (Fig 3.17G,P).

Although CASK was present diffusely along the axon, when axons crossed dendrites stained with Map2, CASK could be seen clustering in higher amounts with vGlut1 (Arrowheads, Fig 3.17F,G,H). This becomes even clearer upon performing a profile analysis to graph the fluorescence imaged along the axon (Profile of white line in 3.17E graphed in I). CASK-G521V behaved in a mostly similar manner. When axons containing CASK-G521V grew past dendrites (Fig 3.17N), CASK levels increased in clusters that colocalized with clusters of vGlut1, (arrowheads, Fig 3.17O,P). A profile analysis of these axons also shows that CASK colocalizes with vGlut1 in the proximity of dendrites (Profile of white line in 3.17N graphed in R). The similar localization of both WT and G521V CASK in hippocampal neurons therefore seems to suggest that the trafficking and retention of CASK to the presynapse are not affected by loss of CASK:Nrxn1β binding.

Figure 3.17 (Next page): CASK localization in neurons is not affected by loss of Neurexin-1β binding. At 7 days *in-vitro* (DIV), hippocampal neurons were transfected by $CaPO_4$ with WT and mutant *RFP-CASK-TV3*. At 14 DIV, the neurons were fixed and stained for the presynaptic marker vGlut1, for the dendritic marker Map2 and for the nucleus with DAPI. In neurons overexpressing CASK-WT **(A)** or CASK-G521V **(B)**, CASK is localized cytosolically both in the soma and in neurites. **(E)** Where axons cross dendrites, CASK **(F)** forms more intense clusters that colocalize with vGlut1 **(G)**, suggesting that CASK is localized presynaptically. Within the axons of neurons overexpressing CASK-G521V **(N)** CASK behaves similarly, forming clusters **(O)** that colocalize with vGlut1 **(P)**, suggesting that CASK:Nrxn1β interaction is not necessary to retain CASK in presynapses. Profile analyses **(I,R)** drawn along axons with WT **(E)** and G521V **(N)** more clearly illustrate the simultaneous rise in CASK and vGlut1 signal in the proximity of dendrites (arrowheads)
Scale bar = 20μm (A-D, J-M), 5μm (E-H, N-Q)

Fig 3.17

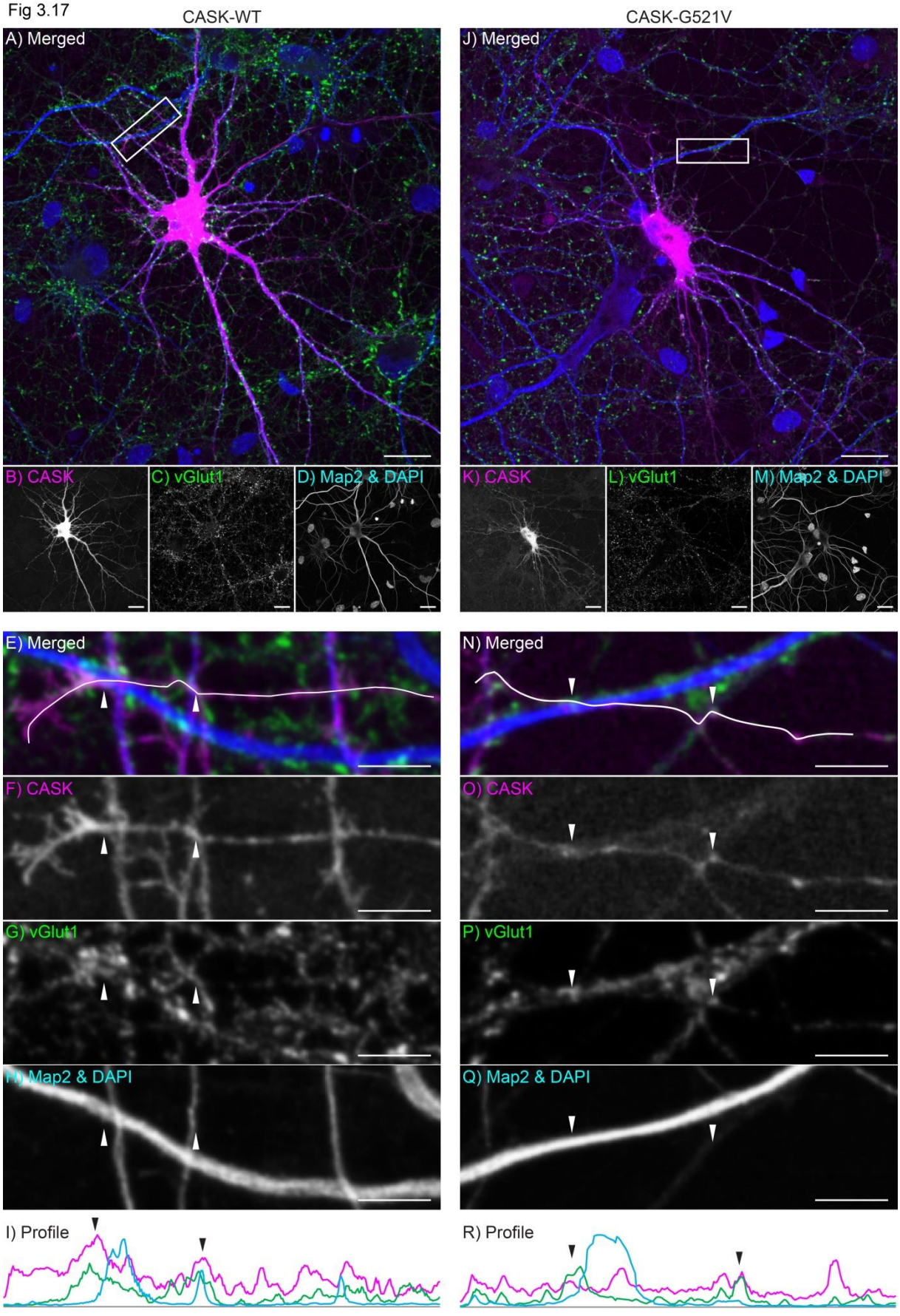
CASK-WT
CASK-G521V
A) Merged
J) Merged
B) CASK
C) vGlut1
D) Map2 & DAPI
K) CASK
L) vGlut1
M) Map2 & DAPI
E) Merged
N) Merged
F) CASK
O) CASK
G) vGlut1
P) vGlut1
H) Map2 & DAPI
Q) Map2 & DAPI
I) Profile
R) Profile

4. Discussion

4.1 Functional relevance of *CASK* transcript variants

Despite many years of study, one aspect of *CASK* that remains poorly studied is the alternative splicing of *CASK* and what functional consequences this may have. While generating *CASK* KO mice by insertional mutagenesis, Laverty and Wilson (1998) discovered that in mice, CASK is present in 2 isoforms: a shorter mCASK-A which only includes the N-terminus of CASK from the CaMK domain to the PDZ domain, and the full length mCASK-B. Ule et al. (2005) studied the neuronal splicing factor Nova using a genome-wide quantitative analysis of alternative splicing and showed that *CASK* was one of the genes whose splicing was regulated by Nova. However, because that was a screening experiment, they did not perform any functional assays nor determine which transcript variants of *CASK* may result from processing by Nova.

In the reference human transcript database, 4 transcript variants of *CASK* have been confirmed, named CASK TV1 to TV4 (GeneBank NM_003688, NM_001126054, NM_001126055, & NM_001367721). The transcript variants differ in their inclusion of 4 alternatively spliced exons: exons 11, 19, 20, and a small 5' extension of exon 23 (23L) (Table 3.1, Fig 3.1B).

We therefore wanted to investigate whether the CASK isoforms resulting from the various *CASK* transcript variants exhibit any functional specialization. To do so, we analyzed 29 CASK cDNA clones derived from human brain mRNA. Among these, we were able to find 3 of the 4 known *CASK* transcript variants: TV1, 2, and 3. Transcript variant 4 was not found among our 29 clones. Surprisingly, these 3 confirmed *CASK* transcript variants accounted for less than 50% of the 29 clones analyzed.

55% of the 29 clones consisted of unreported *CASK* transcript variants, which we have tentatively here called *CASK-TV5* to *TV8*. *CASK-TV5* accounted for 41.4% of the 29 clones, making it the single most abundant variant among our 29 clones. *CASK-TV6, 7,* and *8* were much rarer, accounting for 3.4%, 6.9% and 3.4% respectively.

We then searched the NCBI transcript databases for a match for all of our new *CASK* transcript variants. While *CASK-TV7* was matched to the predicted human *CASK-X2* variant (XM_005272686.4), none of the other transcript variants was matched to any variant in the human database, confirmed or predicted. We then widened our search to other species. Eventually, we were able to find predicted *CASK* variants for *CASK-TV6,* and *TV8* in other mammals. Most interesting, however, was the near perfect match between *CASK-TV5* and the confirmed rat variant of *Cask*. The translated protein sequences of the two transcripts also matched almost perfectly, with only 4 mismatches, 2 of which were conservative.

Three important aspects of these results are worth further discussion.

First, the inability to find even a predicted match for *CASK-TV5, TV6,* and *TV8* in the reference human transcript databases shows that the algorithm used to predict the possible transcript variants may not be accurate enough. This shows the importance of experimentally searching for and confirming the presence of *CASK* transcripts.

This brings up the 2nd aspect: the total number of *CASK* transcript variants that may exist. In our small sample of 29 clones, we were able to identify 4 new *CASK* transcript variants. However, it is highly likely that many other rare transcripts were missed. Indeed, we were not able to detect *CASK-TV4*, which is known to exist. If the 4 alternative spliced exons we identified here are the only ones present in CASK, then there would exist 16 possible transcript variants of CASK, 8 of which are now confirmed.

The third aspect is the relative abundance of the individual transcript variants. The confirmed *CASK* transcript variants (*CASK-TV1 to TV4*) collectively account for ~45% of our 29 clones. *CASK-TV5* on its own accounted for almost as much, accounting for ~40% of the 29 clones, making it the single most abundant *CASK* transcript variant. By contrast, *CASK-TV6, TV7,* and *TV8* were very rare, being found only once or twice among the 29 clones. The absence of *CASK-TV4* among our *CASK* clones also suggests that it may be a rare *CASK* variant.

It should be noted, however, that our sample size was relative small, at 29 clones. It therefore remains difficult to say with certainty whether the proportions we obtained here are reflective of the true proportions of *CASK* variants. Furthermore, *CASK-TV4*, a confirmed *CASK* transcript was not found among our 29 clones. This suggests that other *CASK* transcripts were also missed in our study.

It would be highly interesting to repeat this process with a larger number of samples in order to acquire a more accurate estimation of the relative abundance of various *CASK* transcript variants. Furthermore, it would be very interesting to investigate whether or not certain *CASK* transcript variants may be relatively more or less abundant in certain brain regions. In fact, although *CASK* is most highly expressed in the brain, it is also expressed in non-neuronal tissues (Hata et al., 1996). It may therefore also be interesting to investigate whether certain *CASK* transcript variants are enriched or exclusive to other tissues.

The challenge with such an experiment is the need for an efficient method to sequence and quantify the relative abundance of different *CASK* transcript variants. Methods like RNA-seq which normally allow for high throughput sequencing are not suitable for this application. The technique is based on Next-Generation Sequencing (NGS) which sequences short segments of nucleotides and reassembles them by local overlap alignment during analysis. This approach allows for the detection of the exons and even for the quantification of their relative abundance, but is not well suited to determine which exons were expressed with which other within a specific transcript. Our approach of amplifying the *CASK* cDNA and cloning these into plasmids is labour intensive, but may be the best method to determine which exons are present in individual transcript variants of *CASK*.

4.1.2 Functional specialization of CASK transcript variants

We wanted to investigate whether some of the *CASK* transcript variants may encode CASK isoforms that specialize in certain functions. One mechanism by which CASK isoforms could functionally specialize is to change their binding affinity for a specific interaction partner. I therefore performed coimmunoprecipitation experiments to test how well the different CASK isoforms we identified bind to Tbr1, Sap97, and Neurexin-1β. These three interaction partners were chosen as they are involved in CASK's function in gene regulation, receptor trafficking, and presynaptic scaffolding, respectively.

To find out if certain CASK isoforms may specialize in the regulation of gene transcription, we tested them for their ability to bind to Tbr1. CASK-TV2 emerged as the clear standout, binding significantly more to Tbr1 than CASK-TV3, TV5, and TV6, and near significantly more to CASK-TV1 and TV7 (Fig 3.2B). The mechanism by which CASK-TV2 binds to Tbr1 more strongly than the other CASK isoforms cannot be determined with the current data. Tbr1 binds to the GK domain of CASK (Y.-P. Hsueh et al., 2000) and the amino acid sequence encoded by exon 23L is the closest to the GK domain of CASK. While this segment is absent in CASK-TV2, it is also absent in CASK-TV1, TV5, and TV6, and present in CASK-TV3 and TV7, all of which bound weakly. Thus, the inclusion or exclusion of exon 23L is not predictive of CASK:Tbr1 binding strength. Because no study has specifically investigated the structure of the CASK-GK:Tbr1 complex, it is at this moment not possible to explain how CASK-TV2 achieves higher binding affinity to Tbr1 than other CASK isoforms.

To find out if certain CASK isoforms specialize in receptor trafficking, we tested the various CASK isoforms for their ability to bind to Sap97. The 6 CASK isoforms could be segregated into 2 groups: strong Sap97 binders, consisting of CASK-TV3, TV6, and TV7; and weak Sap97 binders, consisting of CASK-TV1, TV2, and TV5. The distinguishing feature between the strong and weak binders is the inclusion or exclusion of a 6 amino acids long segment encoded by exon 11. This exon 11-encoded segment is located in the linker region between the CaMK domain and L27.1 domain of CASK (Fig 3.1A,B). The strong binders (TV3, TV6, and TV7) all lack the exon 11-encoded segment while the weak binders (TV1, TV2, and TV5) all include the exon 11-encoded segment (Fig 3.3B). This suggests that the exon 11-encoded sequence interferes with the ability of CASK to bind to Sap97.

This is somewhat surprising given the known structure and interaction mode of the complex. Feng et al. (2004) solved the structure of a complex consisting of the rat CASK-L27.1 domain (including the exon 11-encoded segment) bound to the Sap97-L27.1 domain by X-ray crystallography. They showed that CASK-L27.1 and

Sap97-L27 form a tetrameric complex consisting of a dimer of CASK:Sap97 heterodimers. The formation of the dimer of heterodimers is mediated via the L27 domains of both CASK and Sap97. The L27 domains of both proteins are composed of 3 α-helices named αA, αB, and αC. A CASK:Sap97 heterodimer is first formed by an interaction between the αA and αB helices from the L27 domains of both proteins. The 4 α-helices are highly amphipathic and are oriented such that the 4 helices wrap around each other and form a central, hydrophobic core. The L27 domains of CASK and Sap97 both still have their αC helices free, which interact with the 2 αC helices from a second CASK:Sap97 heterodimer, mediating the formation of a tetrameric complex. Thus, CASK and Sap97 bind to each other via hydrophobic interactions.

The correlation between the absence of the exon 11-encoded segment and the higher CASK:Sap97 binding affinity was unexpected because the exon-11 encoded segment lies mostly outside the α-helices that mediate CASK:Sap97 interaction. Exon 11 encodes the LLAAER amino acid segment at positions 340 to 345 (*CASK-TV1* coordinates). Feng et al. (2004) showed that the C-terminal ER (344-345) residues encoded by exon 11 are part of the αA helix of CASK-L27.1, but do not form a part of the hydrophobic core of the 4 helices complex. The other 4 amino acids are part of the unstructured linker region between the CaMK and L27.1 domain of CASK. In CASK isoforms lacking the exon 11-encoded segment, the space upstream of the αA helix is filled by the DPTSSG sequence encoded by exon 10.

It is currently not possible to determine how the absence of exon 11 increases the binding affinity of CASK to Sap97. The structure resolved by Feng et al. (2004) included the segment encoded by *CASK* exon 11. It would be interesting to see whether the structure of the CASK-L27.1:Sap97-L27 complex changes in the absence of the exon 11-encoded segment. If it does not, it may suggest that CASK:Sap97 binding may be regulated by CASK domains other than only the L27.1, possibly the CaMK domain which is N-terminal of the linker region where the exon 11-encoded segment is located.

Finally, to test whether or not certain CASK isoforms may specialize in presynaptic scaffolding, I tested the various CASK isoforms for their ability to bind to Neurexin-1β. However, no CASK isoform bound significantly more to Neurexin-1β than any other isoform.

It would also be very interesting to test how the different isoforms of CASK affect CASK's binding to Liprin-α2 (Olsen et al., 2005), Mint1 (Butz et al., 1998), and CASKIN (Tabuchi et al., 2002). These are all presynaptic CASK partners that bind to the CASK-CaMK domain. Particularly interesting would be the effect of the exon 11-encoded segment, which our results showed to affect CASK:Sap97 binding, possibly through a general change in the conformation of L27.1. It is possible that the CaMK domain's folding could also be changed by the exon 11-encoded segment. Studies have shown that Mint1 can outcompete CASKIN (Tabuchi et al., 2002) and Liprin-α2 (L. E. LaConte et al., 2016) for the CaMK domain of CASK. However, these studies have used rat Cask which includes the exon 11-encoded segment. It would be highly interesting to see if the binding preference of CASK for these 3 CaMK partners changes if the exon 11-encoded segment were missing.

4.2 Functional relevance of CASK missense mutations

Studies of patients with *CASK* loss-of-function mutations suggest that CASK's role as a gene transcription regulator may be a key pathogenic mechanism. Patients with *CASK* loss-of-function mutations exhibit a typical microcephaly with pontine and cerebellar hypoplasia with intellectual deficiency phenotype (MICPCH + ID) (Hackett et al., 2009; Moog et al., 2015; Najm et al., 2008; Takanashi et al., 2012). The CASK:Tbr1:CINAP complex is involved in the transcription of the *Reelin* gene (G.-S. Wang et al., 2004), which is necessary for proper brain lamination and development (D'Arcangelo & Curran, 1998), and transcription of the *GRIN2B* gene which encodes the NR2B subunit of the NMDAR (Y.-P. Hsueh et al., 2000).

However, studies in *Cask-KO* mice suggest that loss of CASK's other functions may also contribute to pathogenicity. *Cask-KO* mice are non-viable, dying within hours of birth. However, they do not exhibit noticeable malformation of the brain (Atasoy et al., 2007). Instead, these mice exhibit more subtle cellular and molecular phenotypes. *Cask*-deficient neurons express fewer NR2B-containing NMDARs, which shifts the ratio of excitatory to inhibitory synapses in acute mouse brain slices towards excitatory (Mori et al., 2019). CASK is both involved in the transcription of the *GRIN2B* gene which encodes the NR2B subunit (G.-S. Wang et al.,

2004) and in the sorting and trafficking of NMDARs (Lin et al., 2013; Setou et al., 2000), giving CASK two mechanisms through which it may cause the loss of postsynaptic NMDARs. Finally, the level of CASK presynaptic partners such as β-Neurexins, Mint1, and Velis are decreased in *Cask-KO* mice (Atasoy et al., 2007), indicating the relevance of CASK as a presynaptic scaffolding protein.

Studies of patients with *CASK* missense mutations also suggest that loss of the gene transcription function is not the only pathogenic mechanism associated with CASK. While certain missense mutations such as L354P (Takanashi et al., 2012), P396S, and Y723C (Hackett et al., 2009) were associated with MICPCH + ID, other mutations like Y268H and W914R were associated with severe intellectual deficiency but not with microcephaly (Hackett et al., 2009), suggesting pathogenic mechanism other than transcription regulation. Furthermore, loss of other molecular functions of CASK, such as CASK:Neurexin interaction, may also be associated with microcephaly. For example, study by L. E. W. LaConte et al. (2018) investigated two CASK missense mutations associated with cerebellar hypoplasia (M519T and G659D), and found that these mutations disrupt CASK:Neurexin-1β binding. These results suggest that even individual *CASK* missense mutations may have a very wide variety of pathogenic mechanisms.

In this study, I investigated 5 previously reported *CASK* missense mutations and 7 new *CASK* missense mutations reported to us by collaborators (Fig 3.1A). The missense mutations are distributed along the length of the *CASK* gene, with no noticeable "hot spots" of mutations that would normally indicate particularly important locations in the protein product of a gene. This suggests that the various missense mutations may have diverse pathogenic mechanisms that affect different CASK functions. I therefore tested the relevance of the 12 missense mutations on all 3 of CASK's known functions.

To find out which mutations are relevant for which CASK function, I first performed a broad screening assay: rather than testing only the mutation located in the CASK binding domain of each partner, all *CASK* missense mutations were tested against all of the studied partners. Once I determined which mutations were relevant for which partner, I performed functional studies to determine how the change of binding to one partner affected the CASK function associated with that partner.

Multiple articles often report *CASK* missense mutations using coordinates based on different *CASK* transcript variants. In this thesis, the coordinates used are in the context of *CASK-TV1*. The experiment that investigated the effects of *CASK* missense mutations were performed with *CASK-TV3* and *CASK-TV5*. *CASK-TV3* was initially used as it was the variant available to me. All coimmunoprecipitation experiments were performed with CASK-TV3 in order to keep them consistent. For some functional assays, I used CASK-TV5, as it most closely resembles the rat Cask protein and I wanted to bring my experiments in line with previously published studies that often used the Rat *Cask* variant (Hata et al., 1996).

4.2.1 CASK as a transcription regulator

I used coimmunoprecipitation experiments to test the binding affinity of the WT and the 12 *CASK* mutants with Tbr1 and CINAP. In initial experiments with cells co-expressing *RFP-CASK (WT or mutant)* and *Myc-Tbr1*, the binding behaviour of Tbr1 to CASK was very inconsistent. A particular CASK mutant could bind to Tbr1 more strongly than WT CASK in one experiment, and then much more weakly in another. I was not able to determine the cause of this seemingly random behaviour. However, knowing that Tbr1, CASK, and CINAP form a complex (G.-S. Wang et al., 2004), I repeated the experiment in cells transfected with *RFP-CASK (WT or mutant)*, *Myc-Tbr1*, and *HA-CINAP*, and analyzed the amount of Tbr1 and CINAP precipitated by CASK. In the presence of CINAP, the binding of Tbr1 to CASK became more consistent.

In this "triple-transfected" condition, CASK:Tbr1 binding was significantly inhibited by the Y723C and W914R mutations (Fig 3.5B). At the same time, the Y723C and W914R mutations increased the CASK:CINAP binding (Fig 3.6B). Interestingly, CASK:CINAP binding was also increased by 3 other missense mutations: Y268H, R489W, and G521V, though Y268H did not do so significantly (P=0.063) (Fig 3.6B). Additionally, CASK:CINAP was further tested in cells transfected with *RFP-CASK (WT or mutant)* and *HA-CINAP*, without *Myc-Tbr1*. In this "double-transfected" condition, CASK:CINAP interaction was also increased by the Y723C and W914R mutations (Fig 3.7B), though the Y268H, R489W, and G521V mutations no longer increased

CASK:CINAP binding. Overall, it appears that the Y723C and W914R mutations are the two mutations relevant for the CASK:Tbr1:CINAP complex formation, and by extension, for CASK to function as a regulator of transcription.

Another question stemming from these results is how Tbr1 and CINAP interact when bound to CASK. In my results, CASK:Tbr1 interaction is unstable but can be stabilized by the addition of CINAP. The fact that it is the Y723C and W914R mutations that disrupt this interaction may provide an indication as to the mechanism underlying this behaviour. As discussed in section 1.2.2, MAGUK can form a PSG supramodule when their PDZ, SH3, and GK domains form intramolecular interactions. The Y723 and W914 residues in CASK correspond to the Y710 and W904 residues which in the MAGUK Sap97 have been identified as being necessary for the SH3:GK interaction (Zhu et al., 2011; Zhu et al., 2016). Both Tbr1 and CINAP are known to bind to the GK domain of CASK, but not to compete for it (Y.-P. Hsueh et al., 2000; G.-S. Wang et al., 2004). It is possible that Tbr1 preferentially binds to the GK domain of CASK when it is in a PSG supramodule or at least binds to the SH3 domain, while CINAP may prefer a more independent CASK-GK domain.

To test the effects of the Y723C and W914R mutations on CASK's function in gene transcription, I performed a dual luciferase experiment based on those performed by Y.-P. Hsueh et al. (2000) and G.-S. Wang et al. (2004). They showed that Tbr1 was able to increase transcription at the *Grin2b* promoter relative to negative control, and that the addition of CASK to Tbr1 further increased the transcriptional activity of Tbr1. However, the addition of CINAP in a non-neuronal context decreased the activity of the CASK:Tbr1 complex.

My results were slightly different (Fig 3.14). Relative to negative control, adding Tbr1 increased transcription activity while CASK-WT alone did not, matching the authors' results. However, when I combined WT or mutant CASK with Tbr1, I did not see a further increase in transcription activity relative to the Tbr1 only level as described by Hsueh et al.. As there was no effect of CASK WT with Tbr1, it was not surprising that CASK-Y723C or -W914R did not lead to any change in transcription activity when these two CASK mutants were combined with Tbr1.

One possible explanation for these results is that HEK293T cells express endogenous CASK. HEK293T cells are based on human embryonic kidney cells (Graham et al., 1977), and CASK is expressed in the kidneys, albeit at a lower level than in the brain (Hata et al., 1996). Interpreted from this perspective, it would mean that my "Tbr1 only" condition would more closely match the "CASK + Tbr1" condition from Hsueh et al.. This would also explain why the mutant forms of CASK had no effect on the transcriptional activity measured.

If the presence of endogenous CASK was the reason why overexpressed CASK did not increase the transcriptional activity of Tbr1, then the simplest approach would be to repeat the assay in a system without CASK. The experiment could be repeated using the same Cos-7 cells or Neuro-A2 cells used by the authors. However, one may assume that these cellular systems also express endogenous CASK. Alternatively, *CASK*-deficient HEK293T cells could be generated with CRISPR technology.

4.2.2 CASK in glutamate receptor trafficking

CASK has been shown to have a role in regulating the trafficking of NMDARs and AMPARs when its L27.1 domain binds to Sap97 (Jeyifous et al., 2009; Lin et al., 2013). Without CASK, Sap97 enters a closed conformation that contributes to the trafficking of AMPARs. When bound to CASK, Sap97 enters an open conformation that associates with and contributes to the trafficking of NMDARs. The binding of CASK to Sap97 is necessary for the trafficking of NMDARs. This was evident in cultured hippocampal neurons where the knock down of CASK caused a 46% decrease in the level of synaptic NMDARs and a corresponding 48% increase in the level of NMDARs in the somatic Golgi complex.

Of the 12 missense mutations I investigated, 2 were located in the L27.1 domain: L354P and P396S. Only the L354P mutation of the L27.1 domain had a significant effect on the CASK:Sap97 interaction, as it decreased interaction to less than 5% of WT (Fig 3.8B).

As briefly discussed earlier, the structure of the CASK-L27.1:Sap97-L27 complex was elucidated by Feng et al. (2004), who showed the two domains each contribute 2 alpha helices that coil around a hydrophobic core. The CASK-L354 residue is located in the αA helix of the CASK-L27.1 domain and is a conserved hydrophobic residue involved in the formation of the 4 helix coil. The replacement of a Leucine by a Proline residue in the CASK L354P mutation thus likely not only disrupts the hydrophobic interaction but also disrupts the formation of the αA helix, disrupting multiple hydrophobic interactions, which explains how it inhibits CASK:Sap97 interaction.

The P396 residue, by contrast, is not an evolutionarily conserved residue nor is it part of the helices of the CASK-L27.1 domain. Its replacements with Serine residue is a non-conservative one, but it likely happens within a region of the CASK-L27.1 domain that isn't critical for CASK:Sap97 binding.

I then tested whether this loss of interaction functionally impacted the ability of CASK to regulate the trafficking of NMDARs and AMPARs to the plasma membrane of neurons. To do so, I infected embryonic rat cortical neurons with lentiviral particles encoding WT and mutant *RFP-CASK* and then measured the amount of surface NMDARs and AMPARs. The surface NMDAR/AMPAR ratio measured in neurons infected with *CASK-L354P* was ~33% of the ratio measured in neurons infected with *CASK-WT* (Fig 3.12B). However, the effect was not statistically significant.

Overall, I expect that the L354P mutation has an effect on the trafficking of NMDARs and AMPARs; failure to detect any statistical significance may be due to 2 reasons. The first is the poor staining quality of the western blot membranes (Fig 3.12A). The antibodies used produced relatively faint bands with a high amount of background, leading to a poor signal-to-noise ratio. Another possibility is that the cortical neurons used in the experiments come from a WT rat background, and therefore still had endogenous CASK present. If the overexpressed CASK-L354P could not bind to Sap97 as our coimmunoprecipitation data suggest (Fig 3.8B), then the endogenous CASK could have been free to bind to Sap97 and mediate NMDAR trafficking.

Two other experiments could be performed to further test the effect of the L354P mutation on NMDAR trafficking. Jeyifous et al. (2009) performed an experiment in HEK293T cells overexpressing a combination of *NMDAR*, *Sap97*, and *CASK*. Using fluorescence imaging, they showed that overexpressed NMDARs trafficked normally to the plasma membrane, but were held back by overexpressed Sap97. They then showed that the further coexpression of CASK could rescue the trafficking of NMDARs to the plasma membrane, but that a CASK construct missing its L27.1 domain could not because it could not bind to Sap97. In principle, the L354P CASK mutant should also be unable to rescue the trafficking of NMDARs in HEK293T overexpressing NMDAR and Sap97.

A second experiment could test the effect of CASK-L354P on NMDAR trafficking in neurons using immunocytochemistry. Jeyifous et al. (2009) knocked down CASK in neurons, and measured the loss of NMDARs at synapses and the associated buildup of NMDARs in the soma by analyzing the colocalization of NMDARs with the synaptic marker Synapsin and the Golgi marker DsRed-ER. One possibility would therefore be to measure synaptic NMDAR levels in WT neurons and CASK knock down neurons, and then see if the overexpression of WT or L354P CASK can rescue the trafficking of NMDARs to the synapses.

4.2.3 CASK in presynaptic scaffolding

CASK was first identified as an interaction partner of Neurexin (Hata et al., 1996). The further discovery of multiple presynaptic CASK interaction partners such as α-Liprins (Olsen et al., 2005) suggest that CASK plays an important role as a presynaptic scaffolding protein. I therefore wanted to determine if any of the 12 missense mutations I studied interfered with the presynaptic scaffolding function of CASK.

I first tested whether the 12 missense mutations could affect the binding strength of CASK to Neurexin-1β and to Liprin-α2. The CASK:Liprin-α2 interaction proved to be extremely resilient and was not affected by any of the mutations tested (Fig 3.9B). By contrast, the CASK:Neurexin-1β interaction was affected by multiple mutations (Fig 3.10B). The R489W and M507I mutations located within the PDZ domain reduced the CASK:Neurexin-1β binding to ~50% of WT. The third mutation of the PDZ domain, G521V, completely

disrupted the CASK:Neurexin-1β binding. The most surprising results, however, were that the Y723C and W914R mutations located in the GK domain of CASK also completely disrupted the CASK:Neurexin-1β binding.

Two questions immediately arise from these results: why do the R489W and M507I mutations only partially disrupt CASK:Neurexin-1β interaction, and why do the Y723C and W914R mutations of the CASK-GK domain affect the binding of Neurexin-1β, which binds to the CASK-PDZ domain.

A study of the MAGUK PALS1 by Li et al. (2014) provides the most likely explanation. They showed that the binding affinity of the isolated PDZ domain of PALS1 and CASK for their PDZ ligands (Crumbs and Neurexin respectively) is lower than the affinity of the combined PDZ-SH3-GK domains. This suggested that both in PALS1 and in CASK, the PDZ, SH3, and GK domains act as an integrated PSG supramodule, a concept that has been previously studied in other MAGUKs (McGee et al., 2001; Nomme et al., 2011; Pan et al., 2011).

Li et al. (2014) solved the crystal structure of the PALS1:Crumbs complex (Fig 4.1). They showed that the PDZ and SH3 domains cooperate to form a binding pocket between them for Crumbs. Furthermore, the GK domain of PALS1 folds back onto the PDZ and SH3 domains in order to provide further binding sites for Crumbs. However, this folded conformation makes it impossible for the SH3 domain to interact with the GK domain the way it normally happens in MAGUKs. This should be a problem for PALS1; studies of the SH3:GK interface in the MAGUKs PSD-95 suggest that the separation of the GK domain from the SH3 domain should destabilize the SH3 domain because the GK domain normally provides 2 β-strands that are necessary for the stable folding of the SH3 domain (McGee et al., 2001). PALS1 solves this problem by dimerizing. As the GK domain folds away, it exposes the previously intramolecular interface between the SH3 and GK domains to the cytoplasm. Two PALS1:Crumbs complexes assemble such that their SH3 domain becomes stabilized by binding to the GK domain of the other PALS1:Crumbs monomer. The emerging picture is one where for PALS1, binding to Crumbs and dimerization are two closely associated phenomena. Given the structural similarity of CASK to PALS1 and the previously described PDZ and PSG supramodule vs PDZ-ligand binding assays where CASK and PALS1 behave in similar ways, it is likely that CASK takes on a similar conformation to PALS1 and dimerizes upon Neurexin-1β binding.

By identifying the PALS1 residues equivalent to the CASK R489, M507, G521, Y723, N798, V849, and W914 residues, it becomes possible to determine how the G521V, Y723C, and W914R mutations differ from the R489W and M507I mutations.

PALS1-G286 is the equivalent amino acid to CASK-G521 and is located in very close proximity to 2 amino acids critical for the PDZ:SH3 interaction: PALS1-R282 and V284 (Li et al., 2014). The G521V mutation likely disrupts the PDZ:SH3 interaction by replacing Glycine (the smallest amino acid) with Valine, a bulkier and more hydrophobic amino acid. The Y723C and W914R mutations are also critical for the formation of the PSG supramodule. In Sap97, the Y710 and W904 residues are critical for SH3:GK interaction by reaching from the GK domain towards the SH3 domain and anchoring the domains together (Zhu et al., 2011; Zhu et al., 2016). Sap97-Y710 and -W904 correspond to PALS1-Y466 and -W688, and to CASK-Y723 and -W914. The Y723C mutation replaces the bulky and hydrophobic Tyrosine side chain with the much smaller Cysteine while the W914R mutation replaces the hydrophobic Tryptophan amino acid with Arginine, a positively charged amino acid. Both mutations therefore likely disrupt the SH3:GK interaction necessary for CASK dimerization, which in turn is necessary to stabilize CASK in the GK-foldover conformation that binds to Neurexin-1β. Thus, the G521V, Y723C, and W914R mutations likely act similarly: they disrupt the formation of the dimerized CASK PSG supramodule, which is necessary for Neurexin binding.

By contrast, the equivalents of the CASK-R489 and -M507 amino acids in PALS1 are not located near the PDZ:SH3 or SH3:GK interfaces. It thus seems that the R489W and M507I mutations may affect CASK:Neurexin interaction by causing a local misfolding of the PDZ domain. However, the loss of binding at the PDZ domain is compensated both by the binding sites in the SH3 domain as well as the supplemental binding sites provided by the folded-over GK domain, hence why these mutations only decrease CASK:Neurexin binding by half.

Fig 4.1

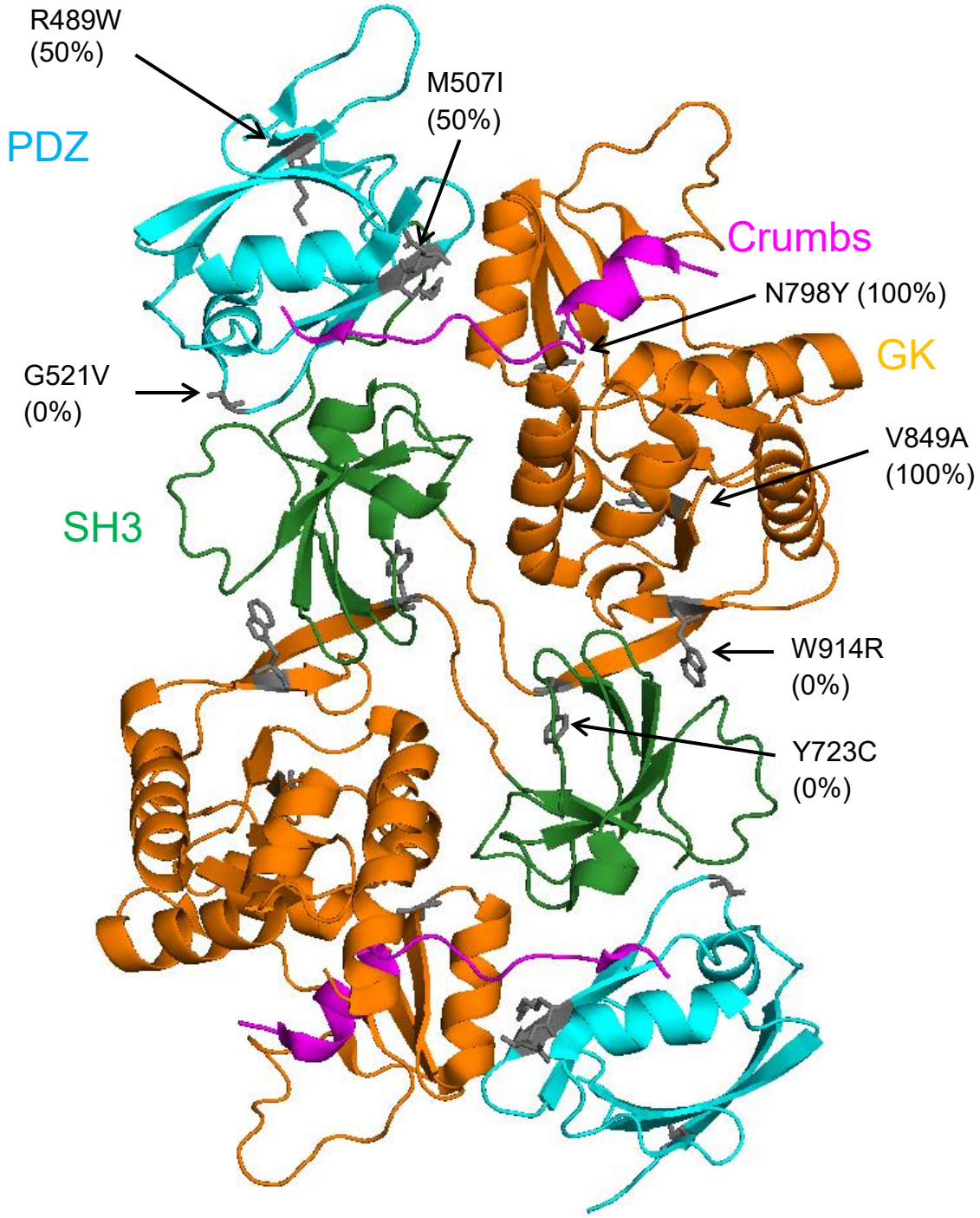

Figure 4.1: Crystal structure of the PALS1-PSG:Crumbs dimer complex. PALS1 residues corresponding to CASK missense mutations are highlighted in grey with CASK:Neurexin-1β affinity noted as percentage of WT. The G521V, Y723C, and W914R equivalent mutations are located within the PDZ-SH3 or SH3:GK interfaces and likely disrupt the formation of the CASK-PSG supramodule, thus disrupting CASK:Neurexin-1β interaction. The R489W and M507I equivalent mutations are located within the PDZ domain and likely cause a change in the folding of the PDZ domain that slightly decreases the affinity of CASK for Neurexin-1β. Figure modified from (Li et al., 2014)

I tested this hypothesis in two ways. The first was to use the SDM (Side Directed Mutator) tool created by Pandurangan, Ochoa-Montaño, Ascher, and Blundell (2017), and the second was to test for the ability of WT and mutant CASK to oligomerize in the presence of Neurexin by split-YFP.

The SDM tool is an online tool which takes a solved structure, and calculates whether the structure should become more or less stable after introducing a single amino acid substitution. Given the dimer structure of PALS1 and the PALS1 equivalents to the CASK mutations, the SDM tool mostly agreed with my previous interpretation and predicted a decrease in structure stability with the G521V, Y723C, and W914R mutation equivalents. By contrast, the R489W and M507I mutations were predicted to stabilize the structure. This indicates a change in the folding of the PDZ domain, potentially one that somehow decreases the affinity of CASK to Neurexin. Interestingly, the N798Y mutation was predicted to increase the stability of the PALS1 structure while the V849A was predicted to have the highest destabilizing effect on PALS1 structure.

CASK mutation	PALS1 equivalent	Δ(ΔG)	Stability
R489W	K255W	+0.76	More
M507I	R272I	+0.59	More
G521V	G286V	-2.99	Less
Y723C	Y466C	-0.09	Less
N798Y	K544Y	+0.09	More
V849A	I594A	-4.58	Less
W914R	W668R	-0.6	Less

Table 4.1: Predicted effect on the stability of PALS1 of mutations corresponding to those found in CASK. The G521V, Y723C, and W914R mutations which completely disrupt CASK:Neurexin-1β interaction are predicted to destabilize the structure of the PALS1. The V849A is also predicted to destabilize PALS1, though it did not disrupt CASK:Neurexin-1β binding.

I also tested whether the G521V, Y723C, and W914R CASK mutants were unable to oligomerize given their inability to bind to Neurexin-1β. I expressed 2 WT or mutant CASK constructs tagged with the N-terminal or C-terminal half of a YFP protein along with Neurexin-1β and Liprin-α2. I measured YFP fluorescence to determine how much WT and mutant CASK oligomerized in the presence of Neurexin-1β and Liprin-α2.

Without binding partners, WT and mutant CASK exhibited a very low amount of oligomerization (Fig 3.15A left group) as indicated by low YFP fluroescence. In the presence of Neurexin-1β (Fig 3.15, centre left group), WT CASK oligomerized. This was quite quite exciting as this is the first experimental evidence that CASK also oligomerizes after binding to PDZ ligands, suggesting that it behaves similarly to PALS1.

The R140G, G161R, and Y268H CASK mutants, which do not disrupt CASK:Neurexin interaction, oligomerized to the same degree as WT CASK. By contrast, the G521V, Y723C, and W914R mutants, which disrupt CASK:Neurexin-1β interaction, failed to oligomerize in the presence of Neurexin. These results support the hypothesis that the binding to Neurexin-1β and oligomerization are closely related phenomena for CASK.

Surprisingly, in the presence of Liprin-α2 (Fig 3.15, centre right group), WT and mutant CASKs behaved in the same manner as with Neurexin-1β. WT, R140G, G161R, and Y268H CASK oligomerized in the presence of Liprin-α2. However, the G521V, Y723C, and W914R CASK mutants which cannot bind to Neurexin-1β fail to oligomerize in the presence of Liprin-α2.

Furthermore, Neurexin-1β and Liprin-α2 could together induce even more CASK oligomerization than either partner could on its own (Fig 3.15, right group vs centre groups). This oligomerization was also disrupted by the G521V, Y723C, and W914R mutations.

There are currently no known mechanisms through which Liprin-α2 could induce the oligomerization of CASK. The fact that the same G521V, Y723C, and W914R mutations that disrupted Neurexin-1β-mediated oligomerization disrupt Liprin-α2-mediated oligomerization suggests that both partners act through a mechanism that requires the formation of the CASK PSG supramodule. However, this is at first glance somewhat surprising, as Liprin-α2 is known to bind to the CaMK and L27.1 domains of CASK (Olsen et al., 2005; Wei et al., 2011). Furthermore, the fact that Neurexin-1β and Liprin-α2 could collectively induce more oligomerization than either on its own suggests that the two partners induce CASK oligomerization through separate, but non-exclusionary mechanisms.

Different aspects of these results may be explained by recent experimental findings on the CASK:Liprin-α2 interaction. Recent work by L. E. LaConte et al. (2016) demonstrated a novel interaction mode between CASK, Neurexin-1β, and Liprin-α2. Normally, Liprin-α2 binds to the CaMK domain of CASK. However, Mint1, another presynaptic partner of CASK usually outcompetes Liprin-α2 for the CaMK binding site. But when CASK binds to Neurexin-1β, the interface between the two proteins create a new binding site to which Liprin-α2, but not Mint1 can bind. It is therefore possible that the addition of Liprin-α2 to the CASK:Neurexin-1β further stabilizes CASK in the dimerized, Neurexin-1β-bound conformation and thus increases the probability that CASK oligomerizes.

The problem with this model is that Liprin-α2 should only be capable of enhancing Neurexin-1β-induced CASK oligomerization, and does not provide an explanation for how CASK may oligomerize just with Liprin-α2 as my data showed (Fig 3.15, centre right group). One possible explanation is the inherent ability of Liprin-α2 to homodimerize (Carles Serra-Pagès et al., 1998). It is possible that Liprin-α2 does not directly induce CASK to oligomerize with other CASK proteins but instead, Liprin-α2 itself may dimerize and indirectly promote CASK oligomerization by bringing CASK proteins into closer proximity to one another.

In presynapses, Liprin-α2 could thus recruit CASK to close proximity to Neurexins which can directly induce CASK oligomerization, the two proteins thus cooperating in the assembly of CASK oligomers.

However, this model is unable to explain why the mutations that disrupt CASK:Neurexin-1β interaction would also disrupt Liprin-α2-induced oligomerization. It could be argued that the G521V, Y723C, and W914R mutations disrupt the PSG supramodule to be completely misfolded. However, this degree of misfolding would likely cause the CASK mutant to be degraded. But as the input blots of my coimmunoprecipitation experiments show (Fig 3.5 to Fig 3.10), the G521V, Y723C, and W914R mutants are not noticeably less well expressed than WT CASK. Thus, if the G521V, Y723C, and W914R mutations cause milder misfolding of the CASK PSG, oligomerization of CASK at the N-terminus should still bring the YFP1 and YFP2 tags at the C-terminus of CASK close enough to fluoresce.

The oligomerization of CASK upon binding to Neurexin is functionally interesting from the perspective of synaptogenesis. Two studies by Scheiffele et al. (2000) and Dean et al. (2003) showed that the clustering of Neurexin is sufficient to induce the development of the presynapse. When presynaptic Neurexin is cross linked using primary and secondary antibodies, axon segments begin to differentiate into presynapses. A similar study in the postsynapse by Graf et al. (2004) showed that clustering of postsynaptic Neuroligin and presynaptic Neurexin could induce postsynaptic differentiation.

However, it is not yet clear which of these 2 receptors clusters "first." Some results by Dean et al. (2003) suggest that Neuroligin may be what clusters first. Neuroligin has an inherent ability to oligomerize thanks to its extracellular domains. Dean et al. showed that Neuroligin deficient in this ability to oligomerize could not induce presynaptic differentiation even when bound to Neurexin. However, this interpretation begs the question: why spontaneous Neuroligin oligomerization does not trigger postsynaptic differentiation even without presynaptic Neurexin.

It therefore seems more likely that the clustering of Neurexin and Neuroligin to trigger pre and postsynaptic differentiation is a cooperative process. However, Neurexin is not known to have an inherent ability to cluster. Its other known interaction partners, Mint1 and Mint2 (Biederer & Südhof, 2000) are also not known to oligomerize. However, we have shown here that CASK oligomerizes when it binds to Neurexin. We may assume that Neurexin also clusters during this process. This is currently the only known mechanism through which Neurexin could oligomerize other than binding to Neuroligin. CASK could therefore simultaneously be a downstream effector of Neurexin to induce presynaptic differentiation as well as an upstream effector that causes Neurexin to cluster Neuroligin and in so doing, induce postsynaptic differentiation.

That being said, *CASK*-KO mice produced by Atasoy et al. (2007) and further characterized by Mori et al. (2019) suggest that CASK may not be necessary for synaptogenesis. Mice deficient for CASK were lethal within 1 day of birth, likely due to the respiratory difficulties observed in these mice. Their only morphological

phenotype in these mice, however, was a cleft palate in 80% of the mice. But their gross brain structure was unaffected. In CASK +/- heterozygous female mice, CASK-deficient neurons had a higher excitatory/inhibitory synapse ratio compared to WT neurons, but had a similar overall density of synapses when compared to WT mice. It would therefore seem that CASK is not essential for synaptogenesis.

One possibility is that while Neurexin and Neuroligin may be sufficient for synaptogenesis in in-vitro cultured systems, they may not be necessary for synaptogenesis under physiological conditions. Indeed, multiple other adhesion proteins are known to be capable of inducing synaptogenesis. LAR-type receptor phosphotyrosine phosphatases (LAR-RPTPs) are a class of presynaptic adhesion proteins that interact with α-Liprins (C. Serra-Pagès et al., 1995; Carles Serra-Pagès et al., 1998). In *Drosophila*, DLAR is necessary for the formation of neuromuscular junctions as growth cones with mutant DLARs tend to overshoot their target. SynCAM (Synaptic Cell Adhesion Molecules) are another family of synaptic adhesion proteins which induce synapse formation by transsynaptic homoadhesion (Biederer et al., 2002). Synaptic adhesion-like molecules (SALMs), which are leucine-rich repeat proteins are also known to play a role in the initial contact that mediates synapse formation (Schroeder & de Wit, 2018).

An interesting note is that CASK-KO, Neurexin-KO, and Neuroligin-KO mice share certain common cellular and physiological traits, suggesting that CASK is an important effector of the Neurexin and Neuroligin pair of adhesion molecules. Neurexin-KO mice have deficiencies in synaptic vesicle release, but also had otherwise normal number of synapses formed on neurons. Interestingly, these mice also were lethal within days of birth, likely due to respiratory difficulties (Missler et al., 2003). Neuroligin-KO mice had similar number of glutamatergic synapse but lower amount of inhibitory synapses compared to WT mice. Like the CASK-KO and Neurexin-KO mice, these mice were lethal within days of birth due to respiratory difficulties (Varoqueaux et al., 2006). The similarity of these three mouse lines suggests that CASK may be involved in a Neurexin:Neuroligin signaling pathway involved in synaptic maturation, though the exact function is not clear.

4.3 Correlating Patient Phenotypes with Molecular Effects

One of the goals of this project had been to correlate the molecular phenotypes resulting from the various *CASK* missense mutations with the symptoms of the patients in whom these mutations had been diagnosed. The hope had been to elucidate the main physiological functions of CASK, which would point towards mechanisms that could be targeted by future therapies for *CASK* mutations.

While our results do not allow a clear 1-to-1 correlation between molecular phenotypes and the patients' symptoms, they nevertheless point towards a promising venue of research for *CASK* mutation therapies. Indeed, another goal of this project had been to determine whether certain pathogenic mechanisms were shared across multiple *CASK* missense mutations. One mechanism that was found to be very common, present in nearly 5 of the 12 mutations studied, was the loss of CASK:Neurexin interaction. A recent study by L. E. W. LaConte et al. (2018) also reports two *CASK* missense mutations, M519T and G659D, that specifically disrupt CASK:Neurexin interaction. These 2 mutations were discovered in 3 patients who exhibited microcephaly and intellectual deficiency.

This was slightly surprising as it was initially believed that it was that loss of CASK:Tbr1 interaction that was behind the microcephaly symptom observed in patients with *CASK* loss-of-function mutations. This was on the basis that the CASK:Tbr1 interaction was shown to upregulate the expression of *Reelin* (G.-S. Wang et al., 2004), a gene required for proper brain laminar development (D'Arcangelo & Curran, 1998). However, if this were the case, it could not have explained why it is that the patients with the R489W, M507I, and G521V mutations all exhibited disruptions of brain morphology including microcephaly.

It therefore seems likely that CASK:Neurexin interaction is also necessary for brain development, though the molecular mechanisms underlying this remain unclear. Our results show that the CASK:Neurexin interaction is necessary for CASK oligomerization in the presynapse. While this is likely beneficial for CASK's ability to play a role as a scaffolding protein within the presynapse, it is not clear how this would allow CASK to influence brain morphology development. Given that CASK also interacts with other adhesion proteins such as Syndecan (Y. P. Hsueh et al., 1998) and SynCAM (Biederer et al., 2002) with its PDZ domain, it is also possible that the

same mutations that affect the CASK:Neurexin interaction also disrupt CASK's ability to bind to these proteins, which in turn may affect neuron migration.

Of course, not all *CASK* missense mutations involve the CASK:Neurexin interaction. For example, the L354P mutation, which disrupts the CASK:Sap97 interaction but does not affect the CASK:Neurexin interaction would not be expected to respond to any kind of therapeutic treatment that targets the interaction between CASK and Neurexin. But combining our 12 mutation and the 2 reported by L. E. W. LaConte et al. (2018), 7 of 14 mutations would be expected to respond to a treatment that targets the CASK:Neurexin interaction.

4.4 Future Directions

Several investigative paths extend from this project to elucidate the function of CASK.

In this study, several *CASK* missense mutations have not yet been linked to a molecular phenotype: the R140G, G161R, and Y268H mutations of the CaMK domain, the P396S mutation of the L27.1 domain, and the N798Y and V849A mutations of the GK domain.

It is possible that some of the mutations being investigated here may simply not be pathogenic. One possibility is the P396S mutation, which has also been found in healthy persons. However, some of the mutations investigated in this study which have not been clearly established as being pathogenic have indicators that they may be.

The N798Y and V849A mutations of the GK domain did not disrupt the binding of CASK to any of the tested partners (Liprin-α2, Sap97, Neurexin-1β, Tbr1, and CINAP). Structurally, the two mutations are located at a certain distance from the Y723C and W914R mutations which decrease CASK:Tbr1 interaction and increase CASK:CINAP interaction. It is possible that the N798Y and V849A mutations may affect the binding of CASK to untested interaction partners such as Bcl11A, which binds to the GK domain of CASK and is also involved in transcriptional regulation. The N798Y and V849A mutations have also not yet been tested for CASK oligomerization in the split-YFP experiments. The SDM program predicts that the V849A mutations should very strongly disrupt the stability of the CASK dimer. Although my results so far have shown a strong correlation between loss of CASK:Neurexin binding and loss of CASK oligomerization, it is conceivable that V849A could disrupt CASK oligomerization even through my results show that it does not disrupt CASK:Neurexin-1β interaction.

Among similar lines, the R489W and M507I mutations, which disrupted CASK:Neurexin-1β interaction to 50% of the WT condition have also not yet been tested for their ability to disrupt CASK oligomerization. It would be highly interesting to see if the 50% decrease in CASK:Neurexin-1β binding also translates into a 50% decrease in oligomerization. Furthermore, my current experimental design cannot determine the nature of the 50% loss in CASK:Neurexin-1β binding caused by these 2 mutations. 2 scenarios are possible: either all CASK-R489W and -M507I proteins exhibit an inherent 50% decrease of their binding affinity for Neurexin, or 50% of the population of CASK-R489W and -M507I proteins becomes incapable of binding to Neurexin-1β while the other half remains affected.

Another frontier of CASK investigation that has not been addressed in this study is the relevance of the CaMK domain of CASK and the mutations present there. The interaction studies performed in this study show that the R140G, G161R, and Y268H mutations failed to affect the binding of CASK to any of the tested interaction partners. It is possible that the pathogenic mechanism underlying these mutations has less to do with loss of partner binding and more to do with the loss of this domain's enzymatic activity. A study by Mukherjee et al. (2008) showed that the CaMK domain of CASK is not an inactive pseudo-kinase as was previously thought, but in fact has an inherent kinase activity that phosphorylates Neurexin. The function of Neurexin phosphorylation is not yet clearly understood, but a study by L. E. LaConte et al. (2016) suggests that phosphorylation of Neurexin tends to decrease the CASK:Neurexin interaction and may be a mechanism that increases Neurexin turnover in the presynapse. The R140G and G161R mutations are located within structures necessary for the kinase activity of CaMK domains (Mukherjee et al., 2008). It is therefore possible that the mutations of CaMK domain do not mediate their pathogenic effect through loss of partner binding but by inhibiting the enzymatic

activity of CASK. This would be a pathogenic mechanism entirely distinct from the mechanisms that have been investigated in this study and represents an exciting venue of research on CASK.

Finally, a new aspect of CASK that I have begun to explore in this study is the relevance of the various *CASK* transcript variants and the CASK isoforms they encode. My results provide the first evidence of the functional specialization of the various *CASK* transcript variants, which provides a new layer of specialization and regulation for CASK. Interesting aspects include how *CASK* transcript variants are spatially and temporally controlled. Although *CASK* is primarily expressed in the brain, it is also present in other tissues such as the uterus, lungs, liver, and kidney (Hata et al., 1996). No studies have currently explored whether the different organs, or different regions of the brain, express a dominant *CASK* transcript variant.

5. References

Atasoy, D., Schoch, S., Ho, A., Nadasy, K. A., Liu, X., Zhang, W., . . . Sudhof, T. C. (2007). Deletion of CASK in mice is lethal and impairs synaptic function. *Proc Natl Acad Sci U S A, 104*(7), 2525-2530. doi:10.1073/pnas.0611003104

Attia, M., Rachez, C., Avner, P., & Rogner, U. C. (2013). Nucleosome assembly proteins and their interacting proteins in neuronal differentiation. *Archives of Biochemistry and Biophysics, 534*(1), 20-26. doi:https://doi.org/10.1016/j.abb.2012.09.011

Bassand, P., Bernard, A., Rafiki, A., Gayet, D., & Khrestchatisky, M. (1999). Differential interaction of the tSXV motifs of the NR1 and NR2A NMDA receptor subunits with PSD-95 and SAP97. *European Journal of Neuroscience, 11*(6), 2031-2043. doi:10.1046/j.1460-9568.1999.00611.x

Betz, A., Okamoto, M., Benseler, F., & Brose, N. (1997). Direct Interaction of the Rat unc-13 Homologue Munc13-1 with the N Terminus of Syntaxin. *Journal of Biological Chemistry, 272*(4), 2520-2526. doi:10.1074/jbc.272.4.2520

Biederer, T., Kaeser, P. S., & Blanpied, T. A. (2017). Transcellular Nanoalignment of Synaptic Function. *Neuron, 96*(3), 680-696. doi:10.1016/j.neuron.2017.10.006

Biederer, T., Sara, Y., Mozhayeva, M., Atasoy, D., Liu, X., Kavalali, E. T., & Südhof, T. C. (2002). SynCAM, a Synaptic Adhesion Molecule That Drives Synapse Assembly. *Science, 297*(5586), 1525. doi:10.1126/science.1072356

Biederer, T., & Südhof, T. C. (2000). Mints as Adaptors: Direct binding to Neurexins and Recruitment of Munc18. *Journal of Biological Chemistry, 275*(51), 39803-39806.

Borg, J.-P., Straight, S. W., Kaech, S. M., de Taddéo-Borg, M., Kroon, D. E., Karnak, D., . . . Margolis, B. (1998). Identification of an Evolutionarily Conserved Heterotrimeric Protein Complex Involved in Protein Targeting. *Journal of Biological Chemistry, 273*(48), 31633-31636.

Boucard, A. A., Chubykin, A. A., Comoletti, D., Taylor, P., & Südhof, T. C. (2005). A Splice Code for trans-Synaptic Cell Adhesion Mediated by Binding of Neuroligin 1 to α- and β-Neurexins. *Neuron, 48*(2), 229-236. doi:10.1016/j.neuron.2005.08.026

Bourne, J. N., & Harris, K. M. (2008). Balancing structure and function at hippocampal dendritic spines. *Annual Review of Neuroscience, 31*, 47-67. doi:10.1146/annurev.neuro.31.060407.125646

Bourne, Y., Taylor, P., Bougis, P. E., & Marchot, P. (1999). Crystal Structure of Mouse Acetylcholinesterase: A PERIPHERAL SITE-OCCLUDING LOOP IN A TETRAMERIC ASSEMBLY. *Journal of Biological Chemistry, 274*(5), 2963-2970. doi:10.1074/jbc.274.5.2963

Bulfone, A., Smiga, S. M., Shimamura, K., Peterson, A., Puelles, L., & Rubenstein, J. L. (1995). T-brain-1: a homolog of Brachyury whose expression defines molecularly distinct domains within the cerebral cortex. *Neuron, 15*(1), 63-78.

Butz, S., Okamoto, M., & Südhof, T. C. (1998). A Tripartite Protein Complex with the Potential to Couple Synaptic Vesicle Exocytosis to Cell Adhesion in Brain. *Cell, 94*(6), 773-782. doi:10.1016/S0092-8674(00)81736-5

Chamma, I., Letellier, M., Butler, C., Tessier, B., Lim, K. H., Gauthereau, I., . . . Thoumine, O. (2016). Mapping the dynamics and nanoscale organization of synaptic adhesion proteins using monomeric streptavidin. *Nat Commun, 7*, 10773. doi:10.1038/ncomms10773

Chang, B. S., Duzcan, F., Kim, S., Cinbis, M., Aggarwal, A., Apse, K. A., . . . Walsh, C. A. (2007). The role of RELN in lissencephaly and neuropsychiatric disease. *American Journal of Medical Genetics Part B: Neuropsychiatric Genetics, 144B*(1), 58-63. doi:10.1002/ajmg.b.30392

Chen, X., Winters, C., Azzam, R., Li, X., Galbraith, J. A., Leapman, R. D., & Reese, T. S. (2008). Organization of the core structure of the postsynaptic density. *Proceedings of the National Academy of Sciences of the United States of America, 105*(11), 4453-4458. doi:10.1073/pnas.0800897105

Chih, B., Gollan, L., & Scheiffele, P. (2006). Alternative Splicing Controls Selective Trans-Synaptic Interactions of the Neuroligin-Neurexin Complex. *Neuron, 51*(2), 171-178. doi:https://doi.org/10.1016/j.neuron.2006.06.005

Chklovskii, D. B. (2004). Synaptic Connectivity and Neuronal Morphology: Two Sides of the Same Coin. *Neuron, 43*(5), 609-617. doi:https://doi.org/10.1016/j.neuron.2004.08.012

Cognet, L., Groc, L., Lounis, B., & Choquet, D. (2006). Multiple Routes for Glutamate Receptor Trafficking: Surface Diffusion and Membrane Traffic Cooperate to Bring Receptors to Synapses. *Science's STKE, 2006*(327), pe13-pe13. doi:10.1126/stke.3272006pe13

Cohen, A. R., Wood, D. F., Marfatia, S. M., Walther, Z., Chishti, A. H., & Anderson, J. M. (1998). Human CASK/LIN-2 Binds Syndecan-2 and Protein 4.1 and Localizes to the Basolateral Membrane of Epithelial Cells. *The Journal of Cell Biology, 142*(1), 129-138. doi:10.1083/jcb.142.1.129

Craig, A. M., & Kang, Y. (2007). Neurexin-neuroligin signaling in synapse development. *Current Opinion in Neurobiology, 17*(1), 43-52. doi:10.1016/j.conb.2007.01.011

D'Arcangelo, G., & Curran, T. (1998). Reeler: new tales on an old mutant mouse. *BioEssays, 20*(3), 235-244. doi:10.1002/(SICI)1521-1878(199803)20:3<235::AID-BIES7>3.0.CO;2-Q

Dean, C., Scholl, F. G., Choih, J., DeMaria, S., Berger, J., Isacoff, E., & Scheiffele, P. (2003). Neurexin mediates the assembly of presynaptic terminals. *Nature neuroscience, 6*(7), 708-716. doi:10.1038/nn1074

DeGiorgis, J. A., Galbraith, J. A., Dosemeci, A., Chen, X., & Reese, T. S. (2006). Distribution of the scaffolding proteins PSD-95, PSD-93, and SAP97 in isolated PSDs. *Brain Cell Biology, 35*(4), 239-250. doi:10.1007/s11068-007-9017-0

Dimitratos, S. D., Stathakis, D. G., Nelson, C. A., Woods, D. F., & Bryant, P. J. (1998). The Location of Human CASK at Xp11.4 Identifies This Gene as a Candidate for X-Linked Optic Atrophy. *Genomics $V 51*(2), 308-309.

Dulubova, I., Sugita, S., Hill, S., Hosaka, M., Fernandez, I., Südhof, T. C., & Rizo, J. (1999). A conformational switch in syntaxin during exocytosis: role of munc18. *The EMBO Journal, 18*(16), 4372-4382. doi:10.1093/emboj/18.16.4372

Ehlers, M. D. (2000). Reinsertion or Degradation of AMPA Receptors Determined by Activity-Dependent Endocytic Sorting. *Neuron, 28*(2), 511-525. doi:10.1016/S0896-6273(00)00129-X

Feng, W., Long, J.-F., Fan, J.-S., Suetake, T., & Zhang, M. (2004). The tetrameric L27 domain complex as an organization platform for supramolecular assemblies. *Nature Structural & Molecular Biology, 11*(5), 475-480. doi:10.1038/nsmb751

Funke, L., Dakoji, S., & Bredt, D. S. (2005). Membrane-associated Guanlylate Kinases Regulate Adhesion and Plasticity at Cell Junctions. *Annual Review of Biochemistry, 74*(1), 219-245. doi:10.1146/annurev.biochem.74.082803.133339

González-Mariscal, L., Betanzos, A., & Ávila-Flores, A. (2000). MAGUK proteins: structure and role in the tight junction. *Seminars in Cell & Developmental Biology, 11*(4), 315-324. doi:https://doi.org/10.1006/scdb.2000.0178

González-Mariscal, L., Islas, S., Contreras, R. G., García-Villegas, M. R., Betanzos, A., Vega, J., . . . Valdés, J. (1999). Molecular Characterization of the Tight Junction Protein ZO-1 in MDCK Cells. *Experimental Cell Research, 248*(1), 97-109. doi:https://doi.org/10.1006/excr.1999.4392

Graf, E. R., Kang, Y., Hauner, A. M., & Craig, A. M. (2006). Structure Function and Splice Site Analysis of the Synaptogenic Activity of the Neurexin-1β LNS Domain. *The Journal of Neuroscience, 26*(16), 4256-4265. doi:10.1523/jneurosci.1253-05.2006

Graf, E. R., Zhang, X., Jin, S.-X., Linhoff, M. W., & Craig, A. M. (2004). Neurexins induce differentiation of GABA and glutamate postsynaptic specializations via neuroligins. *Cell, 119*(7), 1013-1026. doi:10.1016/j.cell.2004.11.035

Graham, F. L., Smiley, J., Russell, W. C., & Nairn, R. (1977). Characteristics of a Human Cell Line Transformed by DNA from Human Adenovirus Type 5. *Journal of General Virology, 36*(1), 59-72. doi:https://doi.org/10.1099/0022-1317-36-1-59

Gray, E. G. (1959). Axo-somatic and axo-dendritic synapses of the cerebral cortex: an electron microscope study. *Journal of anatomy, 93*(Pt 4), 420-433.

Greger, I. H., & Esteban, J. A. (2007). AMPA receptor biogenesis and trafficking. *Current Opinion in Neurobiology, 17*(3), 289-297. doi:https://doi.org/10.1016/j.conb.2007.04.007

Hackett, A., Tarpey, P. S., Licata, A., Cox, J., Whibley, A., Boyle, J., . . . Abidi, F. E. (2009). CASK mutations are frequent in males and cause X-linked nystagmus and variable XLMR phenotypes. *European Journal Of Human Genetics, 18*, 544. doi:10.1038/ejhg.2009.220 https://www.nature.com/articles/ejhg2009220#supplementary-information

Hata, Y., Butz, S., & Südhof, T. C. (1996). CASK: a novel dlg/PSD95 homolog with an N-terminal calmodulin-dependent protein kinase domain identified by interaction with neurexins. *The Journal of Neuroscience, 16*(8), 2488.

Hevner, R. F., Shi, L., Justice, N., Hsueh, Y.-P., Sheng, M., Smiga, S., . . . Rubenstein, J. L. R. (2001). Tbr1 Regulates Differentiation of the Preplate and Layer 6. *Neuron, 29*(2), 353-366. doi:10.1016/S0896-6273(01)00211-2

Hong, S. E., Shugart, Y. Y., Huang, D. T., Shahwan, S. A., Grant, P. E., Hourihane, J. O. B., . . . Walsh, C. A. (2000). Autosomal recessive lissencephaly with cerebellar hypoplasia is associated with human RELN mutations. *Nature Genetics, 26*(1), 93-96. doi:10.1038/79246

Hsueh, Y.-P. (2006). The Role of the MAGUK Protein CASK in Neural Development and Synaptic Function. *Current Medicinal Chemistry, 13*(16), 1915-1927. doi:http://dx.doi.org/10.2174/092986706777585040

Hsueh, Y.-P., Wang, T.-F., Yang, F.-C., & Sheng, M. (2000). Nuclear translocation and transcription regulation by the membrane-associated guanylate kinase CASK/LIN-2. *Nature, 404*(6775), 298-302. doi:10.1038/35005118

Hsueh, Y. P., Yang, F. C., Kharazia, V., Naisbitt, S., Cohen, A. R., Weinberg, R. J., & Sheng, M. (1998). Direct interaction of CASK/LIN-2 and syndecan heparan sulfate proteoglycan and their overlapping distribution in neuronal synapses. *The Journal of Cell Biology, 142*(1), 139-151. doi:10.1083/jcb.142.1.139

Ichtchenko, K., Hata, Y., Nguyen, T., Ullrich, B., Missler, M., Moomaw, C., & Südhof, T. C. (1995). Neuroligin 1: A splice site-specific ligand for β-neurexins. *Cell, 81*(3), 435-443. doi:https://doi.org/10.1016/0092-8674(95)90396-8

Ichtchenko, K., Nguyen, T., & Südhof, T. C. (1996). Structures, Alternative Splicing, and Neurexin Binding of Multiple Neuroligins. *Journal of Biological Chemistry, 271*(5), 2676-2682. doi:10.1074/jbc.271.5.2676

Irie, M., Hata, Y., Takeuchi, M., Ichtchenko, K., Toyoda, A., Hirao, K., . . . Südhof, T. C. (1997). Binding of Neuroligins to PSD-95. *Science, 277*(5331), 1511-1515. doi:10.1126/science.277.5331.1511

Jacob, T. C., Moss, S. J., & Jurd, R. (2008). GABA(A) receptor trafficking and its role in the dynamic modulation of neuronal inhibition. *Nature reviews. Neuroscience, 9*(5), 331-343. doi:10.1038/nrn2370

Jeyifous, O., Waites, C. L., Specht, C. G., Fujisawa, S., Schubert, M., Lin, E. I., . . . Green, W. N. (2009). SAP97 and CASK mediate sorting of NMDA receptors through a previously unknown secretory pathway. *Nat Neurosci, 12*(8), 1011-1019. doi:10.1038/nn.2362

Jo, K., Derin, R., Li, M., & Bredt, D. S. (1999). Characterization of MALS/Velis-1, -2, and -3: a Family of Mammalian LIN-7 Homologs Enriched at Brain Synapses in Association with the Postsynaptic Density-95/NMDA Receptor Postsynaptic Complex. *The Journal of Neuroscience, 19*(11), 4189-4199. doi:10.1523/jneurosci.19-11-04189.1999

Kaech, S. M., Whitfield, C. W., & Kim, S. K. (1998). The LIN-2/LIN-7/LIN-10 Complex Mediates Basolateral Membrane Localization of the C. elegans EGF Receptor LET-23 in Vulval Epithelial Cells. *Cell, 94*(6), 761-771. doi:10.1016/S0092-8674(00)81735-3

Kharazia, V. N., & Weinberg, R. J. (1997). Tangential synaptic distribution of NMDA and AMPA receptors in rat neocortex. *Neuroscience Letters, 238*(1), 41-44. doi:https://doi.org/10.1016/S0304-3940(97)00846-X

Kornau, H., Schenker, L., Kennedy, M., & Seeburg, P. (1995). Domain interaction between NMDA receptor subunits and the postsynaptic density protein PSD-95. *Science, 269*(5231), 1737-1740. doi:10.1126/science.7569905

LaConte, L. E., Chavan, V., Liang, C., Willis, J., Schonhense, E. M., Schoch, S., & Mukherjee, K. (2016). CASK stabilizes neurexin and links it to liprin-alpha in a neuronal activity-dependent manner. *Cell Mol Life Sci, 73*(18), 3599-3621. doi:10.1007/s00018-016-2183-4

LaConte, L. E. W., Chavan, V., Elias, A. F., Hudson, C., Schwanke, C., Styren, K., . . . Mukherjee, K. (2018). Two microcephaly-associated novel missense mutations in CASK specifically disrupt the CASK-neurexin interaction. *Hum Genet, 137*(3), 231-246. doi:10.1007/s00439-018-1874-3

Landis, D. M. D., Hall, A. K., Weinstein, L. A., & Reese, T. S. (1988). The organization of cytoplasm at the presynaptic active zone of a central nervous system synapse. *Neuron, 1*(3), 201-209. doi:https://doi.org/10.1016/0896-6273(88)90140-7

Laverty, H. G., & Wilson, J. B. (1998). Murine CASK Is Disrupted in a Sex-Linked Cleft Palate Mouse Mutant. *Genomics, 53*(1), 29-41. doi:https://doi.org/10.1006/geno.1998.5479

Lee, S., Fan, S., Makarova, O., Straight, S., & Margolis, B. (2002). A novel and conserved protein-protein interaction domain of mammalian Lin-2/CASK binds and recruits SAP97 to the lateral surface of epithelia. *Molecular and cellular biology, 22*(6), 1778-1791. doi:10.1128/mcb.22.6.1778-1791.2002

Leonard, A. S., Davare, M. A., Horne, M. C., Garner, C. C., & Hell, J. W. (1998). SAP97 Is Associated with the α-Amino-3-hydroxy-5-methylisoxazole-4-propionic Acid Receptor GluR1 Subunit. *Journal of Biological Chemistry, 273*(31), 19518-19524. doi:10.1074/jbc.273.31.19518

Li, Y., Wei, Z., Yan, Y., Wan, Q., Du, Q., & Zhang, M. (2014). Structure of Crumbs tail in complex with the PALS1 PDZ–SH3–GK tandem reveals a highly specific assembly mechanism for the apical Crumbs complex. *Proceedings of the National Academy of Sciences, 111*(49), 17444-17449. doi:10.1073/pnas.1416515111

Lin, E. I., Jeyifous, O., & Green, W. N. (2013). CASK regulates SAP97 conformation and its interactions with AMPA and NMDA receptors. *J Neurosci, 33*(29), 12067-12076. doi:10.1523/JNEUROSCI.0816-13.2013

Liu, X.-B., Murray, K. D., & Jones, E. G. (2004). Switching of NMDA receptor 2A and 2B subunits at thalamic and cortical synapses during early postnatal development. *The Journal of neuroscience : the official journal of the Society for Neuroscience, 24*(40), 8885-8895. doi:10.1523/JNEUROSCI.2476-04.2004

Lu, W.-Y., Man, H.-Y., Ju, W., Trimble, W. S., MacDonald, J. F., & Wang, Y. T. (2001). Activation of Synaptic NMDA Receptors Induces Membrane Insertion of New AMPA Receptors and LTP in Cultured Hippocampal Neurons. *Neuron, 29*(1), 243-254. doi:https://doi.org/10.1016/S0896-6273(01)00194-5

MacGillavry, Harold D., Song, Y., Raghavachari, S., & Blanpied, Thomas A. (2013). Nanoscale Scaffolding Domains within the Postsynaptic Density Concentrate Synaptic AMPA Receptors. *Neuron, 78*(4), 615-622. doi:https://doi.org/10.1016/j.neuron.2013.03.009

Maglione, M., & Sigrist, S. J. (2013). Seeing the forest tree by tree: super-resolution light microscopy meets the neurosciences. *Nature neuroscience, 16*, 790. doi:10.1038/nn.3403

Malinow, R., & Malenka, R. C. (2002). AMPA Receptor Trafficking and Synaptic Plasticity. *Annual Review of Neuroscience, 25*(1), 103-126. doi:10.1146/annurev.neuro.25.112701.142758

Maximov, A., & Bezprozvanny, I. (2002). Synaptic Targeting of N-Type Calcium Channels in Hippocampal Neurons. *The Journal of Neuroscience, 22*(16), 6939. doi:10.1523/JNEUROSCI.22-16-06939.2002

Maximov, A., Südhof, T. C., & Bezprozvanny, I. (1999). Association of Neuronal Calcium Channels with Modular Adaptor Proteins. *Journal of Biological Chemistry, 274*(35), 24453-24456. doi:10.1074/jbc.274.35.24453

McGee, A. W., Dakoji, S. R., Olsen, O., Bredt, D. S., Lim, W. A., & Prehoda, K. E. (2001). Structure of the SH3-Guanylate Kinase Module from PSD-95 Suggests a Mechanism for Regulated Assembly of MAGUK Scaffolding Proteins. *Molecular Cell, 8*(6), 1291-1301. doi:10.1016/S1097-2765(01)00411-7

Missler, M., Fernandez-Chacon, R., & Südhof, T. C. (1998). The Making of Neurexins. *Journal of Neurochemistry, 71*(4), 1339-1347. doi:10.1046/j.1471-4159.1998.71041339.x

Missler, M., & Südhof, T. C. (1998). Neurexins: Three genes and 1001 products. *Trends in Genetics, 14*(1), 20-26. doi:https://doi.org/10.1016/S0168-9525(97)01324-3

Missler, M., Zhang, W., Rohlmann, A., Kattenstroth, G., Hammer, R. E., Gottmann, K., & Südhof, T. C. (2003). α-Neurexins couple Ca2+ channels to synaptic vesicle exocytosis. *Nature, 423*(6943), 939-948. doi:10.1038/nature01755

Moog, U., Bierhals, T., Brand, K., Bautsch, J., Biskup, S., Brune, T., . . . Kutsche, K. (2015). Phenotypic and molecular insights into CASK-related disorders in males. *Orphanet J Rare Dis, 10*, 44. doi:10.1186/s13023-015-0256-3

Morel, N., Leroy, J., Ayon, A., Massoulié, J., & Bon, S. (2001). Acetylcholinesterase H and T Dimers Are Associated through the Same Contact: MUTATIONS AT THIS INTERFACE INTERFERE WITH THE C-TERMINAL T PEPTIDE, INDUCING DEGRADATION RATHER THAN SECRETION. *Journal of Biological Chemistry, 276*(40), 37379-37389. doi:10.1074/jbc.M103192200

Mori, T., Kasem, E. A., Suzuki-Kouyama, E., Cao, X., Li, X., Kurihara, T., . . . Tabuchi, K. (2019). Deficiency of calcium/calmodulin-dependent serine protein kinase disrupts the excitatory-inhibitory balance of synapses by down-regulating GluN2B. *Mol Psychiatry*. doi:10.1038/s41380-018-0338-4

Mukherjee, K., Sharma, M., Urlaub, H., Bourenkov, G. P., Jahn, R., Sudhof, T. C., & Wahl, M. C. (2008). CASK Functions as a Mg2+-independent neurexin kinase. *Cell, 133*(2), 328-339. doi:10.1016/j.cell.2008.02.036

Nair, D., Hosy, E., Petersen, J. D., Constals, A., Giannone, G., Choquet, D., & Sibarita, J.-B. (2013). Super-Resolution Imaging Reveals That AMPA Receptors Inside Synapses Are Dynamically Organized in Nanodomains Regulated by PSD95. *The Journal of Neuroscience, 33*(32), 13204-13224. doi:10.1523/jneurosci.2381-12.2013

Najm, J., Horn, D., Wimplinger, I., Golden, J. A., Chizhikov, V. V., Sudi, J., . . . Kutsche, K. (2008). Mutations of CASK cause an X-linked brain malformation phenotype with microcephaly and hypoplasia of the brainstem and cerebellum. *Nat Genet, 40*(9), 1065-1067. doi:10.1038/ng.194

Nakagawa, T., Futai, K., Lashuel, H. A., Lo, I., Okamoto, K., Walz, T., . . . Sheng, M. (2004). Quaternary Structure, Protein Dynamics, and Synaptic Function of SAP97 Controlled by L27 Domain Interactions. *Neuron, 44*(3), 453-467. doi:https://doi.org/10.1016/j.neuron.2004.10.012

Nomme, J., Fanning, A. S., Caffrey, M., Lye, M. F., Anderson, J. M., & Lavie, A. (2011). The Src Homology 3 Domain Is Required for Junctional Adhesion Molecule Binding to the Third PDZ Domain of the Scaffolding Protein ZO-1. *Journal of Biological Chemistry, 286*(50), 43352-43360. doi:10.1074/jbc.M111.304089

Okamoto, M., & Südhof, T. C. (1997). Mints, Munc18-interacting Proteins in Synaptic Vesicle Exocytosis. *Journal of Biological Chemistry, 272*(50), 31459-31464. doi:10.1074/jbc.272.50.31459

Olsen, O., Moore, K. A., Fukata, M., Kazuta, T., Trinidad, J. C., Kauer, F. W., . . . Bredt, D. S. (2005). Neurotransmitter release regulated by a MALS-liprin-alpha presynaptic complex. *J Cell Biol, 170*(7), 1127-1134. doi:10.1083/jcb.200503011

Palay, S. L. (1956). Synapses in the Central Nervous System. *The Journal of Biophysical and Biochemical Cytology, 2*(4), 193-202. doi:10.1083/jcb.2.4.193

Pan, L., Chen, J., Yu, J., Yu, H., & Zhang, M. (2011). The Structure of the PDZ3-SH3-GuK Tandem of ZO-1 Protein Suggests a Supramodular Organization of the Membrane-associated Guanylate Kinase (MAGUK) Family Scaffold Protein Core. *Journal of Biological Chemistry, 286*(46), 40069-40074. doi:10.1074/jbc.C111.293084

Pandurangan, A. P., Ochoa-Montaño, B., Ascher, D. B., & Blundell, T. L. (2017). SDM: a server for predicting effects of mutations on protein stability. *Nucleic Acids Research, 45*(W1), W229-W235. doi:10.1093/nar/gkx439

Papaioannou, V. E. (2014). The T-box gene family: emerging roles in development, stem cells and cancer. *Development, 141*(20), 3819-3833. doi:10.1242/dev.104471

Petralia, R. S., Sans, N., Wang, Y.-X., & Wenthold, R. J. (2005). Ontogeny of postsynaptic density proteins at glutamatergic synapses. *Molecular and Cellular Neuroscience, 29*(3), 436-452. doi:https://doi.org/10.1016/j.mcn.2005.03.013

Racca, C., Stephenson, F. A., Streit, P., Roberts, J. D. B., & Somogyi, P. (2000). NMDA Receptor Content of Synapses in Stratum Radiatum of the Hippocampal CA1 Area. *The Journal of Neuroscience, 20*(7), 2512-2522. doi:10.1523/jneurosci.20-07-02512.2000

Rademacher, N., Kuropka, B., Kunde, S.-A., Wahl, M. C., Freund, C., & Shoichet, S. A. (2019). Intramolecular domain dynamics regulate synaptic MAGUK protein interactions. *eLife, 8*, e41299. doi:10.7554/eLife.41299

Rao, A., Kim, E., Sheng, M., & Craig, A. M. (1998). Heterogeneity in the Molecular Composition of Excitatory Postsynaptic Sites during Development of Hippocampal Neurons in Culture. *The Journal of Neuroscience, 18*(4), 1217-1229. doi:10.1523/jneurosci.18-04-01217.1998

Regan, M. C., Romero-Hernandez, A., & Furukawa, H. (2015). A structural biology perspective on NMDA receptor pharmacology and function. *Current Opinion in Structural Biology, 33*, 68-75. doi:10.1016/j.sbi.2015.07.012

Richmond, J. E., Weimer, R. M., & Jorgensen, E. M. (2001). An open form of syntaxin bypasses the requirement for UNC-13 in vesicle priming. *Nature, 412*(6844), 338-341. doi:10.1038/35085583

Rizo, J., & Südhof, T. C. (2002). Snares and munc18 in synaptic vesicle fusion. *Nature Reviews Neuroscience, 3*(8), 641-653. doi:10.1038/nrn898

Samuels, B. A., Hsueh, Y. P., Shu, T., Liang, H., Tseng, H. C., Hong, C. J., . . . Tsai, L. H. (2007). Cdk5 promotes synaptogenesis by regulating the subcellular distribution of the MAGUK family member CASK. *Neuron, 56*(5), 823-837. doi:10.1016/j.neuron.2007.09.035

Sans, N., Racca, C., Petralia, R. S., Wang, Y.-X., McCallum, J., & Wenthold, R. J. (2001). Synapse-Associated Protein 97 Selectively Associates with a Subset of AMPA Receptors Early in their Biosynthetic Pathway. *The Journal of Neuroscience, 21*(19), 7506-7516. doi:10.1523/jneurosci.21-19-07506.2001

Scheiffele, P., Fan, J., Choih, J., Fetter, R., & Serafini, T. (2000). Neuroligin Expressed in Nonneuronal Cells Triggers Presynaptic Development in Contacting Axons. *Cell, 101*(6), 657-669. doi:https://doi.org/10.1016/S0092-8674(00)80877-6

Schiavo, G., Stenbeck, G., Rothman, J. E., & Söllner, T. H. (1997). Binding of the synaptic vesicle v-SNARE, synaptotagmin, to the plasma membrane t-SNARE, SNAP-25, can explain docked vesicles at neurotoxin-treated synapses. *Proceedings of the National Academy of Sciences of the United States of America, 94*(3), 997-1001. doi:10.1073/pnas.94.3.997

Schnell, E., Sizemore, M., Karimzadegan, S., Chen, L., Bredt, D. S., & Nicoll, R. A. (2002). Direct interactions between PSD-95 and stargazin control synaptic AMPA receptor number. *Proceedings of the National Academy of Sciences, 99*(21), 13902-13907. doi:10.1073/pnas.172511199

Schroeder, A., & de Wit, J. (2018). Leucine-rich repeat-containing synaptic adhesion molecules as organizers of synaptic specificity and diversity. *Experimental & Molecular Medicine, 50*(4), 10. doi:10.1038/s12276-017-0023-8

Serra-Pagès, C., Kedersha, N. L., Fazikas, L., Medley, Q., Debant, A., & Streuli, M. (1995). The LAR transmembrane protein tyrosine phosphatase and a coiled-coil LAR-interacting protein co-localize at focal adhesions. *The EMBO Journal, 14*(12), 2827-2838.

Serra-Pagès, C., Medley, Q. G., Tang, M., Hart, A., & Streuli, M. (1998). Liprins, a Family of LAR Transmembrane Protein-tyrosine Phosphatase-interacting Proteins. *Journal of Biological Chemistry, 273*(25), 15611-15620. doi:10.1074/jbc.273.25.15611

Setou, M., Nakagawa, T., Seog, D.-H., & Hirokawa, N. (2000). Kinesin Superfamily Motor Protein KIF17 and mLin-10 in NMDA Receptor-Containing Vesicle Transport. *Science, 288*(5472), 1796-1802. doi:10.1126/science.288.5472.1796

Sheng, M., & Kim, E. (2011). The postsynaptic organization of synapses. *Cold Spring Harbor perspectives in biology, 3*(12), a005678. doi:10.1101/cshperspect.a005678

Siegelbaum, S. A., Kandel, E. R., & Yuste, R. (2013). Excitatory and Inhibitory Synapses Have Distinctive Ultrastructures *Principles of Neural Science* (5 ed., pp. 213): McGraw Hill Medical.

Sigrist, S. J., & Sabatini, B. L. (2012). Optical super-resolution microscopy in neurobiology. *Current Opinion in Neurobiology, 22*(1), 86-93. doi:https://doi.org/10.1016/j.conb.2011.10.014

Simske, J. S., Kaech, S. M., Harp, S. A., & Kim, S. K. (1996). LET-23 Receptor Localization by the Cell Junction Protein LIN-7 during C. elegans Vulval Induction. *Cell, 85*(2), 195-204. doi:10.1016/S0092-8674(00)81096-X

Spangler, S. A., Schmitz, S. K., Kevenaar, J. T., de Graaff, E., de Wit, H., Demmers, J., . . . Hoogenraad, C. C. (2013). Liprin-alpha2 promotes the presynaptic recruitment and turnover of RIM1/CASK to facilitate synaptic transmission. *J Cell Biol, 201*(6), 915-928. doi:10.1083/jcb.201301011

Stafford, R. L., Ear, J., Knight, M. J., & Bowie, J. U. (2011). The molecular basis of the Caskin1 and Mint1 interaction with CASK. *Journal of Molecular Biology, 412*(1), 3-13. doi:10.1016/j.jmb.2011.07.005

Sudhof, T. C. (2012). The presynaptic active zone. *Neuron, 75*(1), 11-25. doi:10.1016/j.neuron.2012.06.012

Tabuchi, K., Biederer, T., Butz, S., & Südhof, T. C. (2002). CASK Participates in Alternative Tripartite Complexes in which Mint 1 Competes for Binding with Caskin 1, a Novel CASK-Binding Protein. *The Journal of Neuroscience, 22*(11), 4264-4273. doi:10.1523/jneurosci.22-11-04264.2002

Takanashi, J.-i., Okamoto, N., Yamamoto, Y., Hayashi, S., Arai, H., Takahashi, Y., . . . Inazawa, J. (2012). Clinical and radiological features of Japanese patients with a severe phenotype due to CASK mutations. *American Journal of Medical Genetics Part A, 158A*(12), 3112-3118. doi:10.1002/ajmg.a.35640

Tang, A.-H., Chen, H., Li, T. P., Metzbower, S. R., MacGillavry, H. D., & Blanpied, T. A. (2016). A trans-synaptic nanocolumn aligns neurotransmitter release to receptors. *Nature, 536*, 210. doi:10.1038/nature19058 https://www.nature.com/articles/nature19058#supplementary-information

Trotter, J. H., Hao, J., Maxeiner, S., Tsetsenis, T., Liu, Z., Zhuang, X., & Südhof, T. C. (2019). Synaptic neurexin-1 assembles into dynamically regulated active zone nanoclusters. *The Journal of Cell Biology, 218*(8), 2677-2698. doi:10.1083/jcb.201812076

Ule, J., Ule, A., Spencer, J., Williams, A., Hu, J.-S., Cline, M., . . . Darnell, R. B. (2005). Nova regulates brain-specific splicing to shape the synapse. *Nature Genetics, 37*(8), 844-852. doi:10.1038/ng1610

Ullrich, B., Ushkaryov, Y. A., & Südhof, T. C. (1995). Cartography of neurexins: More than 1000 isoforms generated by alternative splicing and expressed in distinct subsets of neurons. *Neuron, 14*(3), 497-507. doi:https://doi.org/10.1016/0896-6273(95)90306-2

Ungar, D., & Hughson, F. M. (2003). SNARE Protein Structure and Function. *Annual Review of Cell and Developmental Biology, 19*(1), 493-517. doi:10.1146/annurev.cellbio.19.110701.155609

Valtschanoff, J. G., & Weinberg, R. J. (2001). Laminar Organization of the NMDA Receptor Complex within the Postsynaptic Density. *The Journal of Neuroscience, 21*(4), 1211-1217. doi:10.1523/jneurosci.21-04-01211.2001

van Spronsen, M., & Hoogenraad, C. C. (2010). Synapse pathology in psychiatric and neurologic disease. *Current neurology and neuroscience reports, 10*(3), 207-214. doi:10.1007/s11910-010-0104-8

Varoqueaux, F., Aramuni, G., Rawson, R. L., Mohrmann, R., Missler, M., Gottmann, K., . . . Brose, N. (2006). Neuroligins Determine Synapse Maturation and Function. *Neuron, 51*(6), 741-754. doi:10.1016/j.neuron.2006.09.003

Walter, P. P., Owen-Hughes, T. A., Côté, J., & Workman, J. L. (1995). Stimulation of transcription factor binding and histone displacement by nucleosome assembly protein 1 and nucleoplasmin requires disruption of the histone octamer. *Molecular and cellular biology, 15*(11), 6178-6187. doi:10.1128/mcb.15.11.6178

Wang, G.-S., Hong, C.-J., Yen, T.-Y., Huang, H.-Y., Ou, Y., Huang, T.-N., . . . Hsueh, Y.-P. (2004). Transcriptional Modification by a CASK-Interacting Nucleosome Assembly Protein. *Neuron, 42*(1), 113-128. doi:https://doi.org/10.1016/S0896-6273(04)00139-4

Wang, T.-F., Ding, C.-N., Wang, G.-S., Luo, S.-C., Lin, Y.-L., Ruan, Y., . . . Hsueh, Y.-P. (2004). Identification of Tbr-1/CASK complex target genes in neurons. *Journal of Neurochemistry, 91*(6), 1483-1492. doi:10.1111/j.1471-4159.2004.02845.x

Wei, Z., Zheng, S., Spangler, S. A., Yu, C., Hoogenraad, C. C., & Zhang, M. (2011). Liprin-mediated large signaling complex organization revealed by the liprin-alpha/CASK and liprin-alpha/liprin-beta complex structures. *Mol Cell, 43*(4), 586-598. doi:10.1016/j.molcel.2011.07.021

Wenthold, R. J., Al-Hallaq, R. A., Swanwick, C. C., & Petralia, R. S. (2008). Molecular Properties and Cell Biology of the NMDA Receptor. In J. W. Hell & M. D. Ehlers (Eds.), *Structural And Functional Organization Of The Synapse* (pp. 317-367). Boston, MA: Springer US.

Wu, H., Luo, J., Yu, H., Rattner, A., Mo, A., Wang, Y., . . . Nathans, J. (2014). Cellular Resolution Maps of X Chromosome Inactivation: Implications for Neural Development, Function, and Disease. *Neuron, 81*(1), 103-119. doi:https://doi.org/10.1016/j.neuron.2013.10.051

Wu, H., Reissner, C., Kuhlendahl, S., Coblentz, B., Reuver, S., Kindler, S., . . . Garner, C. C. (2000). Intramolecular interactions regulate SAP97 binding to GKAP. *The EMBO Journal, 19*(21), 5740-5751. doi:10.1093/emboj/19.21.5740

Zeng, M., Ye, F., Xu, J., & Zhang, M. (2018). PDZ Ligand Binding-Induced Conformational Coupling of the PDZ–SH3–GK Tandems in PSD-95 Family MAGUKs. *Journal of Molecular Biology, 430*(1), 69-86. doi:https://doi.org/10.1016/j.jmb.2017.11.003

Zheng, C. Y., Seabold, G. K., Horak, M., & Petralia, R. S. (2011). MAGUKs, synaptic development, and synaptic plasticity. *Neuroscientist, 17*(5), 493-512. doi:10.1177/1073858410386384

Zhu, J., Shang, Y., Xia, C., Wang, W., Wen, W., & Zhang, M. (2011). Guanylate kinase domains of the MAGUK family scaffold proteins as specific phospho-protein-binding modules. *The EMBO Journal, 30*(24), 4986-4997. doi:10.1038/emboj.2011.428

Zhu, J., Shang, Y., & Zhang, M. (2016). Mechanistic basis of MAGUK-organized complexes in synaptic development and signalling. *Nature Reviews Neuroscience, 17*, 209. doi:10.1038/nrn.2016.18 https://www.nature.com/articles/nrn.2016.18#supplementary-information

Eidesstattliche Versicherung
Declaration on oath

Hiermit erkläre ich an Eides statt, dass ich die vorliegende Dissertationsschrift selbst verfasst und keine anderen als die angegebenen Quellen und Hilfsmittel benutzt habe.

I hereby declare, on oath, that I have written the present dissertation by my own and have not used other than the acknowledged resources and aids.

Hamburg, den 14.01.2020 **Unterschrift** Edward Da

Lebenslauf entfällt aus datenschutzrechtlichen Gründen.